2015

Biorenewable materials from isosorbide

Michael Dennis Zenner
Iowa State University

Biorenewable materials from isosorbide

by

Michael D. Zenner

A dissertation submitted to the graduate faculty in partial fulfillment of the

requirements for the degree of

DOCTOR OF PHILOSOPHY

Major: Organic Chemistry

Program of Study Committee:
Jason S. Chen, Co-Major Professor
Michael R. Kessler, Co-Major Professor
Levi M. Stanley
Arthur H. Winter
Javier Vela

Iowa State University

Ames, Iowa

2015

To my wife, Ashley. Without you this wouldn't have been possible. Thank you.

TABLE OF CONTENTS

ACKNOWLEDGEMENTS

I would like to thank my committee chairs, Jason Chen and Michael Kessler, and my committee members, Levi Stanley, Arthur Winter and Javier Vela, for their guidance and support throughout the course of my research.

In addition, I would also like to thank my friends, colleagues, the department faculty and staff for making my time at Iowa State University a wonderful experience. I would like to thank my advisors, Jason Chen and Michael Kessler. It was with your guidance and encouragement that got me to where I am today. My collaborator, Samy Madbouly, for his rheological contributions to our publications. I would also like to thank my research assistants Cory Barnish and Nick Tucker. I couldn't have asked for better, harder working colleagues.

ABSTRACT

As petroleum feedstocks start to dwindle, it is becoming more important to find acceptable replacements for materials made from these feedstocks. Polyurethanes have classically been synthesized from petroleum-based feedstocks, and depending on its properties, polyurethanes can be used in everything from foams, to construction plastics. In recent years there has been an increasing amount of research trying to replace petroleum-based chemicals those derived from biobased sources. One such compound, isosorbide, is a rigid diol that has seen an increasing amount of research as a replacement for hard segments of polymers. While there has been much work incorporating isosorbide into polyurethanes as a diol, there has been relatively little work incorporating isosorbide as a diisocyanate. Previously, isosorbide has been directly functionalized via and S_N2 and oxidation-reduction method. Our approach introduced a tether, succinic anhydride, which is increasingly produced through fermentation. Reaction of isosorbide with succinic anhydride results in a dicarboxylic acid that can be subsequently converted to a diacid chloride. The diacid chloride then undergoes a two-step Curtius Rearrangement to afford an isosorbide-based diisocyanate. Subsequent proof of concept polyurethanes were synthesized and characterized to analyze the properties of our newly synthesized diisocyanate.

Tackifiers are a relatively unknown class of molecules that are used extensively in the adhesives industry. Usually derivatives of resin acids (diterpenes), terpenes, or petroleum-based starting materials, tackifiers, are used to improve wetting, tack and adjust the glass transition temperature of an adhesive. While most small molecules are crystalline and have a very distinctive transition from a solid to a liquid, tackifiers are glassy amorphous small molecules that have a glass transition, like a polymer. Tackifiers are usually blend with block copolymers to form pressure sensitive adhesives, i.e. tape.

It was during the synthesis of our biorenewable diisocyanate that we discovered a molecule which possessed interesting properties. The succinate diacid derivative of isosorbide was extremely viscous and therefore difficult to transfer to the next reaction. It also made everything it touched extremely sticky. With this interesting result, several analogs were synthesized to gain some insights into this emergent property. Increasing the tether length attached to isosorbide by one methylene group had no effect on how tacky the material was, but shifted the temperature at which it was most tacky down by approximately 30 °C. Conversely, introducing rigidity into the tether, increased the temperature of max tack by 30 °C. We believed the carboxylic acids of the tethers were contributing to this emergent property of tack, therefore methyl ester derivatives were synthesized and tested. While the max tack temperature shifted, there was little to no effect on maximum tack of these molecules. Further derivatives are being investigated to hopefully gain insights into the structural aspects of these molecules that are leading to tack.

The extra functionality (internal alkene) of our maleate-based tackifier led us to investigate the ability to make "smart" tackifiers, by either permanently or reversibility converting our tackifier using an external stimuli, such as heat or UV-light. Two proof of concept polymers were synthesized, one from a maleate diacid-based monomer and the other from a maleate methyl ester-based monomer. Interestingly, we discovered these monomers polymerize at significantly different temperatures and result in varying morphology. This led us to investigate the polymerization of our diacid-based polymerization. It was discovered, using ^{1}H NMR, FTIR, and GPC studies, that our diacid-based tackifier was polymerizing through a condensation mechanism rather than through a radial mechanism.

CHAPTER 1

SUSTAINABILITY AND ISOSORBIDE

1.1 Sustainability

Historically, since the late 1980's to early 2000's, crude oil prices remained relatively stable at $30 to $40 per barrel. It was during the early 2000's that the United States saw an almost exponential increase in price per barrel, stabilizing around $100 in the last few years. According to the U.S. Energy Information Administration, oil prices have been project to follow one of three project routes, see Figure 1. If prices continue on the current trend, oil prices are expect to reach $200 per barrel by 2040. This would result in doubling, or more, of the price seen at the pump circa 2010. A second projection has oil prices reaching $150 per barrel by 2040, which is still an increase of 50% over the next 30 years. Finally, most optimistically and least likely, stabilization around current price would result in gas prices competitive to that of prices around 2010. While the general public mostly associates high oil prices with high prices at the gas pump, many does not make the link between high oil prices with the cost of commodity chemicals. Today, a large majority of chemicals that go into things such as plastic bottles and packaging are still derived from petroleum feedstocks.[1]

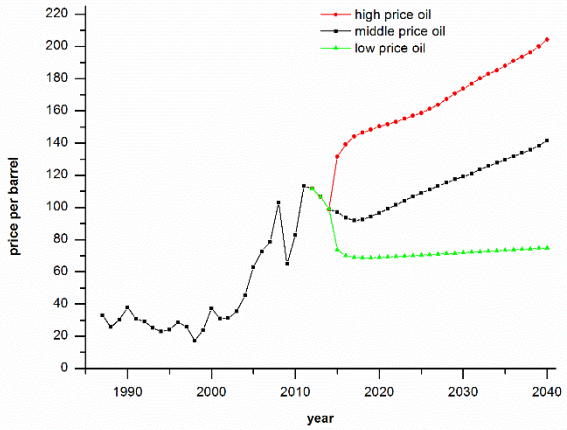

Figure 1: historical and predicted oil prices.

This need for alternative chemicals for use in materials has led to two different approaches when it comes to replacement of petroleum–based materials. The first, is production and replacement of petroleum based chemicals with those produces from renewable resources.[2,3] This allows for an easy transition from the stand point of being a drop-in replacement since there would

be no difference in structure or properties of the end product. The second route is the synthesis and incorporation of bio-based chemicals with new structures, and potential properties.[4] For the purposes of this discussion, we are going to focus on the latter.

Within the field of using new, biorenewable, chemicals there are two main subcategories, those who are making new materials from natural sources, such as cellulose, with little to no chemical modification and those converting biofeedstocks into more refined chemicals. One example, is finding new uses for cellulose through new processing technology with no chemical modification.[5] While appealing, the use of cellulose has two major draw backs that severely limits its use. First, cellulose has low thermal stability, therefore use in any high temperature application is not feasible, and secondly, the high functionality (alcohol groups) makes cellulose a poor choice in environments where alcohol reactivity could occur. Reaction of the alcohols on cellulose could result in alteration of its chemical and physical properties, something usually avoided when used for a particular purpose. It is the drawbacks of these types of molecules that has led efforts to find new, less functionalized molecules for use in biobased materials.

1.2 Isosorbide

One molecule isosorbide, derived from cellulose, has been the focus of much research in the last 20 years, Figure 2. Isosorbide is made from the depolymerization of cellulose to glucose. Glucose is then hydrogenated to sorbitol, which can be made in quantities of 1 million tons per year.[6] Sorbitol then undergoes a double dehydration resulting in isosorbide as the final product, Figure 3. Isomannide, a stereoisomer, is made from the less available mannitol, and can be

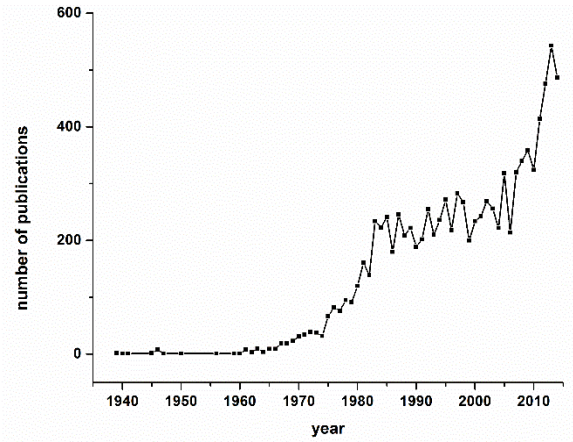

Figure 2: publication of isosorbide per year.

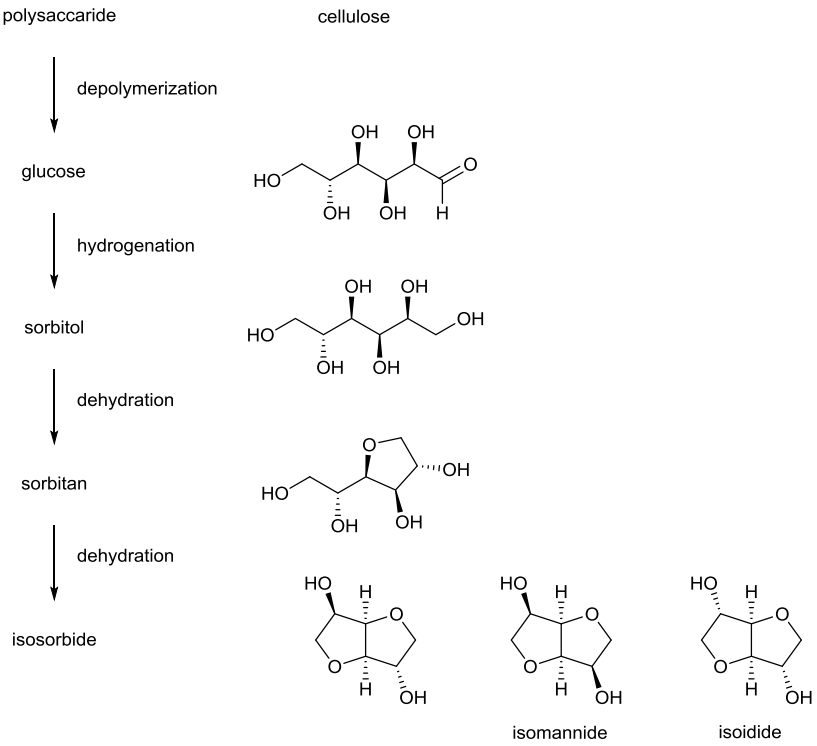

Figure 3. Synthesis of isosorbide from cellulose.

purchased as a specialty chemical, but isoidide cannot be made from natural sources and therefore must be synthesized in the lab. Recently Van Es. et. al. reported the isomerization of isosorbide to isoidide using a ruthenium based catalyst.[7] There has also been considerable progress increasing the efficiency and scalability of isosorbide production, which has increased its appeal as a replacement for petroleum-based chemicals.[8]

Isosorbide is a small molecule diol with a melting point of 60 °C and a decomposition temperature of 270 °C. It consists of two cis-fused furan rings, with an internal angle of approximately 120°, Figure 4. This puts one alcohol convex, **a**, (less hindered) and one concave, **b**, (more hindered) with respect to the ring which leads to a difference in reactivity of the two alcohols. The concave alcohol, due to its position, hydrogen bonds with the oxygen on the neighboring ring, resulting in the concave alcohol being slightly more nucleophilic than the corresponding convex alcohol.[4,9] What makes isosorbide more appealing than its

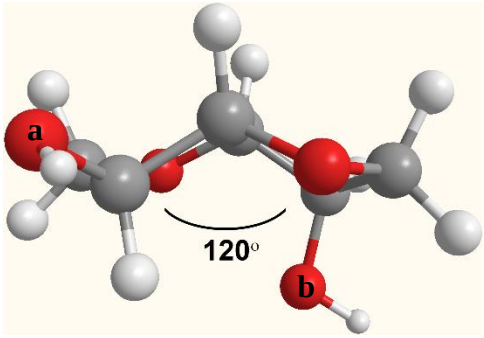

Figure 4. Isosorbide.

carbohydrate counter parts, i.e. glucose and sorbitol, is its reduced functionality (two alcohols compared to five on glucose) and higher thermal stability.

1.3 Succinic Acid

One molecule, succinic acid, was once made entirely from petroleum-based feedstock. Recently, however, there has been substantial effort made to synthesize succinic acid from biorenewable resources. In 2010 succinic acid was produced on a relatively small scale (30,000 tons per year) and with a net market worth of $225 million per year. DSM partnered with Roquette to build a plant capable of producing 10,000 to 20,000 tons per year, with the ability to produce upwards of 50,000 tons per year using either bacterial or non-bacterial production methods. US-based Myriant constructed a bio-succinic acid plant capable of producing 15,000 tons per year with the infrastructure to produce 80,000 tons per year using an E. coli production method. It is these efforts that is taking succinic acid from a

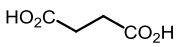

Figure 5. Succinic acid

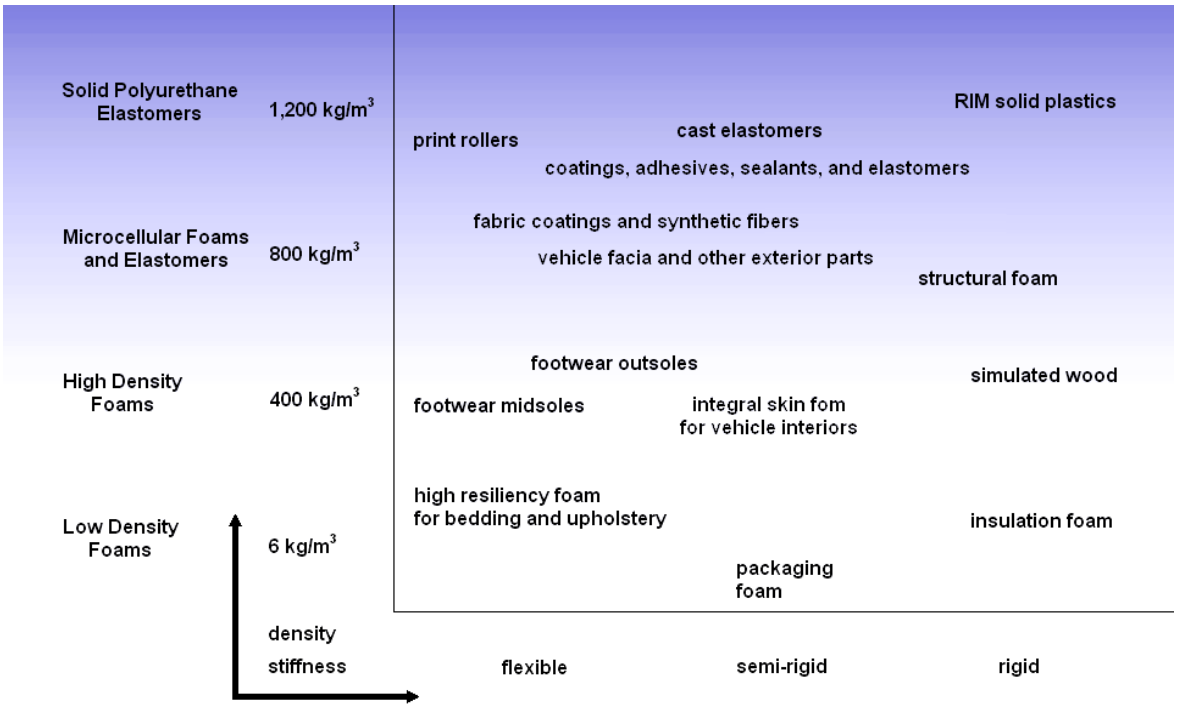

Figure 6. Polyurethane properties combinations.

specialty chemical to a cheap, readily available commodity chemical. Between these two plants alone, here is enough production capacity to exceed that of petroleum-based succinic acid.[10, 11]

1.4 Polyurethanes

One area of focus for the incorporation of isosorbide is polyurethanes. In 2012, polyurethane production totaled 5.5 billion pounds (2.75 million tons) in the United States alone.[12] Depending on the properties, Figure 6,[13] polyurethanes can be used in a variety of ways. For example, if a polyurethane is flexible with a low density, it can made into a material that is suitable for things such as bedding. On the other hand if a polyurethane is hard and dense, it becomes a material suitable for use in construction. It is this diversity that makes polyurethanes common in everyday life, from the foam insulation in the walls of a house, bed and seat cushions, to the clear coats on furniture and wood floors. Not too surprisingly, a majority of these materials are still made from petroleum-based feedstock, and as oil prices increase, so do the prices of materials.

As previously stated, there has been in increasing amount of research incorporating isosorbide as a biorenewable diol.[4] It wasn't until relatively recently there has been research functionalizing isosorbide into a diisocyanate, Figure 7. One approach, as demonstrated by Thiem et. al. was the direct functionalization of isosorbide via an S_N2 route.[14—16] For this approach, isosorbide was first reacted with 4-toluenesulfonyl chloride to generate a good leaving group.

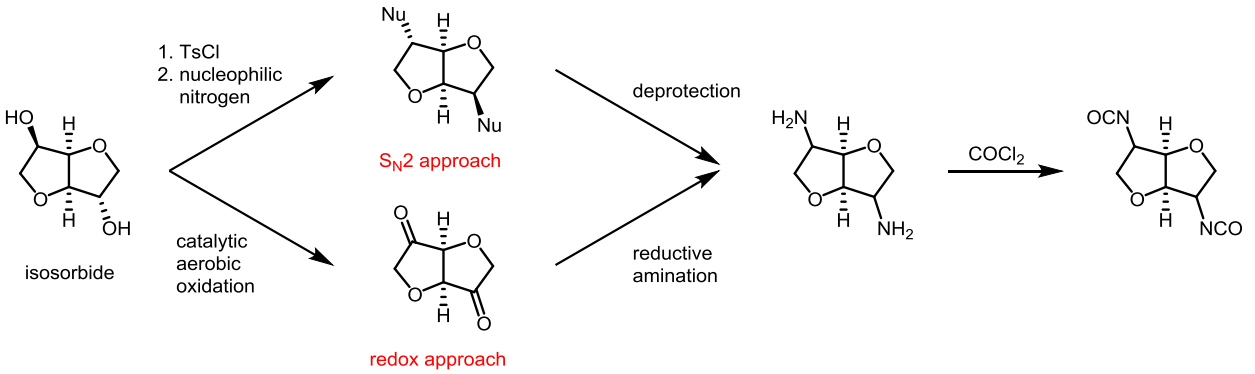

Figure 7. S_N2 and redox synthesis of isosorbide diisocyanate.

Next, the activated oxygen's were displaced via an S_N2 mechanism using a protected amine nucleophile. Following deprotection, the diamine was phosgenated to form the stereochemically well defined diisocyanate. One of the difficulties with the S_N2 approach stems from the core structure of isosorbide. Since the cis-fused bicycle has an internal angle of 120°, displacement of the convex oxygen is quite difficult due to severe steric hindrance as the amine approaches from the concave side of the molecule. Another route, demonstrated by Schneider et. al., takes an oxidation-reduction approach.[17—20] For this approach, isosorbide is oxidized to the diketone. The diketone then undergoes a reductive amination to afford the diamine, followed by phosgenation to give the diisocyanate. While this synthesis is more applicable on industrial scale, it no longer has the well-defined stereochemistry achieved via the S_N2 approach. Synthesis of this diisocyanate is impractical on laboratory scale due to the extreme pressure needed (500 bar) for the reductive amination. These pressure are likely needed to suppress side reactions common of reductions to primary amines.[20]

1.5 Tackifiers

Another area of research, which sees little to no attention in academia, but is quite important in industry and everyday life, is the synthesis of tackifiers. A tackifier is a small molecule that renders materials tacky (sticky). Tack, as defined by ASTM standards is, "the property of an adhesive that enables it to form a bond of measureable strength immediately after the adherend and adhesive are brought into contact under low pressure."[21] So what makes a tackifier different from all other small molecules? Besides being sticky, where most small molecules are crystalline solids and melt into liquids, tackifiers have a glass transition instead of a melt, a property known mostly to polymers. Tackifiers are placed into one of three categories, resin acids (diterpenes), terpenes, and petroleum-based. Resin acids are by far the most widely used and applicable

tackifier. Most resin acids are either derivatized or oligomerized to reduce the acid count (increase compatibility) and increase the glass transition temperature of the tackifier. Tackifiers, while display tack on their own, are not suitable for use in adhesives alone, since they do not have enough cohesive strength, and therefore can be separated easily from the surface to which they are attached. Tackifiers, since there is no crosslinking or chain entanglement are also susceptible to creep. It is therefore necessary to blend tackifiers with polymers to make pressure sensitive adhesives (i.e. tapes).[22, 23]

1.6 Pressure sensitive adhesives

Pressure sensitive adhesives were traditionally made from natural rubber.[24] It wasn't until recently that pressure sensitive adhesives were made using synthetic polymers. Current pressure sensitive adhesive technology focuses on block co-polymers which follow an A-B-A type structure, where the A block is usually a hard end-block with a glass transition above room temperature and the B block is a soft/flexible, with a glass transition below room temperature. Some common block co-polymers used in industry are styrene-butadiene-styrene, and styrene-isoprene-styrene.[25] In recent years acrylic co-polymers have also become more commercially available.[26] The different blocks have sufficiently different properties, which results in the two blocks being incompatible with one another, resulting in microphase separation. The mid-block serves as a soft viscoelastic phase and the end-block serves as a physical crosslinker. The goal, when making an adhesive, is to have the tackifier compatible with the mid-block, and not the end-block. The tackifier increases wetting ability of the adhesive with the surface. The physical crosslink, caused by π-stacking of the styrene segments over a chemical crosslink, allows the pressure sensitive adhesive to be melt cast since heating the polymer above the glass transition of

the end-block results in separation of the end-blocks. This allows the polymer to be processed and cooled, at which time the end-blocks re-crosslink.

The realization that oil will not last forever has caused an increase in the amount of research involving bio-based or biorenewable materials. Isosorbide, which as seen an increased interest in the past 20 years has shown great promise towards reducing our dependence of petroleum-based chemicals and materials. That being said, there is still much to be learned and be discovered about the fused bicycle. In the next few chapters I will describe the planned syntheses and the unplanned discoveries from isosorbide.

References

[1] AEO2014 Early Release Overview, Annual Energy Outlook 2014 Early Release Overview, *U.S. Energy Information Administration*, **2014**. http://www.eia.gov/forecasts/aeo/er/pdf/0383er(2014).pdf

[2] Y. Xu, M. A. Hanna, L. Isom, *The Open Agriculture Journal*, **2008**, 2, 54 – 61.

[3] J. B. McKinlay, C. Vieille, J. G. Zeikus, *Appl. Microbiol. Biotechnol.* **2007**, *76*, 727 – 740.

[4] M. Rose, R. Paklovits, *ChemSusChem.* **2012**, 5, 167 – 176.

[5] D. Klemm, F. Kramer, S. Moritz, T Lindstrom, M. Ankerfors, D. Gray, A. Dorris, *Angew. Chem. Int. Ed.* **2011**, 50, 5438 – 5466.

[6] M. Patel, M. Crank, V. Domburg, B. Hermann, L. Roes, "Medium and Long-term Opportunities and Risks of the Biotechnological Production of Bulk Chemicals from Renewable Resources," **2006**, http://brew.geo.uu.nl/BREW_Final_Report_September_2006.pdf, pp 75 – 76.

[7] D. S. van Es, Rigid Biobased Building Blocks, *J. Renew. Mater.* **2013**, 1, 61 – 72.

[8] K. Stensrud, E. Hagberg, S. Howard, E. M. Rockafellow, International Patent, **2014**, WO 2014/137619 A1

[9] G. Fleche, M. Huchette, *Starch/Staerke*, **1986**, 38, 26 – 30.

[10] M. Patel, M. Crank, V. Domburg, B. Hermann, L. Roes, "Medium and Long-term Opportunities and Risks of the Biotechnological Production of Bulk Chemicals from Renewable Resources," **2006**, http://brew.geo.uu.nl/BREW_Final_Report_September_2006.pdf, pp 39 – 44.

[11] K.-K. Cheng, X.-B. Zhao, J. Zeng, J.-A. Zhang, *Biofuels, Bioprod., Bioref.* **2012**, *6*, 302 – 318.

[12] The Economic Benefits of the U.S. Polyurethanes Industry, *American Chemistry Council*, **2014**. http://polyurethane.americanchemistry.com/Resources-and-Document-Library/Economic-Benefits-of-Polyurethanes-2013.pdf

[13] http://en.wikipedia.org/wiki/List_of_polyurethane_applications

[14] J. Thiem, H. Lüders, *Makromol. Chem.* **1986**, *187*, 2775 – 2785.

[15] F. Bachmann, J. Reimer, M. Ruppenstein, J. Thiem, *Macromol. Chem. Phys.* **2001**, *202*, 3410 – 3419.

[16] S. Thiyagarajan, L. Gootjes, W. Vogelzang, J. van Haveren, M. Lutz, D. S. van Es, *ChemSusChem* **2011**, 4, 1823 – 1829.

[17] G. Limberg, J. Thiem, *Synthesis* **1994**, 3, 317 – 321.

[18] S. Imm, S. Bahn, M. Zhang, L. Neubert, H. Neumann, F. Klasovsky, J. Pfeffer, T. Haas, M. Beller, *Angew. Chem*. **2011**, 123, 7741 – 7745; *Angew. Chem., Int. Ed.* **2011**, 50, 7599 – 7603.

[19] U. Dingerdissen, J. Pfeffer, T. Tacke, H. Schmidt, F. Klasovsky, R. Sheldon, M. Volland, M. Rimbach, S. Rinker, **2011**, U.S. patent application US 2011/0251399 A1.

[20] G. Streukens, C. Lettmann, S. Schneider, **2012**, international patent application WO 2012/010385 A1.

[21] For the definition of tack and tackifiers, see: a) Standard Terminology of Adhesives D907-11a, *American Society for Testing and Materials*, Philadelphia, PA, Vol. 15.06, **2012**, 33 – 44

[22] I. Benedek, M. M. Feldstein (eds.), *Technology of Pressure-Sensitive Adhesives and Products*, CRC Press, Boca Raton, **2009**, p. 576

[23] A. V. Pocius, *Adhesion and Adhesives Technology*, 2nd ed., Hanser, Cincinnati, **2002**, pp. 242 – 259.

[24] I. Benedek, M. M. Feldstein (eds.), *Technology of Pressure-Sensitive Adhesives and Products*, CRC Press, Boca Raton, **2009**, pp. 2-8 – 2-10.

[25] Y. Hu, C. W. Paul, "Block Copolymer-Based Hot-Melt Pressure-Sensitive Adhesives" in *Technology of Pressure-Sensitive Adhesives and Products* (I. Benedek, M. M. Feldstein, eds.), CRC Press, Boca Raton, **2009**, pp. 3-1 – 3-45

[26] I. Benedek, M. M. Feldstein (eds.), *Technology of Pressure-Sensitive Adhesives and Products*, CRC Press, Boca Raton, **2009**, pp. 3-33 – 3-42.

CHAPTER 2

ISOSORBIDE-BASED DIISOCYANATES AND POLYURETHANES THEREOF

PUBLISHED: M. D. Zenner, Y. Xia, J. S. Chen. M. R. Kessler, Isosorbide-based Diisocyanates and Polyurethanes Thereof, *ChemSusChem*, **2013**, 6, 1182.

Introduction

Polyurethanes are versatile materials generated through the polymerization of polyols with polyisocyanates.[1] Their properties may be tailored to afford elastomers, foams, coatings, adhesives, and fibers. The vast majority of polyurethanes are petroleum-derived, but there is growing success in employing biorenewable polyols.[2,3] In contrast, there has been comparatively little work on the development of biorenewable polyisocyanates.[4–7]

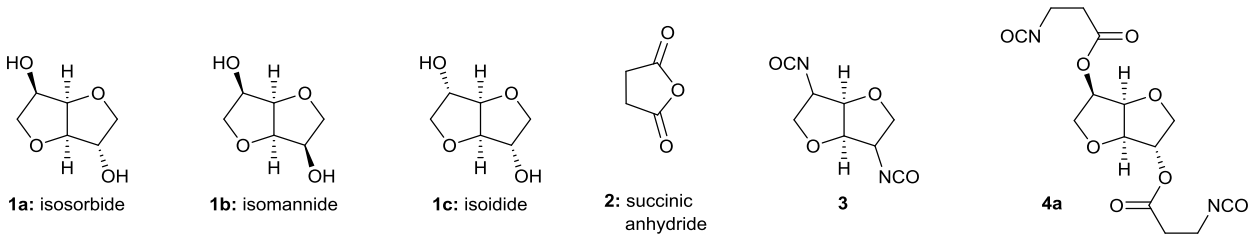

Figure 1. Structures of biorenewable building blocks (**1a** – **c**, **2**) and selected isosorbide-based diisocyanates (**3**, **4a**).

Manufactured by the dehydration of sorbitol (1 million tons of sorbitol is produced annually[8]), isosorbide (**1a**, Figure 1) is a promising non-toxic precursor to biobased materials.[8,9] Isomannide (**1b**) also is readily available, but isoidide (**1c**) is quite scarce. Its rigidity and thermal stability render isosorbide (**1a**) a useful reinforcing agent for thermoplastic polymers[10] and a promising surrogate for petroleum-derived diols.[3] There are few reports of isosorbide-based diisocyanates (e.g., **3**) and diamines.[4–6] Due to unfavorable sterics and electronics, S_N2 approaches to diisocyanate **3**[4] proceed acceptably for isomannide (**1b**) only. Oxidation–reductive amination strategies[5] deliver diisocyanate **3** in high yield from isosorbide (**1a**), but as a mixture of diastereomers.

Results and Discussion

Our first attempts were towards the direct funtionalization of isosorbide to a diisocyanate, Scheme 1. In order to increase the chances of success we chose isomannide. The C2 symmetry of isomannide made for convinent characterization and the concave alcohols on isomannide force both nucleophiles to approach from the less hindered, convex, side of the molecule. An S_N2 approach was previously reported using triflate as the leaving group. In order to increase scaleaility and reduced cost, mesylate, although a less favorable leaving group, was chosen. While reaction of isomannide with mesyl chloride in methylene chloride and amine base proceeds in quantitative yields, attempts at an S_N2 displacement with potassium isocyantate (refluxing DMF, and DMSO at 160 °C) resulted in appearance of starting material. Having no indication of product formation, we shifted our attention to a redox approach.

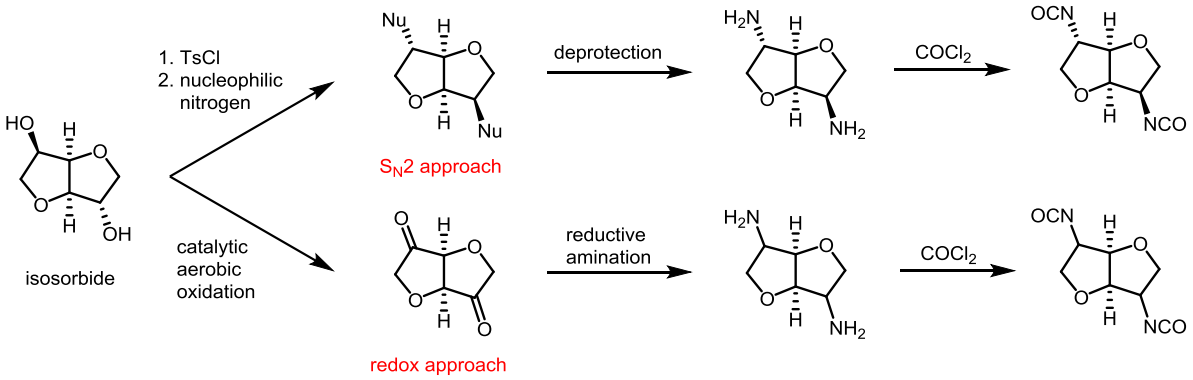

Scheme 1. S_N2 and redox synthesis of isosorbide diisocyanate.

The synthesis of an isosorbide-based diketone was previously reported.[5] It was from this point we pursured an isosorbide-based diisocyanate. Our first attempt at conversion of the diketone to an amine, through the imine intermediate, using Pd/C and ammonium acetate under a hydrogen atmosphere, resulted in starting diketone. For our second approach, the diketone was dissolved in methanol saturated with ammonia and heated to 65 °C in a sealed container. After 2.5 hr Pd/C was added to the reaction and pressurized to 30 bar under a hydrogen atmosphere. Only starting material was observed. Our second attempt at synthesis of the isosorbide-based diisocyanate

proceeded through an oxime intermediate. The isosorbide-based diketone was reacted with hydroxylamine in methanol, but NMR characterization was incoclusive. It was therefore decided that conversion to the oxime followed by immediate reduction to the amine was the most practical way to decide whether there was oxime formation and subsiquently, amine formation was successful. All attempts reacting the diketone with hydroxylamine followed by redution using Pd/C and either hydrogen or formic acid, as the hydrogen source, only resulted in starting material. It was here that we decided a different approach was necessary for the synthesis of an isosorbide-based diisocyanate. It is important to note that shortly after we abandoned the redox approach to a diamine, a patent application was published where successful reduction of the diketone was achieve, using Pd/C and hydrogen at 500 bar.[5]

We envisaged the use of a second biobased building block as a short tether in order to access a stereochemically pure isosorbide-based diisocyanate. Succinic anhydride (**2**) was identified as an ideal co-starting material in view of the extensive progress towards manufacturing biosuccinic acid at a competitive price.[12] Herein we report the preparation of diisocyanates **4** using no stoichiometric petroleum-based reagents and the characterization of representative biorenewable polyurethanes thereof.

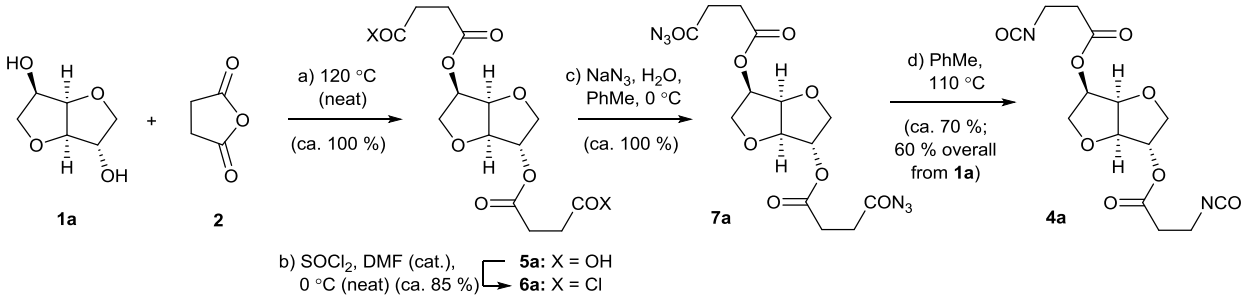

Scheme 2. Synthesis of diisocyanate **4a**: a) **1a** (1.0 equiv), **2** (2.3 equiv), 120 °C, 24 h; b) $SOCl_2$ (13.8 equiv), DMF (0.01 equiv.), 0 °C, 2 h; c) NaN_3 (5.0 equiv), H_2O, PhMe, 1 h; PhMe, 110 °C, 1 h. DMF = *N*,*N*-dimethylformamide.

The synthesis of diisocyanate **4a** is shown in Scheme 2. Double esterification of isosorbide (**1a**) with succinic anhydride (**2**) proceeded in quantitative yield under solvent-free conditions

when both reactants were melted (120 °C). Due to sublimation of succinic anhydride at those temperatures, it was therefore necessary to fully submerge the round bottom in an oil bath to achieve complete reaction. While reaction in solvents such as DMF and pyridine ran to completion, removal of residual solvent proved to be quite challenging due to the extreme viscosity of the product. Diacid **5a** could be purified with difficulty by vacuum sublimation of excess succinic anhydride (**2**) from the viscous mixture, but it was not necessary to do so. A one-step Schmidt reaction would be the most direct route to diisocyanate **4a**, but was ruled out because of the explosive and toxic nature of the low-boiling reagent hydrazoic acid (HN_3, b.p. 37 °C). Diisocyanate formation through a Curtius rearrangement[13] was deemed the safer option. Therefore, crude diacid **5a** was converted into diacid chloride **6a** through the action of thionyl chloride. The uncatalyzed reaction at 75 °C proceeded in ca. 70 % chemical yield.[14] The yield was improved to ca. 85 % by cooling the reaction mixture to 0 °C and adding 1 mol % of DMF.[15] Excess thionyl chloride was recovered by distillation and used in the synthesis of subsequent batches of material.

A two-step Curtius rearrangement of diacid chloride **6a** through the intermediacy of diacyl azide **7a** gave diisocyanate **4a**. Thus, diacyl azide **7a** was formed through exposure to sodium azide under aqueous biphasic conditions. This process was quantitative[16] in various organic solvents. Unexpectedly, all impurities were eliminated during aqueous workup, affording a solution of pure diacyl azide **7a** that could be used directly in the next step. (**Warning:** Diacyl azide **7a** may be explosive in concentrated form.) The yield of the thermal conversion of diacyl azide **7a** into diisocyanate **4a** was insensitive to temperature in a range from 45 °C to 140 °C, but strongly dependent on solvent selection. Various solvents such as DMSO, ethyl acetate, benzene, toluene, xylenes, and nitrobenzene were screened. Aromatic solvents were chosen over other organic

solvents, with toluene proving optimal, due to their higher boiling points and thus increased safety (see below), as well as higher yields, during the Curtius rearrangement. For safety on large scale,[13] the solution of diacyl azide **7a** was added into a small amount of toluene that had been heated to 110 °C. The reaction was "instantaneous" at this temperature, and any runaway exotherm could be halted immediately by stopping the addition of diacyl azide **7a**. On larger scales, 30 g, a jacketed addition funnel was used to keep diacyl azide **7a** cool using dry ice and acetone, for increased safety. Pure diisocyanate **4a** (b.p. 186 – 189 °C, 230 mTorr) was distilled in 60 % overall yield from isosorbide (**1a**) (ca. 70 % yield from diacyl azide **7a**).

One difficulty we encountered during the distillation was the thermal instability of diisocyanate **4a**. While the distillation occurs from 186 – 189 °C at 230 mTorr, if the distillation pot is heated to 200 °C or higher, partial E1cB like elimination occurs, Scheme 3 and supporting information, due to the acidic hydrogen alpha to the ester. Interestingly, the amount of elimination product is seemingly random, when deliberately heating the distillation pot to 260 °C only 1.5 % elimination was observed. At other times, when great care was taken during the distillation set-up, and the pot temperature reached 205 °C, upwards of 15 % elimination was observed. We believed residual Lewis acids, such as $MgSO_4$ from the aqueous work-up, might be catalyzing the elimination. Various drying agents such as Na_2SO_4 and molecular sieves were tested during the aqueous work-up of acyl azide, converted to the diisocyanate and distilled. Elimination was observed for all samples tested. Radical inhibitors were also added during the distillation to test if high temperatures were causing a radical type

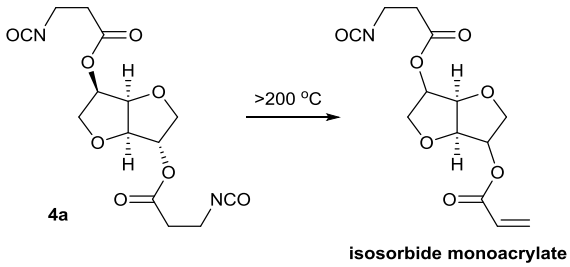

Scheme 3, elimination of **4a**.

elimination, but resulted in similar amounts of elimination. The distillation has, thus far, been limiting the amount pure diisocyanate **4a** obtained, to17 grams.

To assess whether elimination of **4a** was due to the acidity of the hydrogen alpha to the ester, a gluterate linked diisocyanate **12a** was synthesized, Scheme 4. While synthesis of the diacid and acid chloride proceed in similar yields as the succinate tether, conversion to the diacyl azide **11a** is not as clean. Approximately 50 % of the material is lost during the aqueous work up, we believe this is due to the increased solubility of the gluterate linker in water due to its increased ability to intermolecularly hydrogen bond with water over that of the succinate linker. Optimization of the aqueous work-up should result in less loss of material, but was deemed unnecessary for the purposes of the study. Distillation of **12a** occurred at 229 – 230 °C at 600 mTorr, with the distillation pot reaching a maximum temperature of 270 °C. Characterization of purified **12a** showed no evidence of elimination, further suggesting elimination of **4a** is due to the acidic hydrogen alpha to the ester.

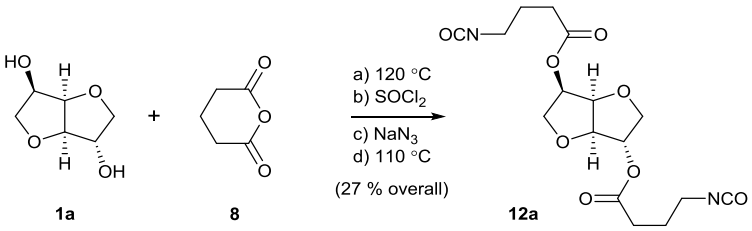

Scheme 4. Synthesis of diisocyanate **12a**: a) **1a** (1.0 equiv), **8** (2.3 equiv), N,N-dimethyl benzylamine (0.01 equiv.), 120 °C, 4 h; b) $SOCl_2$ (3 equiv), DMF (0.01 equiv.), 70 °C, 25 min; c) NaN_3 (2.5 equiv), tetrabutylammonium bromide (0.002 equiv.), H_2O, PhMe, 1 h; d) PhMe, 110 °C, 1 h.

Table 1. optimization of synthesis of diacid **5a**.

Entry	catalyst	amount / mol %	time / min	% conversion
1	DMBA	1	180	100
2	H_2SO_4	1	5	74[a]
3	H_2SO_4	1	10	90[a]
4	H_2SO_4	1	20	87[b]
5	H_2SO_4	0.1	20	75[a]

[a] incomplete reaction; [b] resulted in 13 % oligomerization.

After publication, we were contacted by a few companies (Johnson Controls Inc. in particular showing great interest) to use diisocyanate **4a** with their technology to increase the biocontent of their thermosets. Although, and unfortunately, the collaboration fell through due to a disagreement over royalties with ISURF and JCI, we decided to further optimize for synthesis of diisocyanate **4a** on kilogram scale. With this in mind, optimization was focused around three areas; time, waste, and most importantly safety.

There were two main problems encountered during the synthesis of diacid **5a**; first, it took 24 h to complete and second, at 120 °C there is significant sublimation of succinic anhydride. It was therefore necessary to fully submerge the round bottom in oil to ensure complete reaction, which posed a major issue as scales increased much beyond 100 grams. The use of dimethylbenzyl amine as a catalyst to reduces the reaction time of isosorbide with maleic anhydride to 3 h was recently published, and was applicable for use with succinic anhydride, reducing the formation of diacid **5a** to 3 h.[17] Temperature reduction was not an option, since 120 °C is necessary to melt succinic anhydride, but reduction in reaction time, while sublimation still occurs, is negligible, making it unnecessary to fully submerge the entire round bottom. Use of sulfuric acid as a catalyst was also investigated and resulted in conversion to diacid **5a** in 20 min, but gave partial oligomerization, therefore depending on the end use of the material, use of sulfuric acid may be advantageous, Table 1. With optimization of diacid **5a** complete, we turned our attention to optimization of acid chloride **6a**.

Although the conversion to acid chloride **6a** goes in high yield, the actual logistics of getting the reaction set up is quite tedious and time consuming. Diacid **5a** is an extremely viscous, and sticky material, making it quite difficult to handle. In order to transfer diacid **5a** to the round bottom containing cold thionyl chloride, it was necessary to heat (80 °C) diacid **5a** to a free flowing

liquid to transfer the material. This posed a second problem, once diacid **5a** was in the cold thionyl chloride it either heated the thionyl chloride making the reaction occur above 0 °C or re-solidified before it dissolved, resulting in the need to heat the reaction to get diacid **5a** dissolved since the reaction could no longer stir. To get around this problem, diacid **5a** had to be heated to a free flowing liquid and poured it into a mortar. The mortar containing diacid **5a** was then cooled using acetone and dry ice. Once frozen, diacid **5a** could then be crushed using a pestle, which also had to be cooled using dry ice. Powdered diacid **5a** could then be transferred, using a cold scoopula, to cold thionyl chloride. The transfer had to occur quickly to a avoid reheating of diacid **5a**, which results in a sticky mess. Conversion to diacid chloride **6a** can be done in refluxing thionyl chloride, but results in slightly lower yields and still used excess thionyl chloride, which has to be removed after the reaction is complete. With reducing waste in mind and wanting to increase the ease of the reaction, we came up with a quite simple solution, change the order of addition.

After complete reaction of diacid **5a** the temperature was reduced to 95 °C and 1 mol % DMF was added. Thionyl chloride was then added dropwise to the reaction, after the viscosity of the reaction began to decrease, the temperature could be further lowered to 70 °C, to prevent refluxing of thionyl chloride. Reaction progress was monitored using a bubbler. Once bubbling slowed, almost to a stop, 10 drops of thionyl chloride was added rapidly to the reaction. If bubbling increased, the reaction was incomplete, but if no increase in bubble rate was observed after addition, then the reaction was complete. This not only allowed us to take a two pot two step reaction and reduce it to a one pot, two step reaction, with little to no effect on yield, it also eliminated the use of excess thionyl chloride. This reduced not only waste but the need to remove any remaining thionyl chloride. With optimization of diacid **5a** and acid chloride **6a** complete, we turned our attention to the Curtius rearrangement.

One of the main concerns with the conversion to acyl azide **7a** was the risk of hydrazoic acid (a toxic explosive) formation. In our previous synthesis, 4 eq. of sodium azide was necessary to drive the reaction to completion. This not only increased the risk of hydrazoic acid formation, if the aqueous layer became acidic, but also used 2 eq. more than necessary to achieve complete reaction. In order to reduce on the amount of sodium azide needed, tetrabutylammonium bromide was introduced as a phase transfer catalyst. This decreased the amount of sodium azide needed from 4 eq. to 2.5 eq. which not only reduces the amount of azide needed but substantially increases safety. 2.5 eq. is only necessary because of the presence of approximately 0.2 eq. of succinyl chloride in the reaction. We are also working towards monitoring the pH of the aqueous layer via a pH probe or indicator. This would allow us to determine if the solution is becoming acidic and therefore add base as necessary to keep the reaction at a safe, basic, pH. Attempts at optimization of the aqueous workup to remove the need for addition of a drying agent were unsuccessful, with the best achieved water content after the workup was 0.1 equivalents of water after washing with a 10 % potassium carbonate solution followed by a brine wash. We are now turning our attention to the second step of the Curtius rearrangement. We believe use of a transition metal catalyst will raise the purity to the point where it could be used for synthesis of thermoset polymers, since absolute purity isn't not a strict necessity for these types of polymers.

As shown in Scheme 5, isomannide-derived diisocyanate **4b** (b.p. 197 – 199 °C, 230 mTorr) was prepared from isomannide (**1b**) and succinic anhydride (**2**) in 52 % overall yield under identical reaction conditions to that of un-optimized diisocyanate **4a**. Unlike

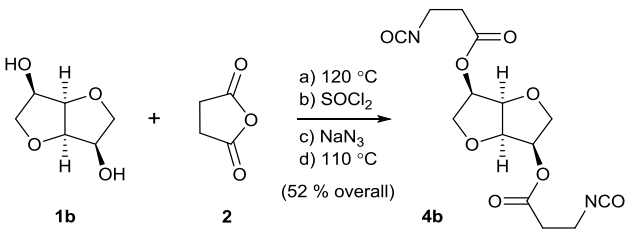

Scheme 5. Synthesis of diisocyanate **4b**: a) **1b** (1.0 equiv), **2** (2.3 equiv), 120 °C, 24 h; b) $SOCl_2$ (13.8 equiv), DMF (0.01 equiv.), 0 °C, 2 h; c) NaN_3 (5.0 equiv), H_2O, PhMe, 1 h; d) PhMe, 110 °C, 1 h.

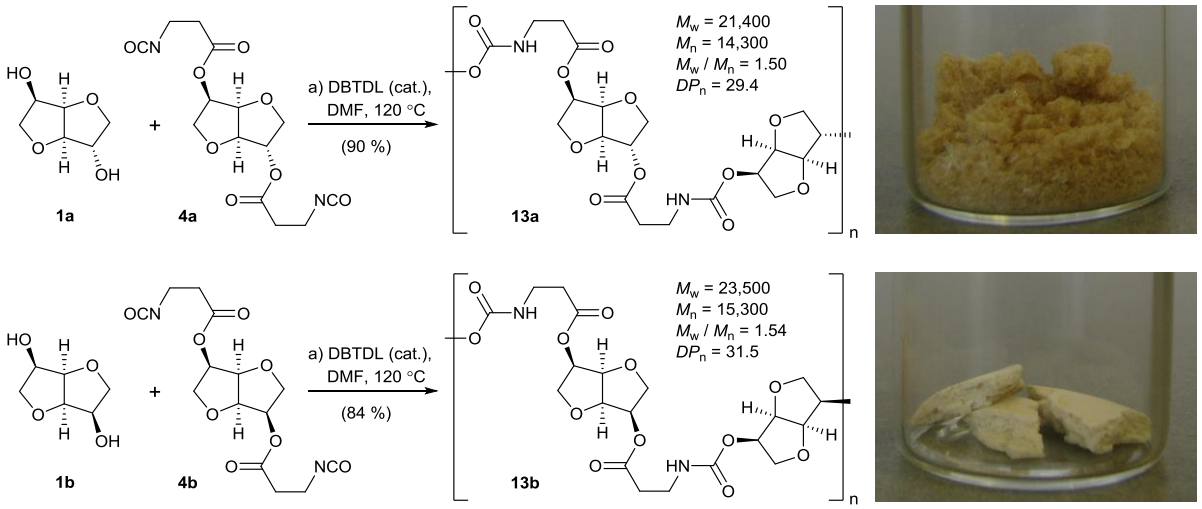

Scheme 6. Synthesis of polyurethanes **13a** and **13b**: a) **1** (1.0 equiv), **4** (1.0 equiv), DBTDL (0.001 equiv), DMF, 120 °C, 48 h; then MeOH. Polyurethane **13a** is stereo-irregular; for clarity, only one stereochemical combination is shown. Each vial (28 mm outer diameter) contains 700 mg of polymer.

isosorbide-based diisocyanate **4a**, isomannide-based diisocyanate **4b** is C_2-symmetrical. Therefore, whereas polymerizations with isosorbide-based diisocyanate **4a** lead to stereo-irregular polyurethanes, polymerizations with isomannide-based diisocyanate **4b** can lead to stereo-regular polyurethanes.[18]

Representative thermoplastic polyurethanes were synthesized in order to assess the suitability of diisocyanates **4a** and **4b** for the design of high-performance materials. Thus, polymerization of isosorbide-derived diisocyanate **4a** with isosorbide (**1a**) in the presence of dibutyltin dilaurate (DBTDL) followed by precipitation from methanol afforded polyurethane **13a** (Scheme 6) in 90 % yield. Analysis of this opaque light-brown powder by gel permeation chromatography (GPC; calibrated to polystyrene) revealed a degree of polymerization competitive with that of other isosorbide-derived polyurethanes[3,4a,b,6a] (M_w = 21,400; M_n = 14,300) and low polydispersity (M_w / M_n = 1.50). Polymerization of isomannide-derived diisocyanate **4b** with isomannide (**1b**) under identical conditions delivered polyurethane **13b**, possessing a comparable degree of polymerization (M_w = 23,500; M_n = 15,300) and similarly low polydispersity (M_w / M_n = 1.54), in 84 % yield. Both polymers possess excellent thermal stability (T_d = 253 °C for **13a**,

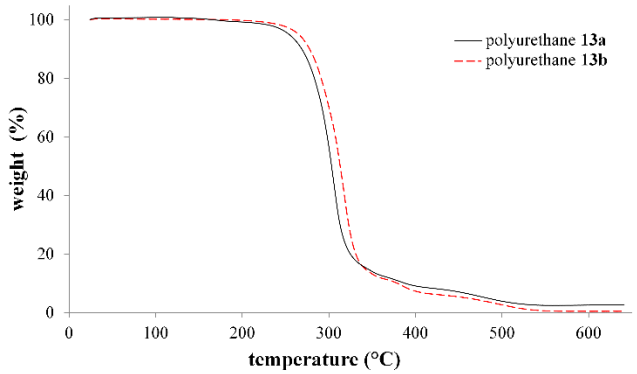

Figure 2. TGA curves for polyurethanes **13a** and **13b**. Samples were heated at 20 °C / min.

265 °C for **13b**; measured at 5 % mass loss, see Figure 2) as determined by thermogravimetric analysis (TGA) which is consitant with most polyurethanes having a thermal stability ranging from 100 °C to 300 °C.

To our surprise, whereas isosorbide-based material (**13a**) is a fluffy powder, the isomannide-derived substance (**13b**) is an opaque white solid. Differential scanning calorimetry (DSC) of these materials at a heat rate of 10 °C min^{-1} revealed a significantly more endothermic melt of isomannide-derived polyurethane **13b** (ΔH = 23 J g^{-1}; compare with 1.0 J g^{-1} for **13a**, see Figure 3), suggesting a higher level of crystallinity for this material. This dramatic and reproducible difference in morphology under identical processing conditions is consistent with the stereo-regular nature of isomannide-derived polyurethane **13b** and the stereo-irregular nature of isosorbide-derived polyurethane **13a**.[18] However, once thermal histories are erased (i.e., after pre-heating to 175 °C at 10 °C min^{-1} and cooling back down at the same rate), polyurethanes **13a** and **13b** undergo glass transitions at 78 °C and 81 °C, respectively, and do not exhibit a melt. Further characterization of these materials is ongoing.

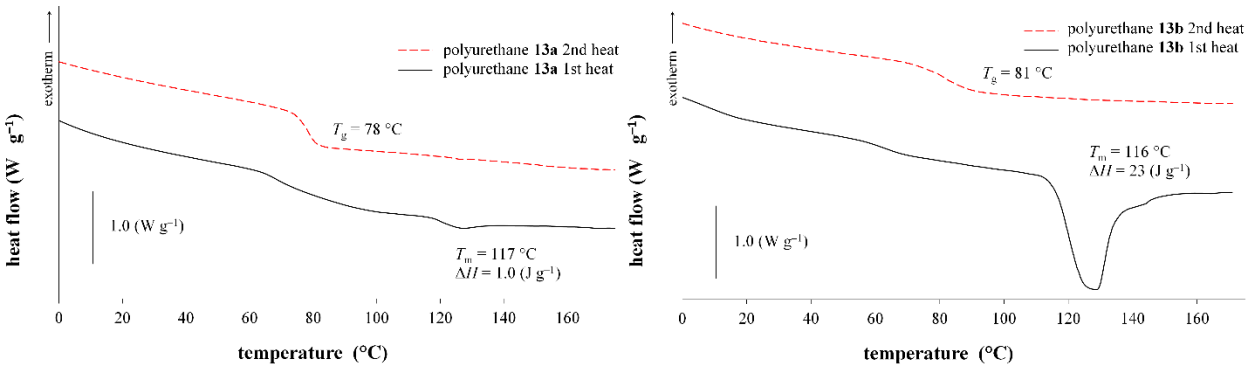

Figure 3. DSC curves for polyurethanes **13a** (top) and **13b** (bottom). Samples were heated at 10 °C min^{-1} from –50 to 175 °C, cooled back to –50 °C at a rate of 10 °C min^{-1}, then heated again at 10 °C min^{-1}.

Conclusion

In summary, we prepared stereochemically well-defined diisocyanates (**4a** and **4b**) from isosorbide (**1a**) or isomannide (**1b**) and succinic anhydride (**2**). The diisocyanates have low vapor pressures, and thus should present minimal inhalation hazards. If biobased succinic anhydride is used, then 100 % of the carbon content is from biorenewable sources, and no stoichiometric petroleum-derived reagents are consumed. Representative polyurethanes made from these diisocyanates have excellent thermal stability and stereochemistry-dependent morphology. Related diisocyanates and polyurethanes will be prepared and evaluated in due time.

I would like to thank Nick Tucker for his help in optimization of diacid **5a** and the conversion to diacyl azide **7a**. I would also like to thank Ying Xia for his help in obtaining thermal characterization of polyurethanes **13a** and **13b** as well as training me on the thermal characterization equipment.

Experimental Section

General procedures. Unless otherwise noted, all reactions were performed with stirring under an argon atmosphere under anhydrous conditions. Isosorbide was purchased from Acros Organics. Isomannide was purchased from Sigma-Aldrich. Other reagents were purchased at the most economical grade. All chemicals were used as received, without purification. HPLC grade toluene was used without prior drying. Dry *N*,*N*-dimethylformamide (DMF) was obtained by passing ACS grade DMF through a Glass Contour solvent purification system. The pressures for vacuum distillations were measured during the collection of the distillate. Yields of monomeric materials refer to distilled and spectroscopically (^{1}H NMR) homogeneous samples. Thin-layer chromatography (TLC) was performed on Grace Davison Davisil silica TLC plates using UV light and common stains for visualization. NMR spectra were calibrated using residual undeuterated

solvent as an internal reference. Apparent couplings were determined for multiplets that could be deconvoluted visually. Gel permeation chromatography (GPC) was performed on filtered samples (0.45 micron PTFE filters) dissolved in DMF containing 10 mM LiBr with a flow rate of 0.8 mL min^{-1} through two PSS Gram Analytical GPC columns in series (8 × 300 mm, 10 micron, 100 Å porosity for one column, 1000 Å porosity for other column) at 50 °C using refractive index (RI) for detection, and calibrated to polystyrene. Differential scanning calorimetry (DSC) was performed on ca. 5 mg samples under a helium atmosphere from –50 to 175 °C at a heat rate of 10 °C min^{-1}; samples were then cooled back to –50 °C at a rate of 10 °C min^{-1} for a second heat. Thermogravimetric analysis (TGA) was performed on ca. 5 mg samples exposed to ambient air from 50 to 650 °C at a heat rate of 20 °C min^{-1}.

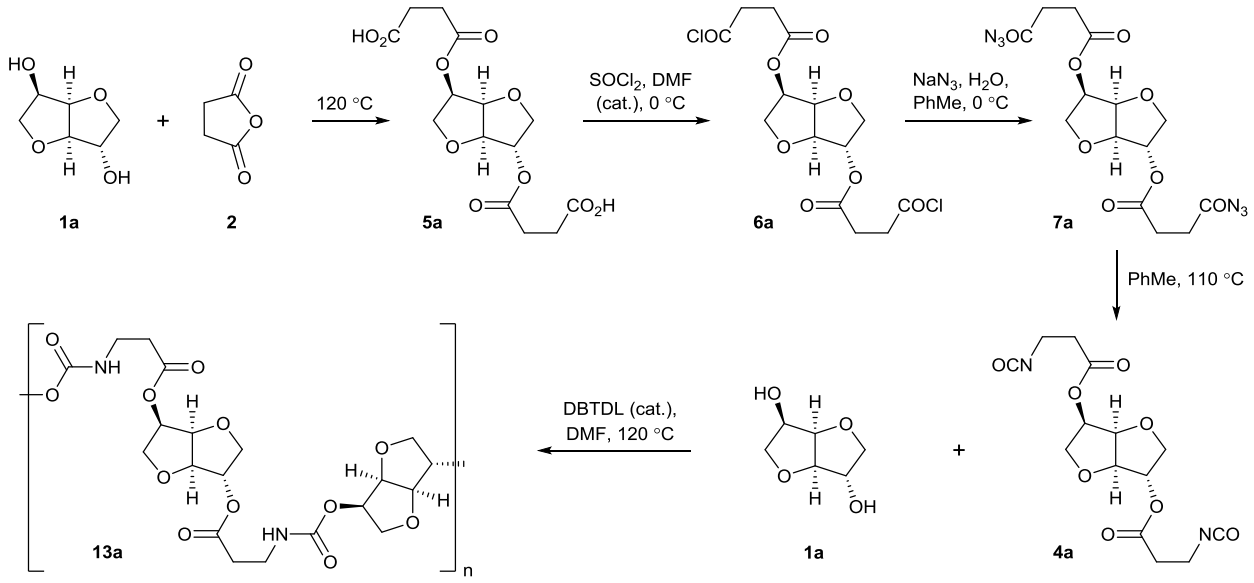

Scheme 1. Synthesis of isosorbide-based diisocyanate **4a** and polyurethane **13a**.

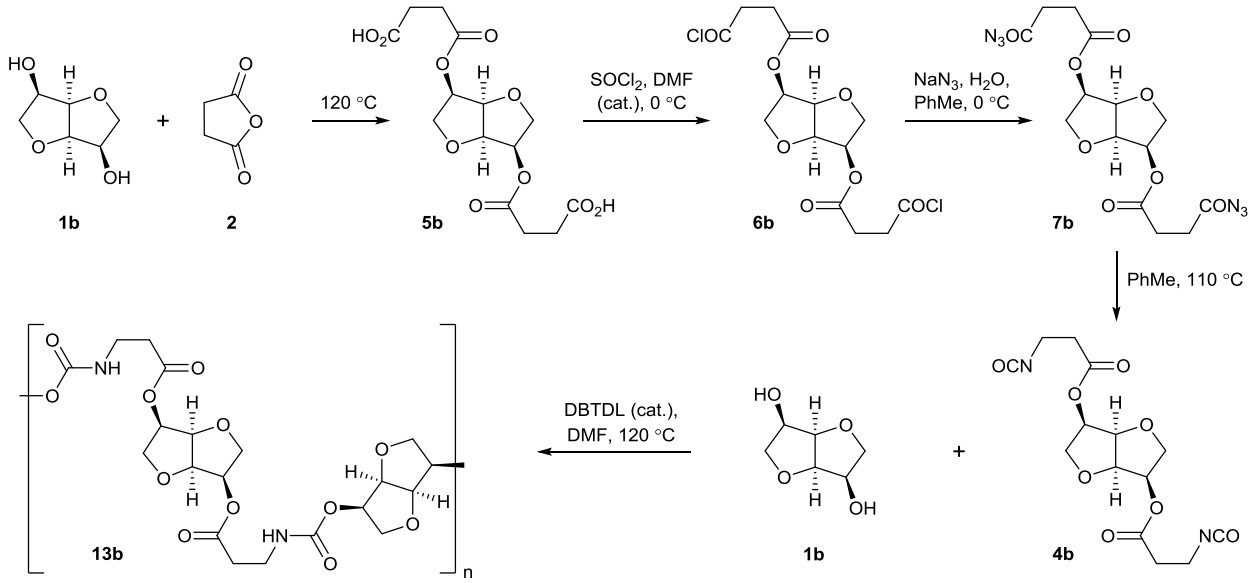

Scheme 2. Synthesis of isomannide-based diisocyanate **4b** and polyurethane **13b**.

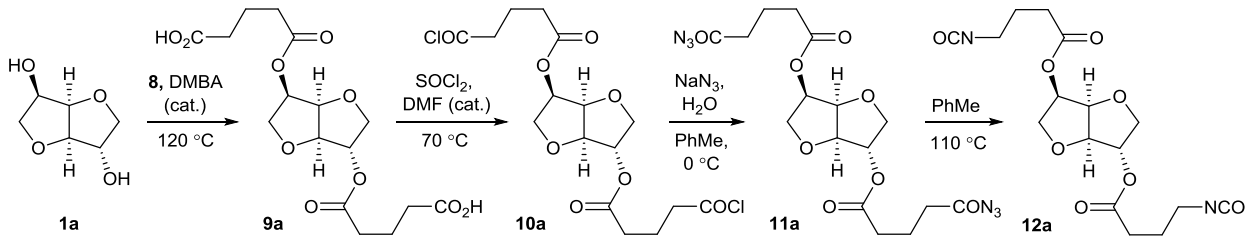

Scheme 3. Synthesis of isosorbide-based diisocyanate **12a**.

Diacid 5a. A mixture of isosorbide (**1a**, 7.31 g, 50 mmol) and succinic anhydride (**2**, 11.51 g, 115 mmol, 2.3 equiv) was heated at 120 °C for 24 h to give diacid **5a** as a viscous orange oil. Note: Heating of the entire reaction vessel was necessary in order to minimize evaporative loss of succinic anhydride (**2**). Vacuum sublimation of succinic anhydride (**2**) from the crude material gave a sample of diacid **5a** for analysis. **5a**: R_f = 0.43 (silica, EtOAc); $[\alpha]_D^{23}$ = +90.9 $cm^3\ g^{-1}\ dm^{-1}$ (*c* = 1.00 g cm^{-3}, $CHCl_3$); IR (thin film): ν_{max} = 1739, 1716 cm^{-1}; ^1H NMR (400 MHz, $CDCl_3$): δ = 10.51 (br, 2H), 5.21 (s, 1H), 5.18 (q, *J* = 5.4 Hz, 1H), 4.83 (t, *J* = 5.1 Hz, 1H), 4.47 (d, *J* = 4.6, 1H), 4.00 – 3.94 (m, 2H), 3.93 (dd, *J* = 10.0, 5.9 Hz, 1H), 3.81 (dd, *J* = 10.0, 5.1 Hz, 1H), 2.69 (s, 4H), 2.68 – 2.60 (m, 4H) ppm; ^{13}C NMR (100 MHz, $CDCl_3$): δ = 178.01, 177.95, 171.71, 171.33, 85.88, 80.87, 78.37, 74.42, 73.33, 70.54, 29.04, 29.01, 28.98, 28.76 ppm; HRMS (ESI-QTOF) calcd for $C_{14}H_{17}O_{10}^-$ [M – H^+]: 345.0822, found: 345.0827.

Diacid 5b was synthesized following the above procedure. **5b**: R_f = 0.38 (silica, EtOAc); $[\alpha]_D^{23}$ = +116.9 $cm^3\ g^{-1}\ dm^{-1}$ (*c* = 1.00 g cm^{-3}, $CHCl_3$); IR (thin film): ν_{max} = 1741, 1717 cm^{-1}; ^1H NMR (400 MHz, $CDCl_3$): δ = 8.29 (br, 2H), 5.10 (d, *J* = 5.8 Hz, 2H), 4.68 (dd, *J* = 9.3, 3.8 Hz, 2H), 4.01 (dd, *J* = 9.6, 6.1 Hz, 2H), 3.79 (dd, *J* = 9.6, 6.3 Hz, 2H), 2.77 – 2.70 (m, 4H), 2.70 – 2.65 (m, 4H) ppm; ^{13}C NMR (100 MHz, $CDCl_3$): δ = 178.20, 171.37, 80.58, 73.98, 70.72, 29.40, 29.25 ppm; HRMS (ESI-QTOF) calcd for $C_{14}H_{17}O_{10}^-$ [M – H^+]: 345.0822, found: 345.0821.

Diacid 9a synthesis was previously reported.[1]

[1] M.D. Zenner, S. A. Madbouly, J. S. Chen, M. R. Kessler, *ChemSusChem*, **2015**, 10.1002/cssc.201402667

Diacid chloride 6a. To a solution of crude diacid **5a** (50 mmol) in thionyl chloride (50 mL, 690 mmol, 13.8 equiv) at 0 °C was added DMF (39 μL, 0.5 mmol, 0.01 equiv). Vigorous gas evolution was observed for the first 30 min. After another 1.5 h at 0 °C, the reaction mixture was concentrated under reduced pressure to recover excess thionyl chloride and give diacid chloride **6a** as an orange oil. Note: The gasses evolved during the reaction were bubbled into water to minimize corrosion of nearby objects. A sample of diacid chloride **6a** for analysis was obtained by the reaction of a purified sample of diacid **5a**. **6a**: R_f = 0.35 (silica, EtOAc); $[\alpha]_D^{23}$ = +49.0 cm^3 g^{-1} dm^{-1} (*c* = 1.00 g cm^{-3}, $CHCl_3$); IR (thin film): ν_{max} = 1794, 1747 cm^{-1}; ^1H NMR (400 MHz, $CDCl_3$): δ = 5.22 (d, *J* = 2.8 Hz, 1H), 5.17 (q, *J* = 5.4 Hz, 1H), 4.84 (t, *J* = 5.1 Hz, 1H), 4.46 (d, *J* = 4.7 Hz, 1H), 4.00 – 3.94 (m, 2H), 3.93 (dd, *J* = 10.0, 5.9, 1H), 3.83 (dd, *J* = 10.1, 4.9 Hz, 1H), 3.32 – 3.14 (m, 4H), 2.74 (td, *J* = 6.6, 2.9 Hz, 2H), 2.69 (t, *J* = 6.4 Hz, 2H) ppm; ^{13}C NMR (100 MHz, $CDCl_3$): δ = 173.11, 173.02, 170.45, 170.15, 85.89, 80.83, 78.68, 74.70, 73.28, 70.58, 41.76, 41.68, 29.40, 29.14 ppm; HRMS (ESI-QTOF): does not ionize.

Diacid chloride 6b was synthesized following the above procedure.

Diacid chloride 10a. To crude diacid **9a** (18.7 g, 50 mmol, 1 equiv.) at 70 °C was added DMF (39 μL, 0.5 mmol, 0.01 equiv). Thionyl chloride (7.3 mL, 100 mmol, 2 equiv.) was added dropwise. Vigorous gas evolution was observed. Reaction progression was monitored via bubble evolution. The gasses evolved during the reaction were bubbled into water to minimize corrosion of nearby objects.

Diacyl azide 7a. A solution of crude diacid chloride **6a** (50 mmol) in toluene (125 mL) was added dropwise over the course of 40 min to an aqueous solution of sodium azide (16.25 g, 250 mmol, 5.0 equiv) at 0 °C. The rate of addition was controlled so that the internal temperature of the reaction did not exceed 3 °C. After an additional 20 min at 0 °C, the reaction mixture was partitioned into two phases, and the organic phase was washed with 1 × 100 mL 10 % potassium carbonate solution, 1 × 100 mL water, and 2 × 100 mL brine, then dried over Na_2SO_4. Diacyl azide **7a** was not isolated due to its instability in concentrated form. **7a**: R_f = 0.60 (silica, EtOAc); IR (thin film): ν_{max} = 2138, 1747, 1721 cm^{-1}; ^1H NMR (400 MHz, $CDCl_3$ + ca. 5 % PhMe + trace EtOAc): δ = 5.23 (br, 1H), 5.16 (q, *J* = 5.5 Hz, 1H), 4.83 (t, *J* = 4.9 Hz, 1H), 4.47 (d, *J* = 4.7 Hz, 1H), 4.06 – 4.01 (m, 2H), 3.98 (dd, *J* = 10.0, 5.9 Hz, 1H), 3.82 (dd, *J* = 10.1, 5.1 Hz, 1H), 2.79 – 2.59 (m, 8H) ppm; HRMS (ESI-QTOF): does not ionize.

Diacyl azide 7b was synthesized following the above procedure.

Diacyl azide 11a A solution of crude diacid chloride **10a** (50 mmol) in toluene (50 mL) was added dropwise over the course of 40 min to an aqueous solution of sodium azide (8.13 g, 125 mmol, 2.5 equiv) and tetrabutylammonium bromide (0.32g, 0.1 mmol, 0.002 equiv.) at 0 °C. The rate of addition was controlled so that the internal temperature of the reaction did not exceed 10 °C. After an additional 15 min at 0 °C, the reaction mixture was partitioned into two phases, and the organic phase was washed with 1 × 50 mL 10 % potassium carbonate solution, 1 × 50 mL water, and 2 × 50 mL brine, then dried over $MgSO_4$.

Diisocyanate 4a. A toluene solution of diacyl azide **7a** (50 mmol, toluene from previous reaction step) was added dropwise over the course of 45 min to 10 mL of toluene at 110 °C. The rate of addition was controlled so that steady reflux and gas formation were observed. After an additional 15 min at 110 °C, the reaction mixture was concentrated under reduced pressure to give crude diisocyanate **4a** as a dark orange oil. Diisocyanate **4a** was distilled (186 – 189 °C, 230 mTorr) to give a light orange oil [10.19 g, 60 % overall yield from isosorbide (**1a**)]. **4a**: R_f = 0.70 (silica, EtOAc); $[\alpha]_D^{23}$ = +69.0 $cm^3\ g^{-1}\ dm^{-1}$ (*c* = 1.00 g cm^{-3}, $CHCl_3$); IR (thin film): ν_{max} = 2274, 1747 cm^{-1}; ^1H NMR (600 MHz, $CDCl_3$): δ = 5.26 (d, *J* = 2.8 Hz, 1H), 5.21 (q, *J* = 5.5 Hz, 1H), 4.87 (t, *J* = 5.1 Hz, 1H), 4.49 (d, *J* = 4.7 Hz, 1H), 4.01 – 3.96 (m, 2H), 3.95 (dd, *J* = 10.0, 5.9, 1H), 3.85 (dd, *J* = 10.1, 5.0 Hz, 1H), 3.66 – 3.55 (m, 4H), 2.67 (t, *J* = 6.4 Hz, 2H), 2.62 (t, *J* = 6.3 Hz, 2H) ppm; ^{13}C NMR (150 MHz, $CDCl_3$): δ = 170.18, 169.90, 123.40, 123.30, 85.97, 80.81, 78.57, 74.57, 73.35, 70.55, 38.67, 38.65, 35.69, 35.46 ppm; HRMS (ESI-QTOF) calcd for $C_{14}H_{17}N_2O_8^+$ [M + H^+]: 341.0985, found: 341.0979.

Diisocyanate 4b was synthesized following the above procedure. Diisocyanate **4b** was distilled (197 – 199 °C, 230 mTorr) to give a light yellow oil [8.91 g, 52 % overall yield from isomannide (**1b**)]. **4b**: R_f = 0.81 (silica, EtOAc); $[\alpha]_D^{23}$ = +155.9 $cm^3\ g^{-1}\ dm^{-1}$ (*c* = 1.00 g cm^{-3}, $CHCl_3$); IR (thin film): ν_{max} = 2278, 1738 cm^{-1}; ^1H NMR (400 MHz, $CDCl_3$): δ = 5.18 – 5.11 (m, 2H), 4.74 – 4.71 (m, 2H), 4.06 (dd, *J* = 9.5, 6.4 Hz, 2H), 3.83 (dd, *J* = 9.5, 6.7 Hz, 2H), 3.62 (td, *J* = 6.3, 3.1 Hz, 4H), 2.68 (t, *J* = 6.3 Hz, 4H) ppm; ^{13}C NMR (100 MHz, $CDCl_3$): δ = 170.20, 123.27, 80.39, 74.27, 70.47, 38.67, 35.43 ppm; HRMS (ESI-QTOF) calcd for $C_{14}H_{16}N_2O_8Na^+$ [M + Na^+]: 363.0804, found: 363.0792.

Diisocyanate 12a was synthesized following the above procedure. Diisocyanate **9a** was distilled (229 – 230 °C, 600 mTorr) to give a light yellow oil [5.73 g, 27 % overall yield from isosorbide (**1a**)] **9a**: R_f = 0.79 (silica, EtOAc); $[\alpha]_D^{23}$ = +81.93 cm^3 g^{-1} dm^{-1} (*c* = 1.00 g cm^{-3}, $CHCl_3$); IR (thin film): ν_{max} = 2279, 1739 cm^{-1}; ^{1}H NMR (600 MHz, $CDCl_3$): δ = 5.20 (br, 1H), 5.16 (q, *J* = 5.5 Hz, 1H), 4.84 (t, *J* = 5.0 Hz, 1H), 4.47 (d, *J* = 4.4 Hz, 1H), 3.96 (d, *J* = 2.0 Hz, 2H), 3.93 (dd, *J* = 10.0, 6.0 Hz, 1H), 3.82 (dd, *J* = 9.8, 5.0 Hz, 1H), 3.42 (t, *J* = 6.4 Hz, 2H), 3.40 (t, *J* = 6.4 Hz, 2H), 2.49 (dt, *J* = 7.5, 2.4 Hz, 2H), 2.44 (t, *J* = 7.3 Hz, 2H), 1.98 – 1.86 (m, 4H) ppm; ^{13}C NMR (150 MHz, $CDCl_3$): δ = 172.05, 171.74, 122.26, 122.25, 86.03, 80.82, 78.29, 74.23, 73.42, 70.55, 42.25, 42.18, 31.01, 30.76, 26.32, 26.20 ppm; HRMS (ESI-QTOF) calcd for $C_{14}H_{16}N_2O_8Na^+$ [M + H^+]: 369.1292, found: 369.1293.

Polyurethane 13a. A mixture of diisocyanate **4a** (3.97 g, 11.7 mmol), isosorbide (**1a**, 1.71 g, 11.7 mmol), DMF (6 mL), and dibutyltin dilaurate (6 μL, 0.01 mmol, 0.001 equiv) was heated at 120 °C for 48 h. The reaction mixture was poured into methanol (50 mL) to give a white precipitate that was rinsed three times with methanol. Polyurethane **10a** was dried at 23 °C for 12 h and 50 °C under reduced pressure for 12 h to give an opaque light-brown foam (5.14 g, 90 % yield). **10a**: $[\alpha]_D^{23}$ = +37.0 cm^3 g^{-1} dm^{-1} (*c* = 1.00 g cm^{-3}, DMF); IR (thin film): ν_{max} = 3339, 1726, 1532, 1249 cm^{-1}; ^{1}H NMR (600 MHz, DMSO-d_6): δ = 7.47 – 7.33 (m, 2H), 5.09 (q, *J* = 4.9 Hz, 1H), 5.04 (s, 1H), 4.97 (q, *J* = 5.0 Hz, 1H), 4.91 (s, 1H), 4.74 (t, *J* = 5.0 Hz, 1H), 4.66 (t, *J* = 4.8 Hz, 1H), 4.41 (d, *J* = 4.6 Hz, 1H), 4.36 (d, *J* = 3.6 Hz, 1H), 3.89 – 3.77 (m, 6H), 3.75 (dd, *J* = 9.8, 3.6 Hz), 3.62 (*J* = 9.4, 4.9 Hz, 1H), 3.27 – 3.16 (m, 4H), 2.53 – 2.43 (m, 4H) ppm; ^{13}C NMR (150 MHz, DMSO-d_6): δ = 170.48, 170.37, 155.37, 155.13, 85.54, 85.36, 80.71, 80.30, 77.70, 77.58, 73.80, 73.50, 72.77, 72.35, 70.08, 69.98, 36.38, 34.12, 34.04, 33.80, 33.76 ppm; GPC: M_w = 21,400 g / mol, M_n

= 14,300 g / mol, M_w / M_n = 1.50, DP_n = 29.4; TGA: T_d = 253 °C (5 % mass loss), 50 % mass loss at 304 °C.

Polyurethane 13b was synthesized following the above procedure, scaled to 1.90 g (5.59 mmol) of diisocyanate **4b**. Polyurethane **10b** was made as an opaque white solid (2.34 g, 84 % yield). **10b**: $[\alpha]_D^{23}$ = +212.0 cm^3 g^{-1} dm^{-1} (c = 1.00 g cm^{-3}, DMF); IR (thin film): ν_{max} = 3335, 1726, 1532, 1253 cm^{-1}; ^{1}H NMR (600 MHz, DMSO-d_6): 7.32 (t, J = 5.2 Hz, 2H), 5.00 (q, J = 5.5 Hz, 2H), 4.88 (q, J = 5.3 Hz, 2H), 4.60 (d, J = 4.3 Hz, 2H), 4.54 (d, J = 3.1 Hz, 2H), 3.92 (dd, J = 9.3, 6.3 Hz, 2H), 3.90 (dd, J = 8.9, 6.8 Hz, 2H) 3.65 (dd, J = 8.7, 6.8 Hz, 2H), 3.57 (t, J = 8.1 Hz, 2H), 3.28 – 3.16 (m, 4H), 2.58 – 2.40 (m, 4H) ppm; ^{13}C NMR (150 MHz, DMSO-d_6): δ = 170.46, 155.35, 80.16, 79.83, 73.52, 69.74, 69.70, 36.37, 33.74 ppm; GPC: M_w = 23,500 g / mol, M_n = 15,300 g / mol, M_w / M_n = 1.54, DP_n = 31.5; TGA: T_d = 265 °C (5 % mass loss), 50 % mass loss at 317 °C.

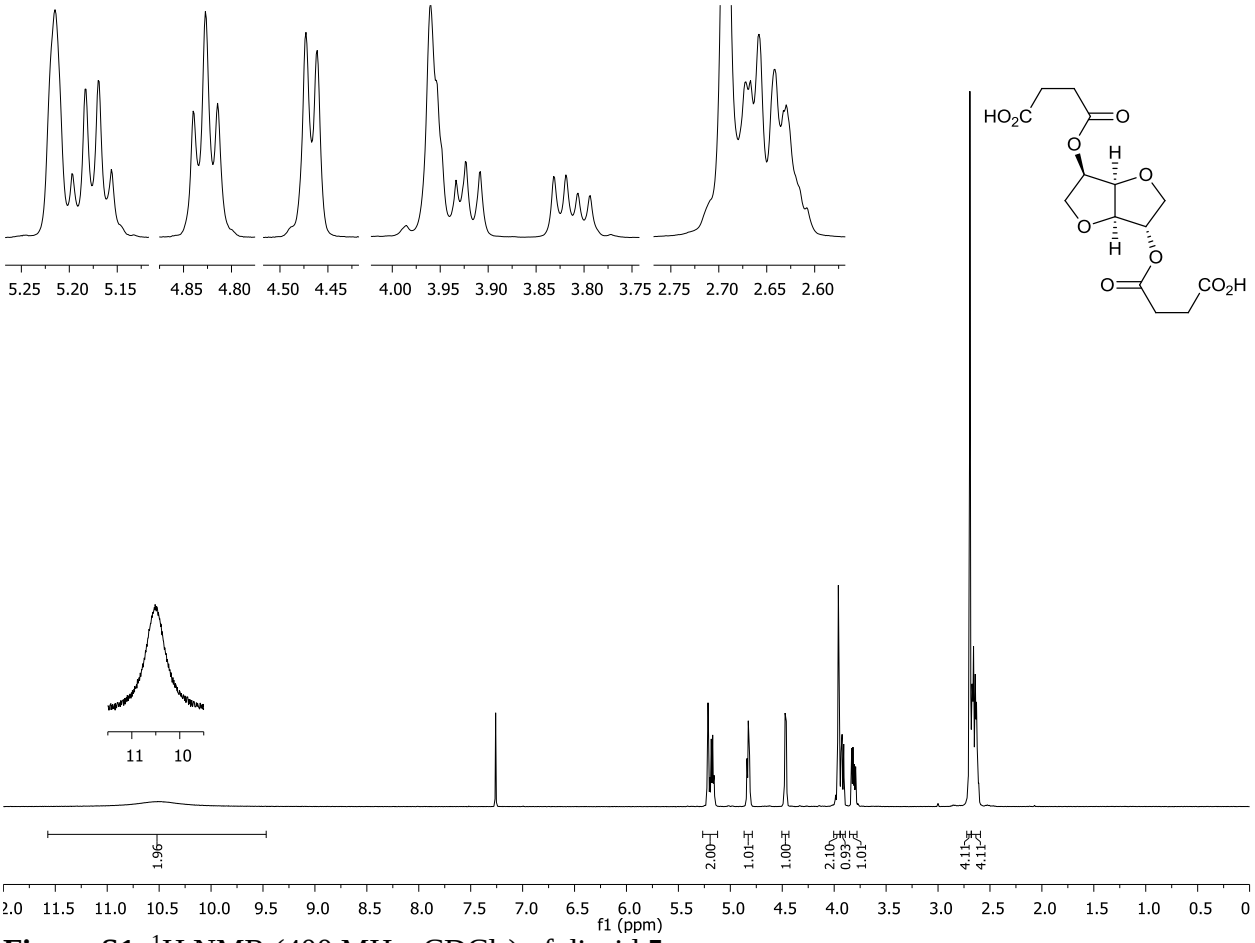

Figure S1. ^{1}H NMR (400 MHz, $CDCl_3$) of diacid **5a**

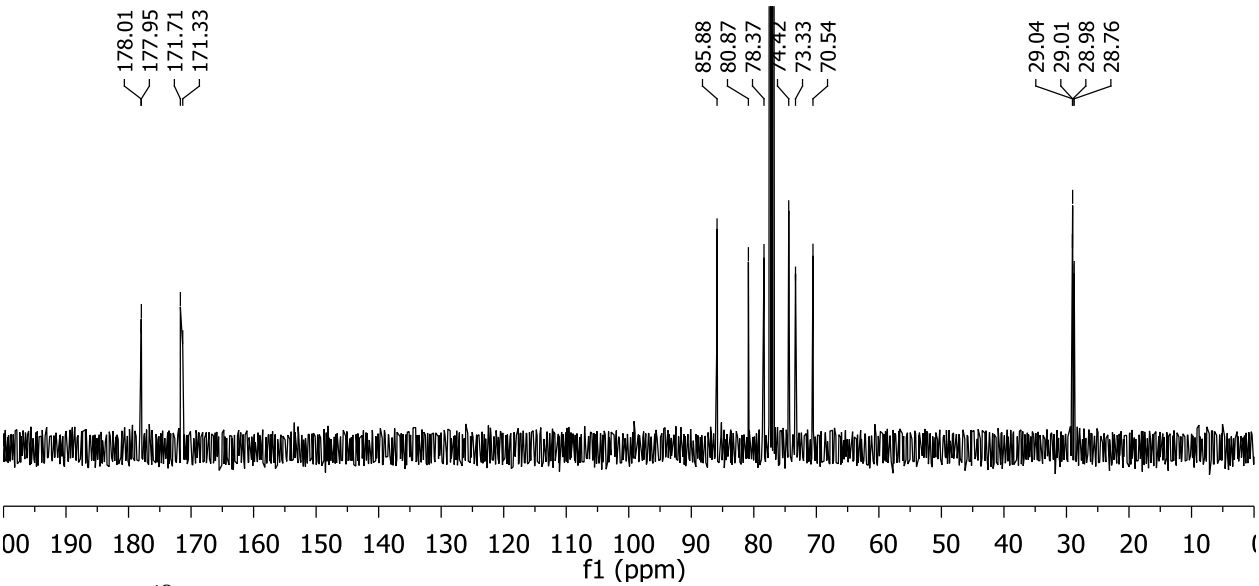

Figure S2. ^{13}C NMR (100 MHz, $CDCl_3$) of diacid **5a**

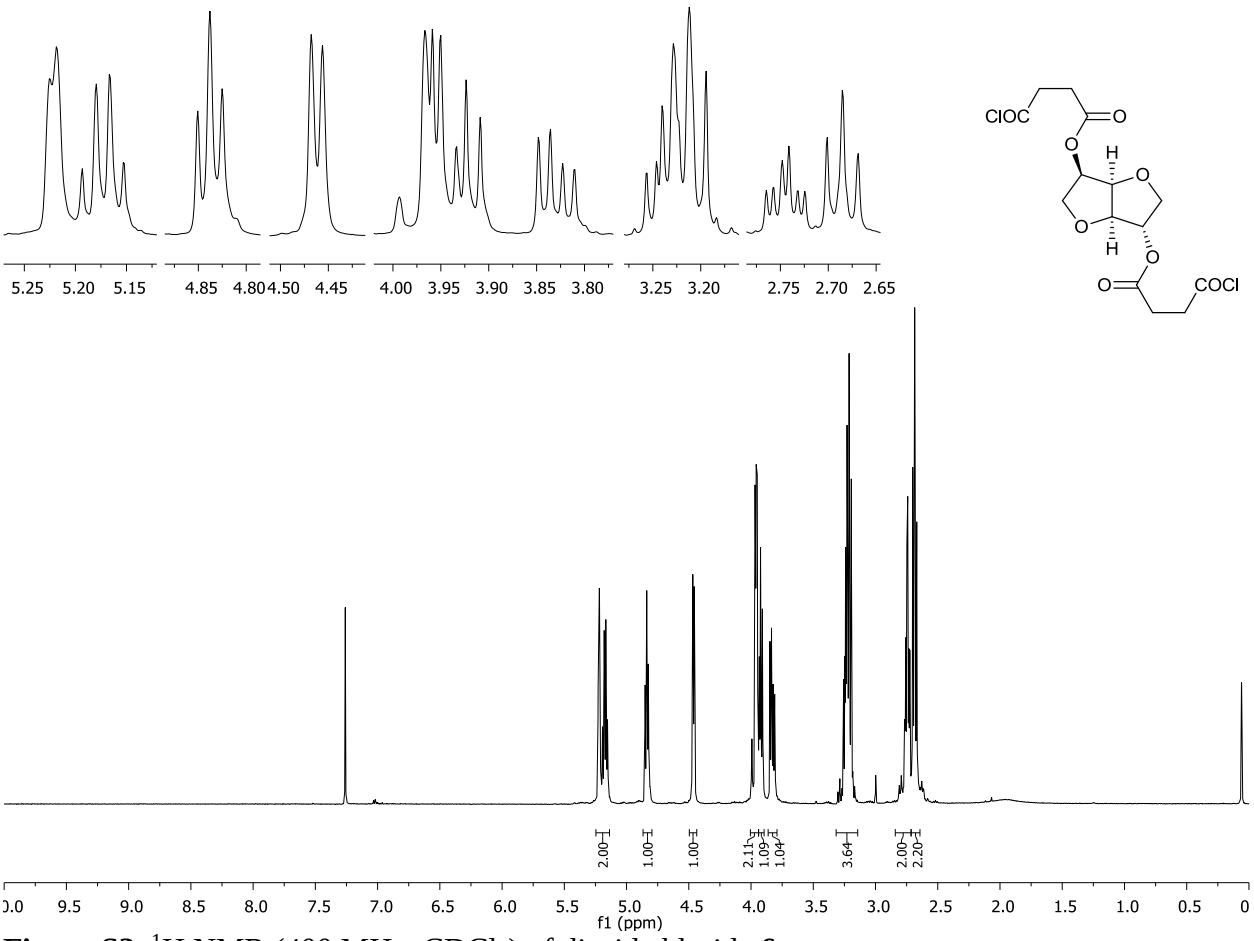

Figure S3. ^{1}H NMR (400 MHz, $CDCl_3$) of diacid chloride **6a**

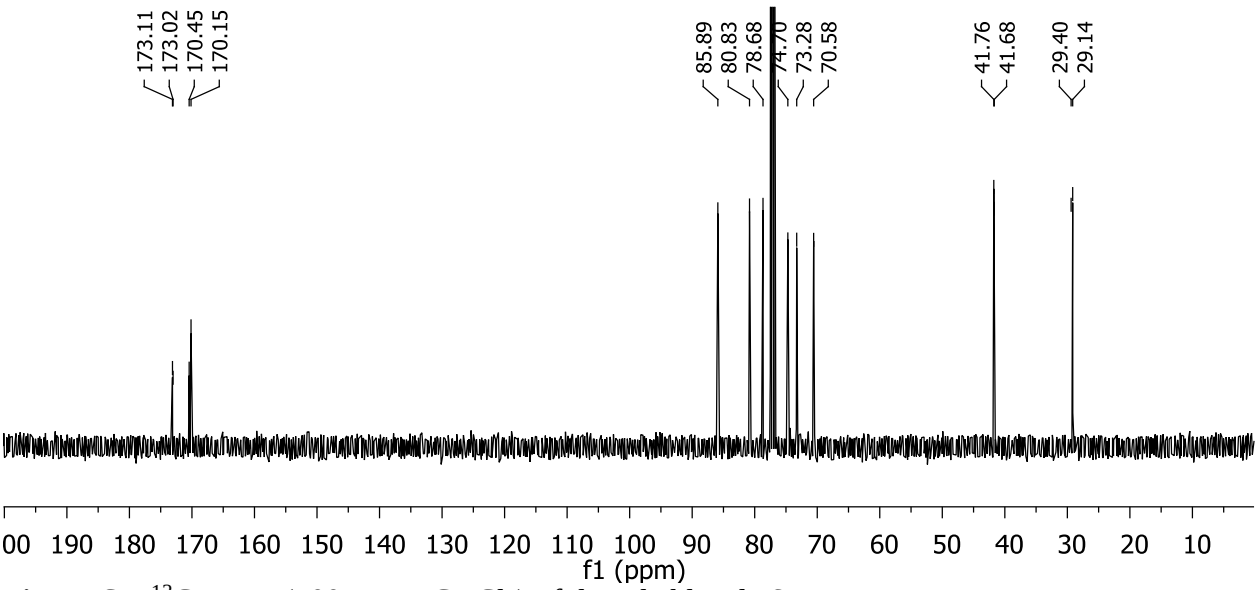

Figure S4. ^{13}C NMR (100 MHz, $CDCl_3$) of diacid chloride **6a**

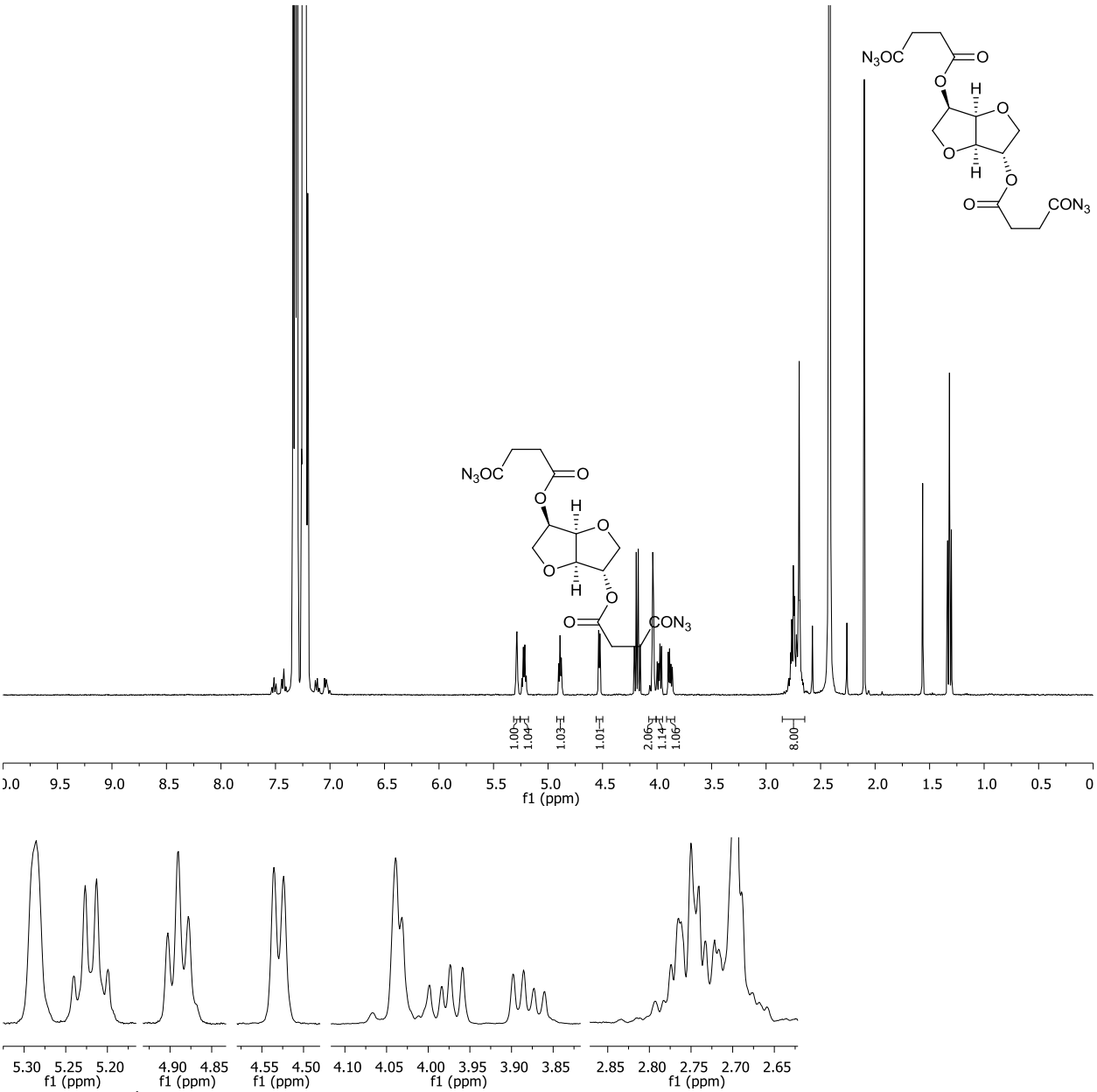

Figure S5. ^{1}H NMR (400 MHz, $CDCl_3$ + ca. 5 % PhMe + trace EtOAc) of diacyl azide **7a**
Note: EtOAc was added as an internal standard to allow yield determination.

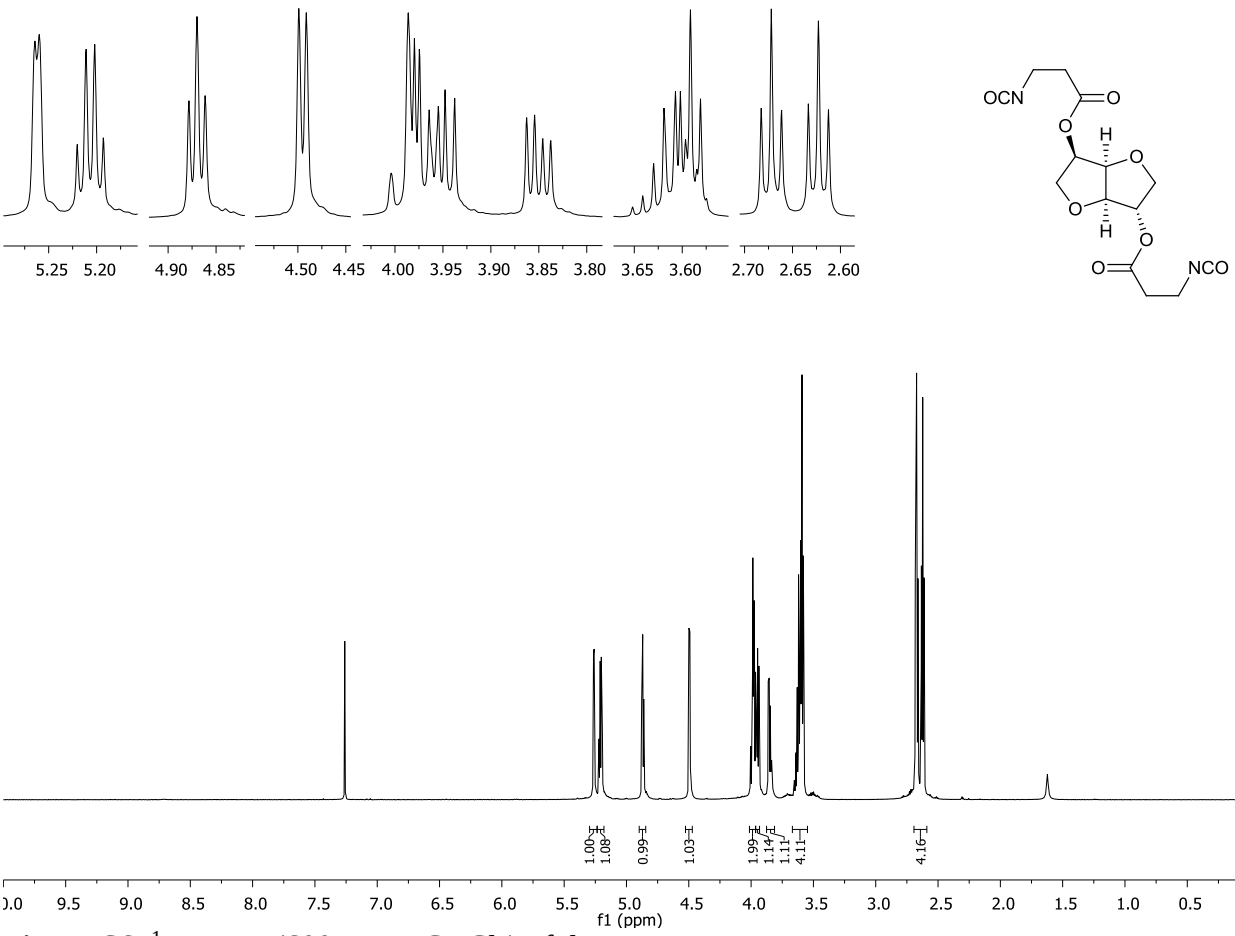

Figure S6. ^{1}H NMR (600 MHz, $CDCl_3$) of diisocyanate **4a**

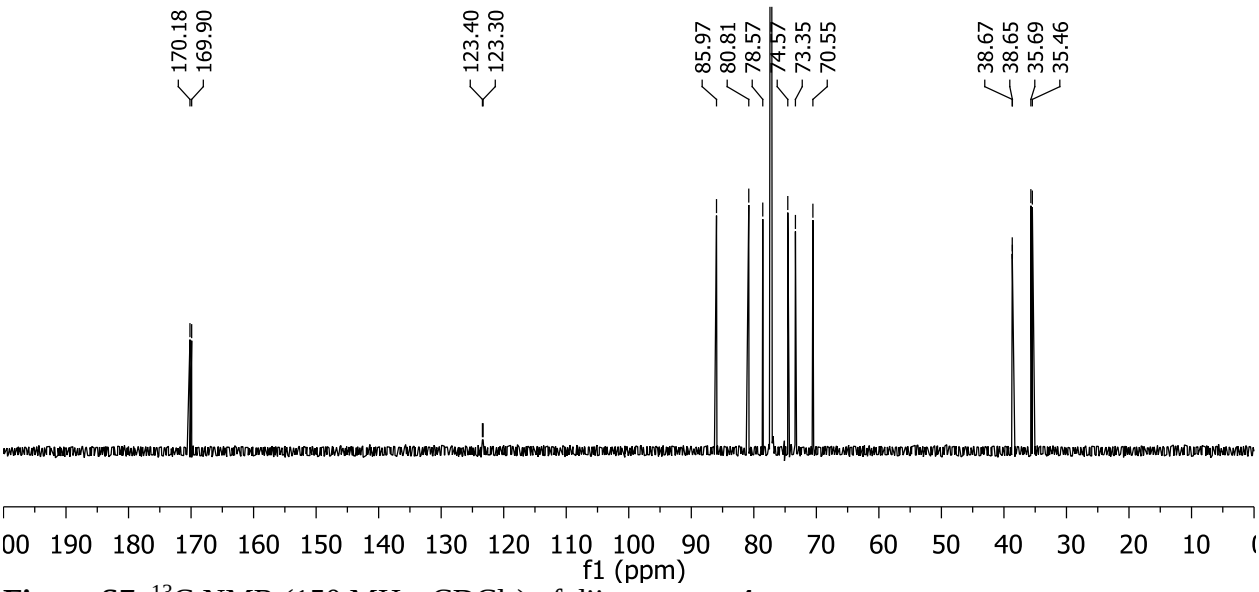

Figure S7. ^{13}C NMR (150 MHz, $CDCl_3$) of diisocyanate **4a**

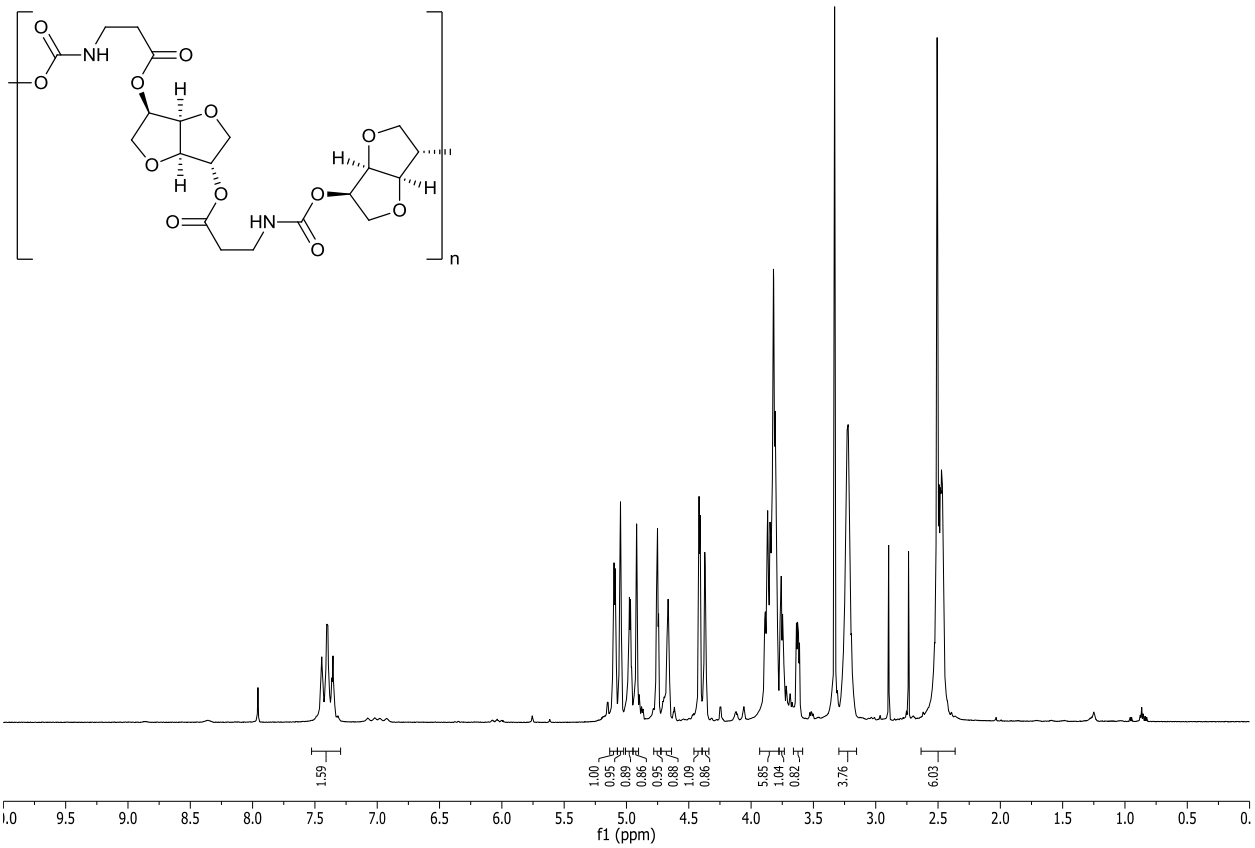

Figure S8. ^{1}H NMR (600 MHz, DMSO-d_6) of polyurethane **13a**

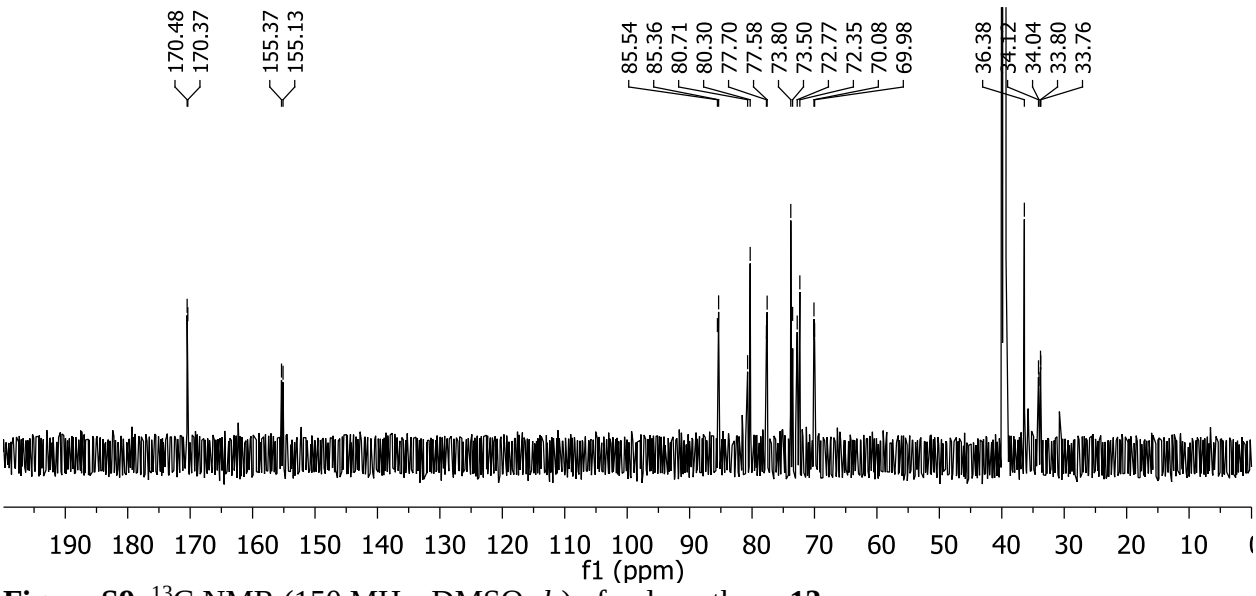

Figure S9. ^{13}C NMR (150 MHz, DMSO-d_6) of polyurethane **13a**

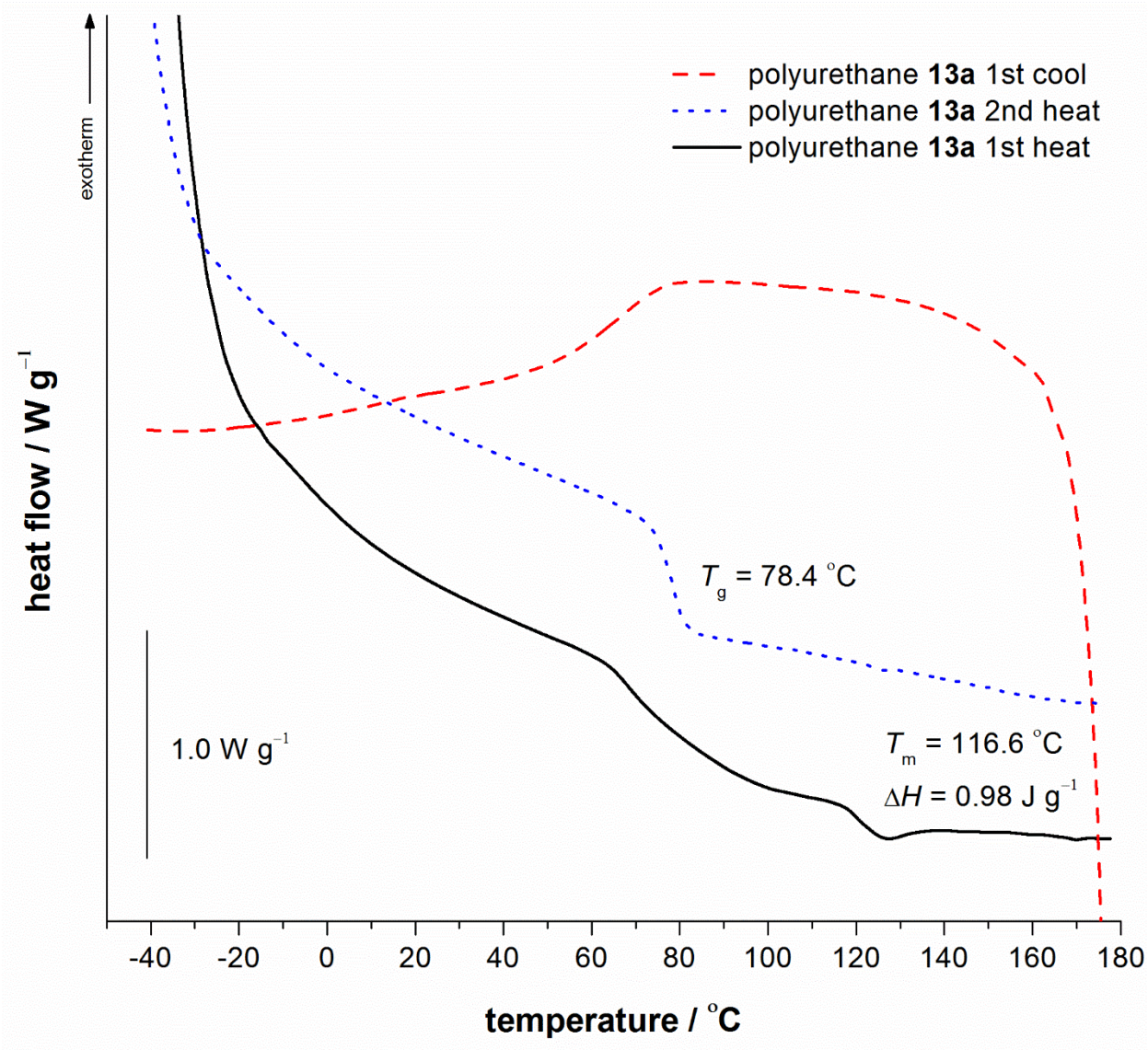

Figure S10. DSC curves (He, 10 °C min^{-1}) for polyurethane **13a**

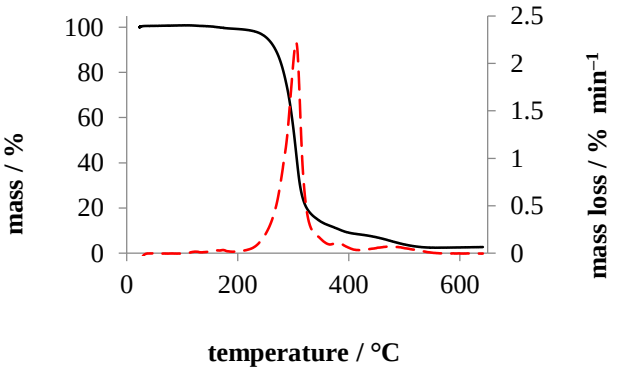

Figure S11. TGA curve (air, 20 °C min^{-1}) for polyurethane **13a**

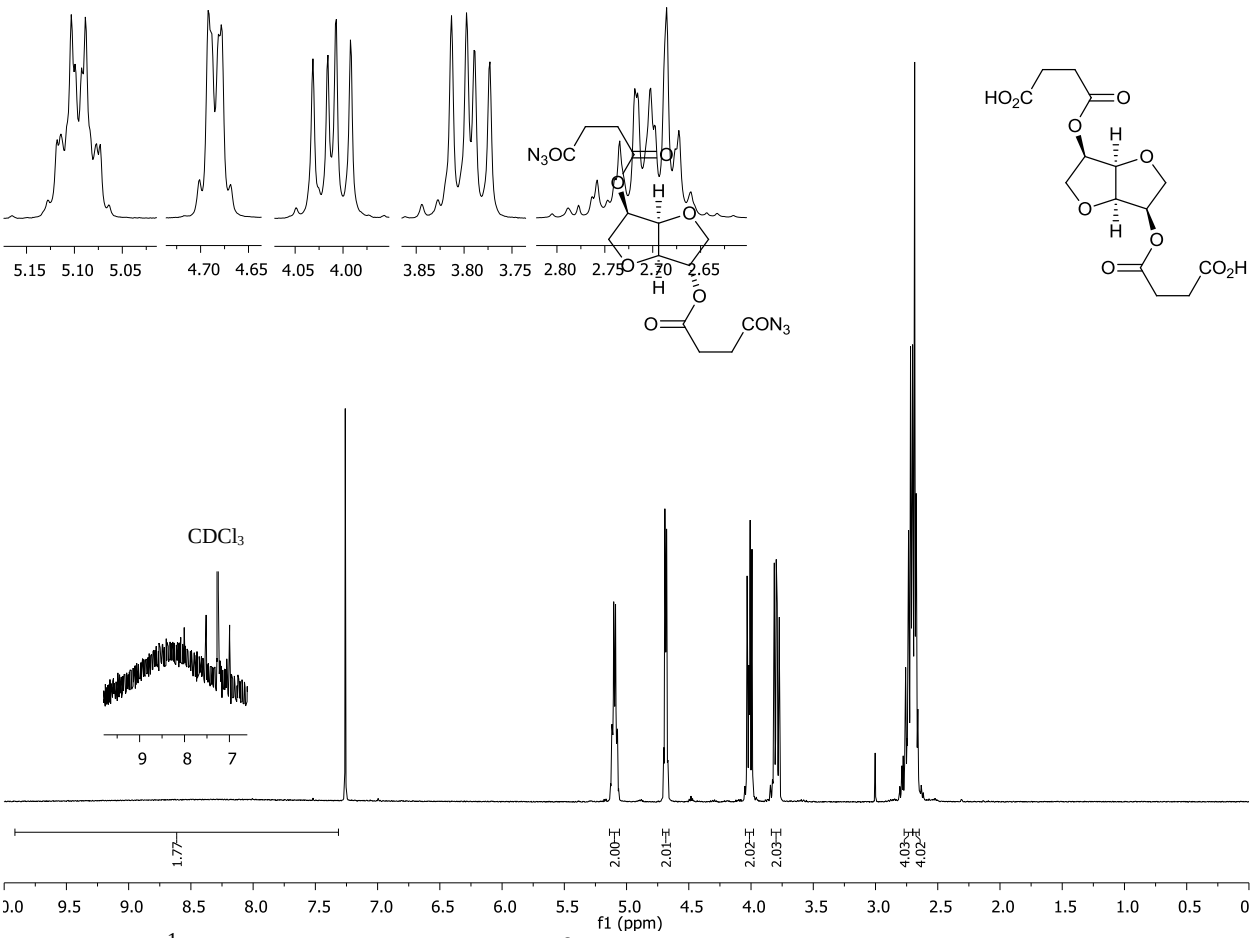

Figure S12. ^{1}H NMR (400 MHz, $CDCl_3$) of diacid **5b**

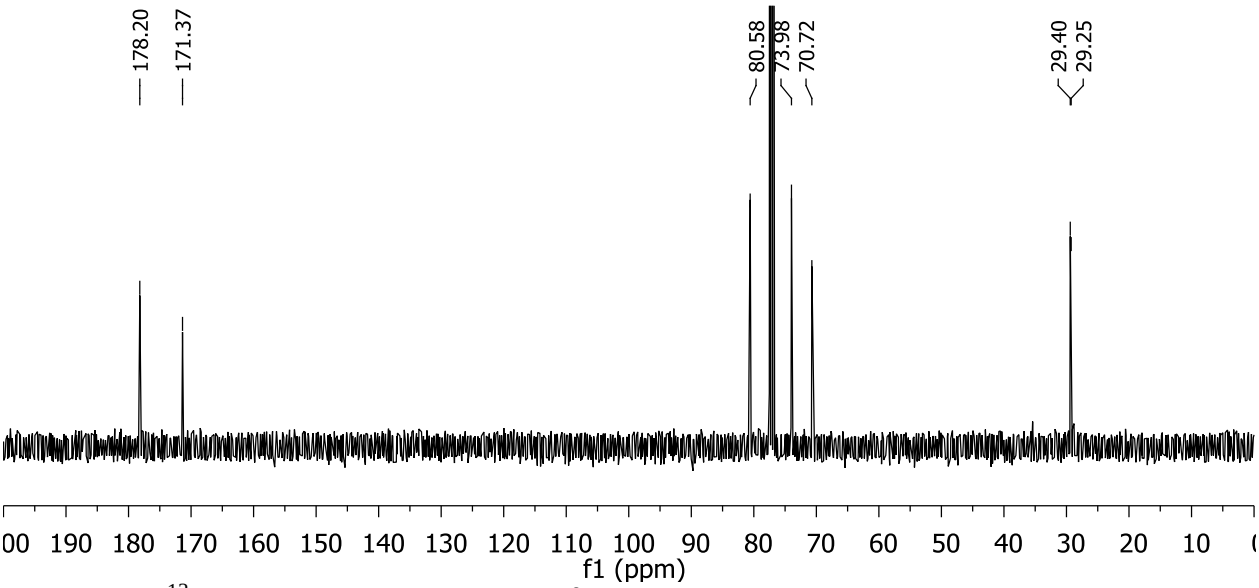

Figure S13. ^{13}C NMR (100 MHz, $CDCl_3$) of diacid **5b**

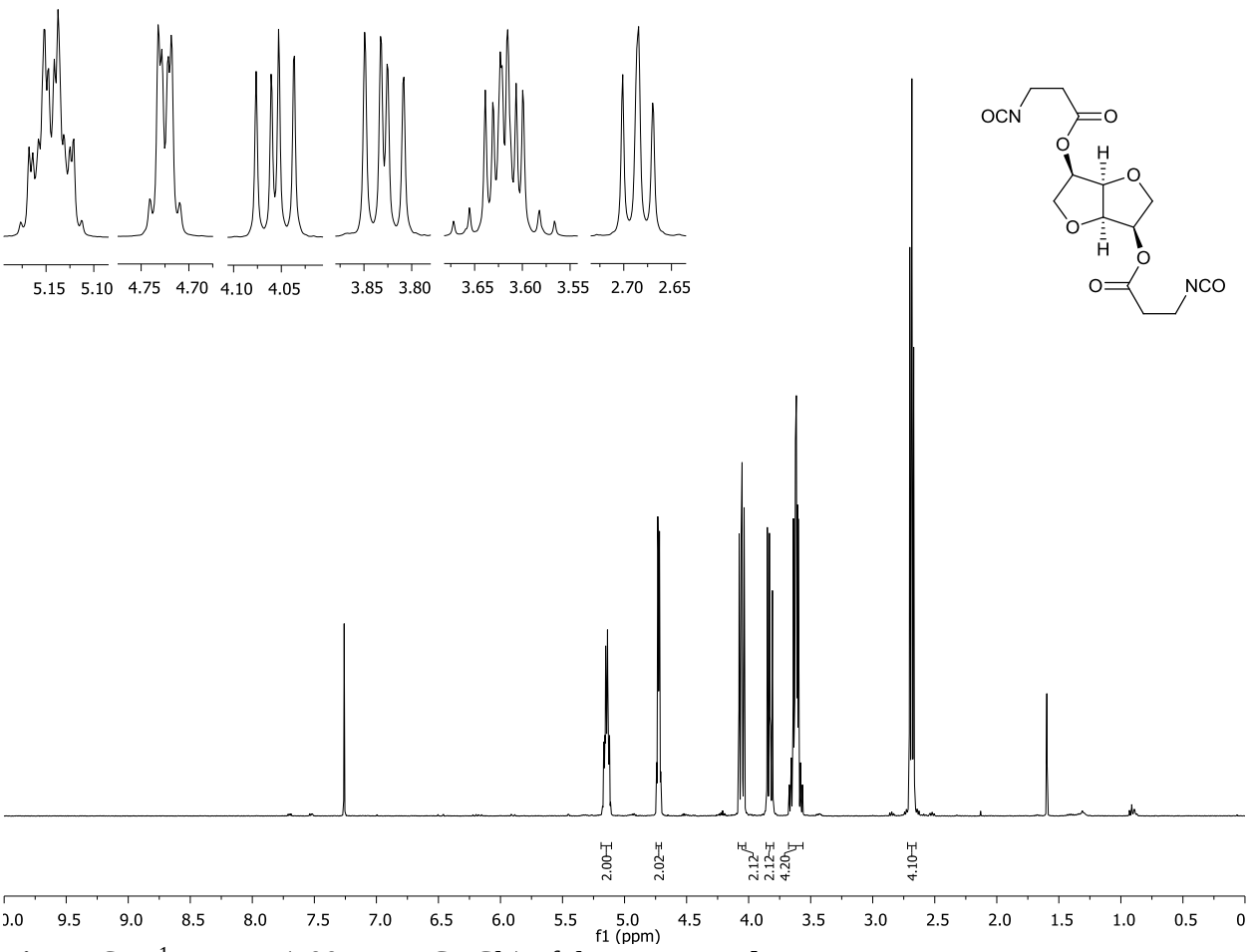

Figure S14. ^{1}H NMR (400 MHz, $CDCl_3$) of diisocyanate **4b**

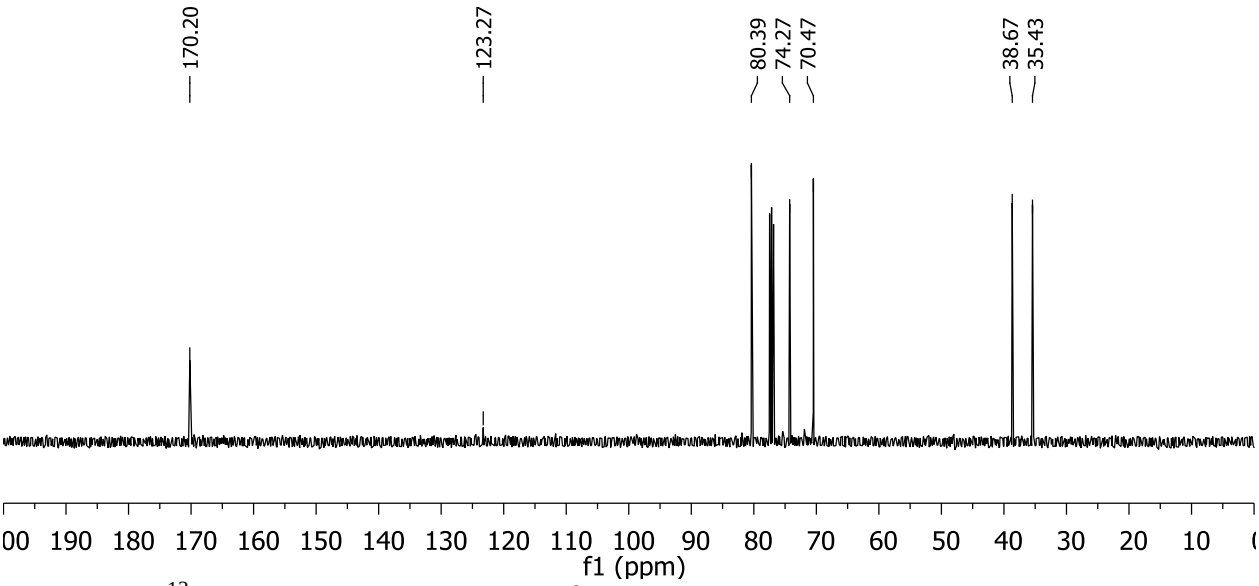

Figure S15. ^{13}C NMR (100 MHz, $CDCl_3$) of diisocyanate **4b**

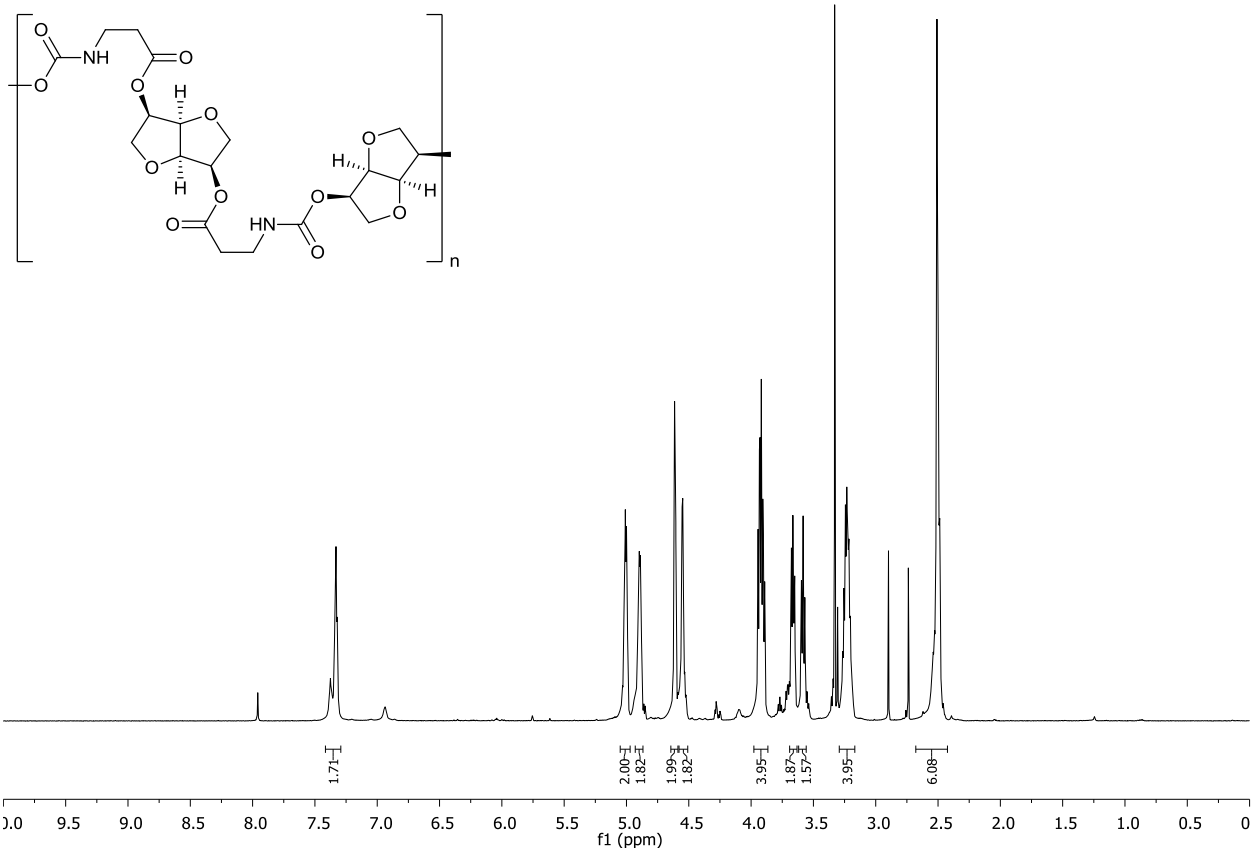

Figure S16. ^{1}H NMR (600 MHz, DMSO-d_6) of polyurethane **13b**

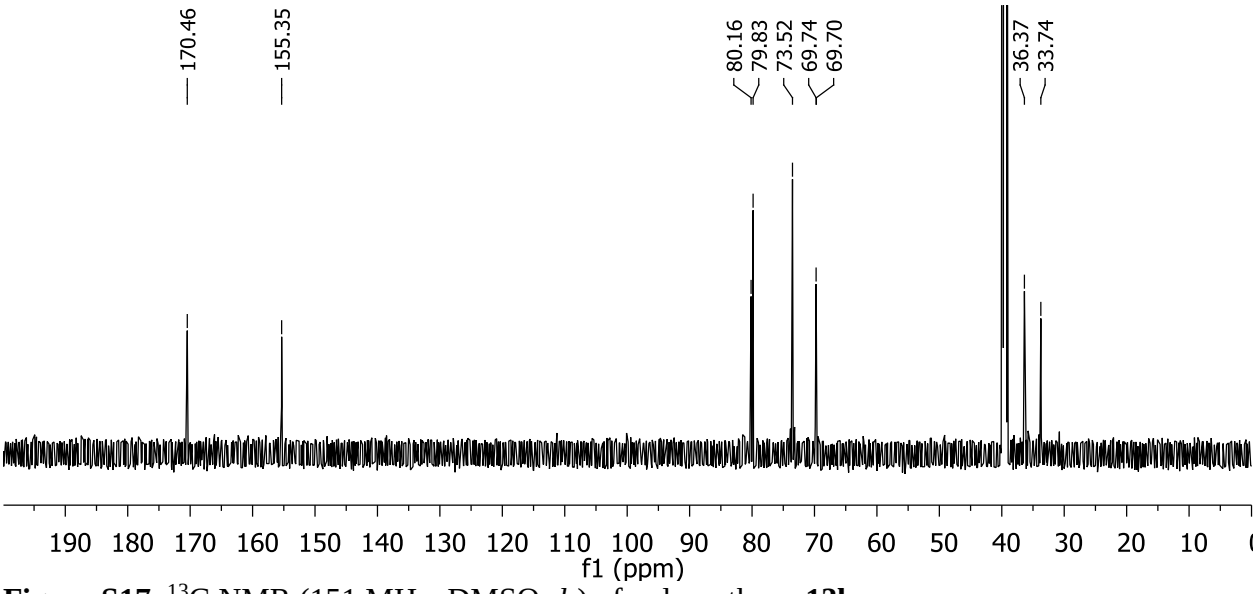

Figure S17. ^{13}C NMR (151 MHz, DMSO-d_6) of polyurethane **13b**

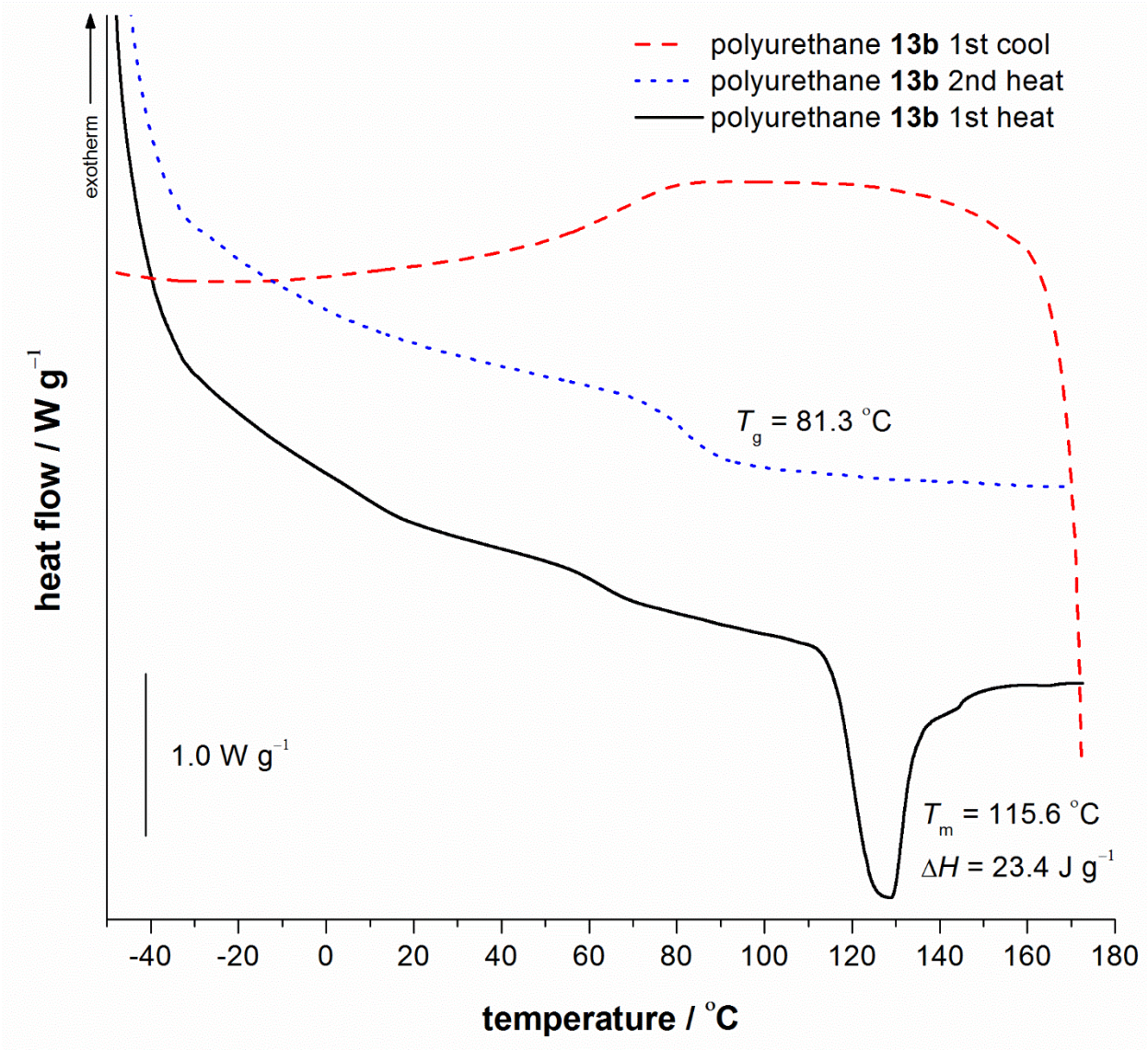

Figure S18. DSC curves (He, 10 °C min^{-1}) for polyurethane **13b**

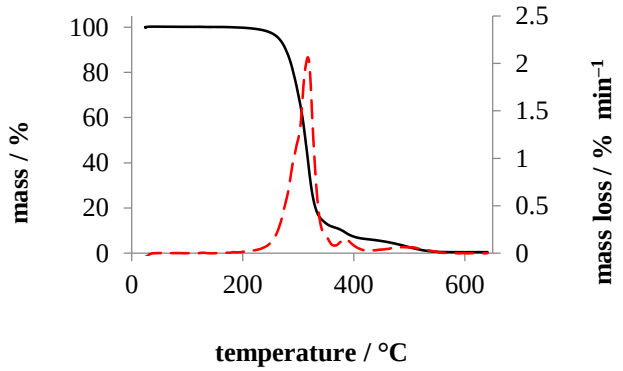

Figure S19. TGA curve (air, 20 °C min^{-1}) for polyurethane **13b**

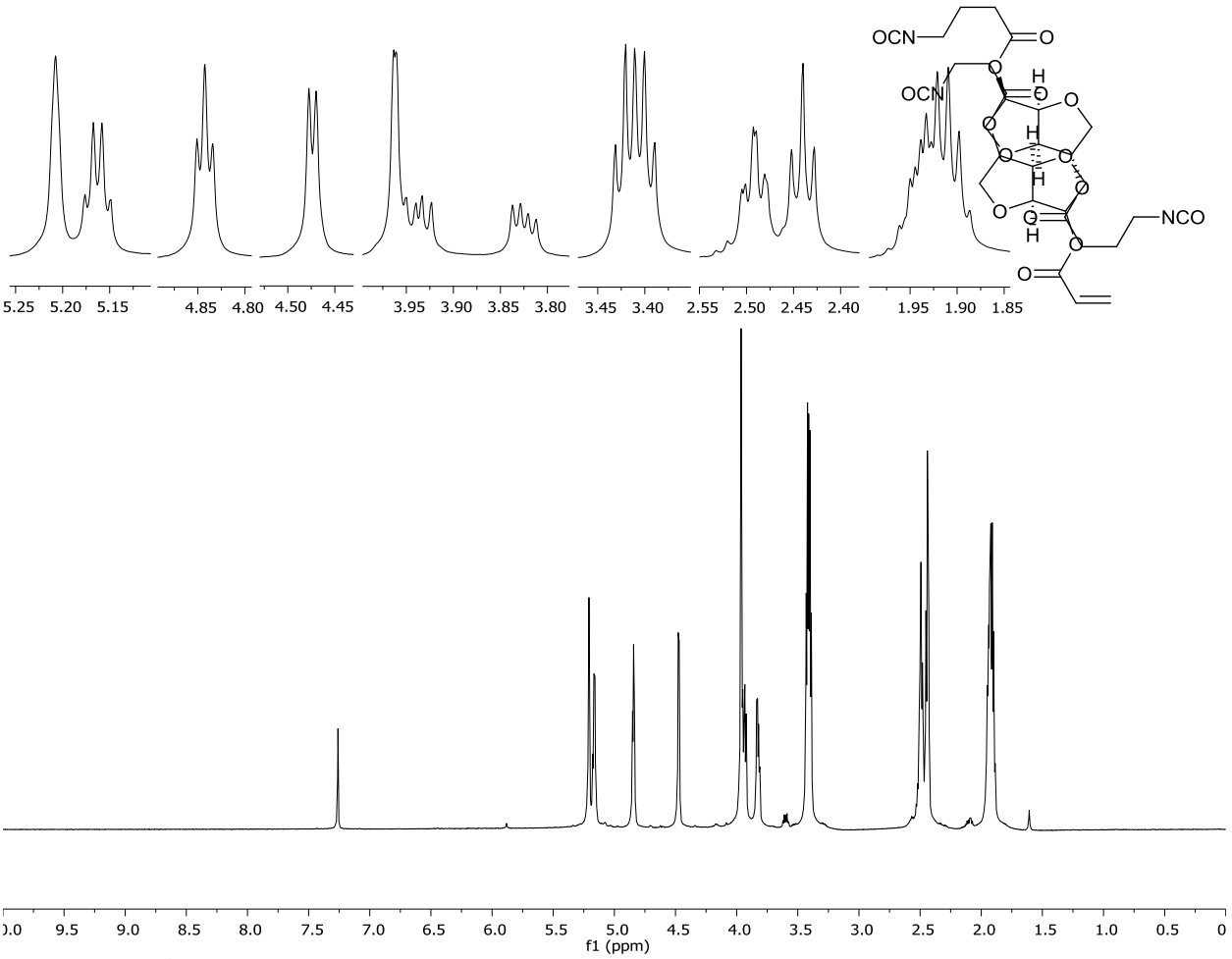

Figure S20. ^{1}H NMR (600 MHz, $CDCl_3$) of diisocyanate **12a**

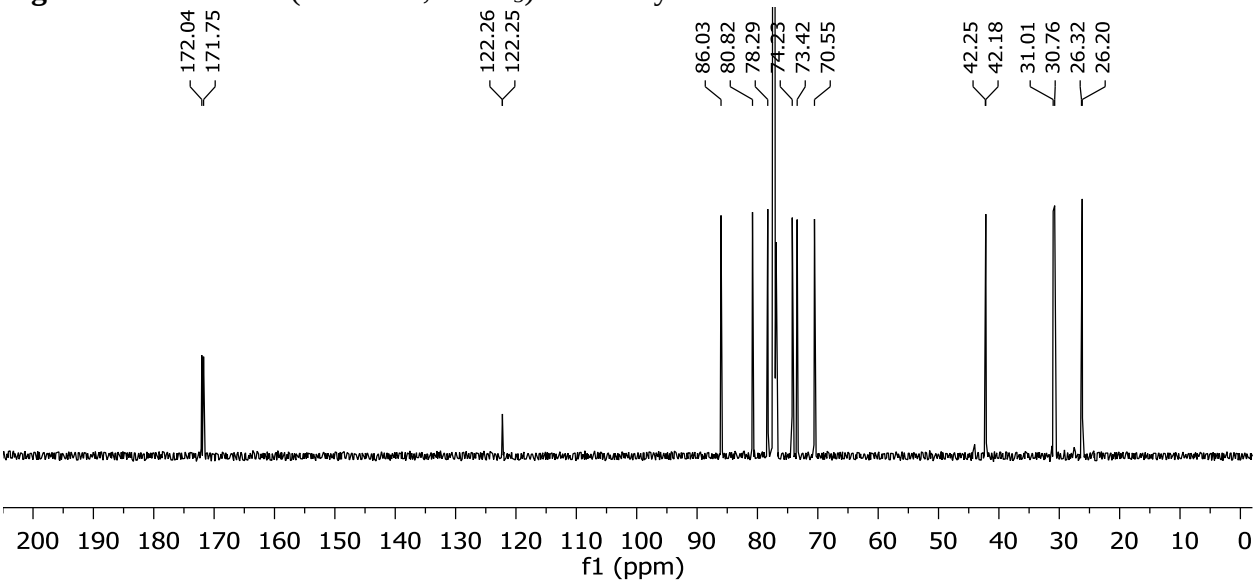

Figure S21. ^{13}C NMR (150 MHz, $CDCl_3$) of diisocyanate **12a**

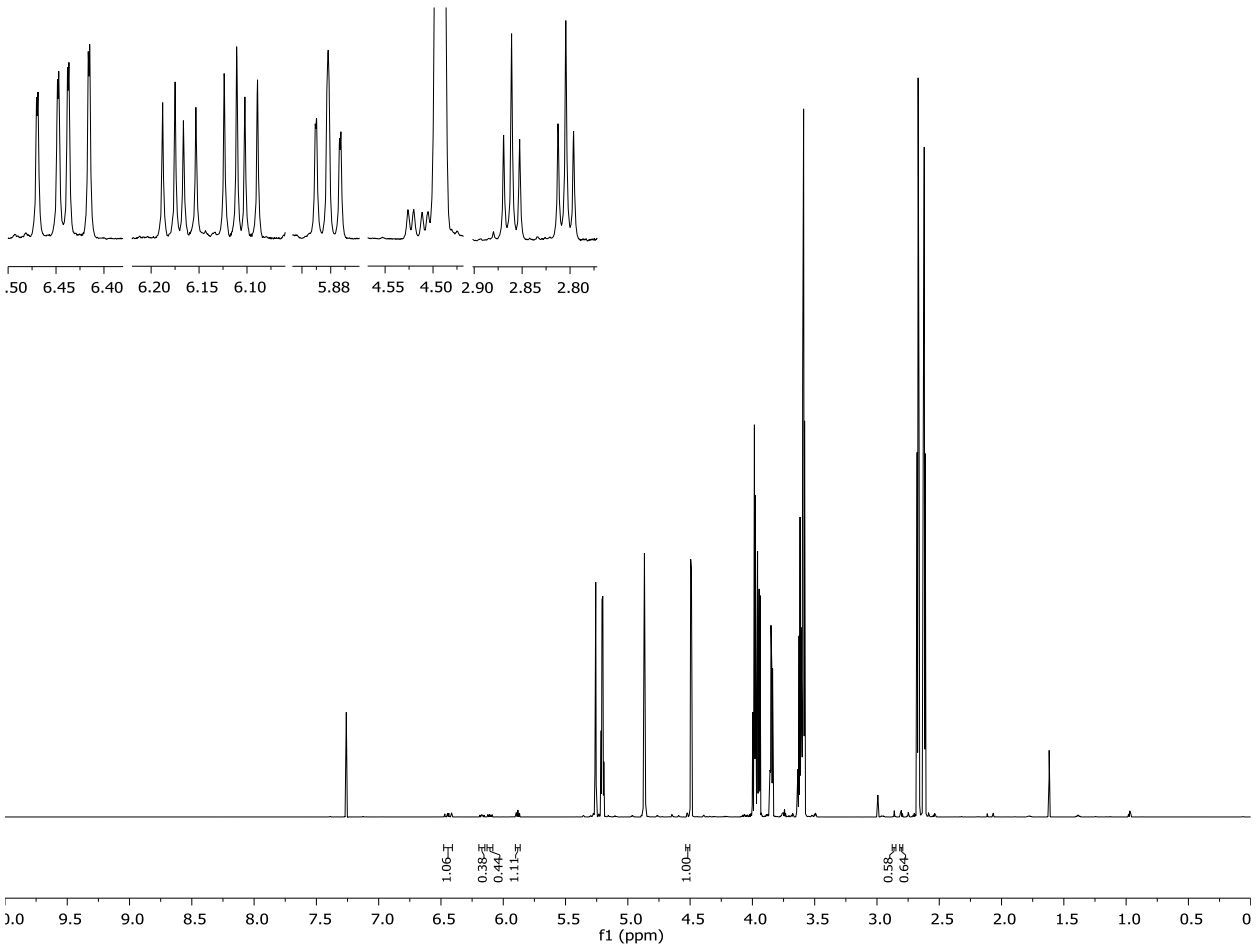

Figure S22. ^{1}H NMR (800 MHz, $CDCl_3$) of **isosorbide monoacrylate**.

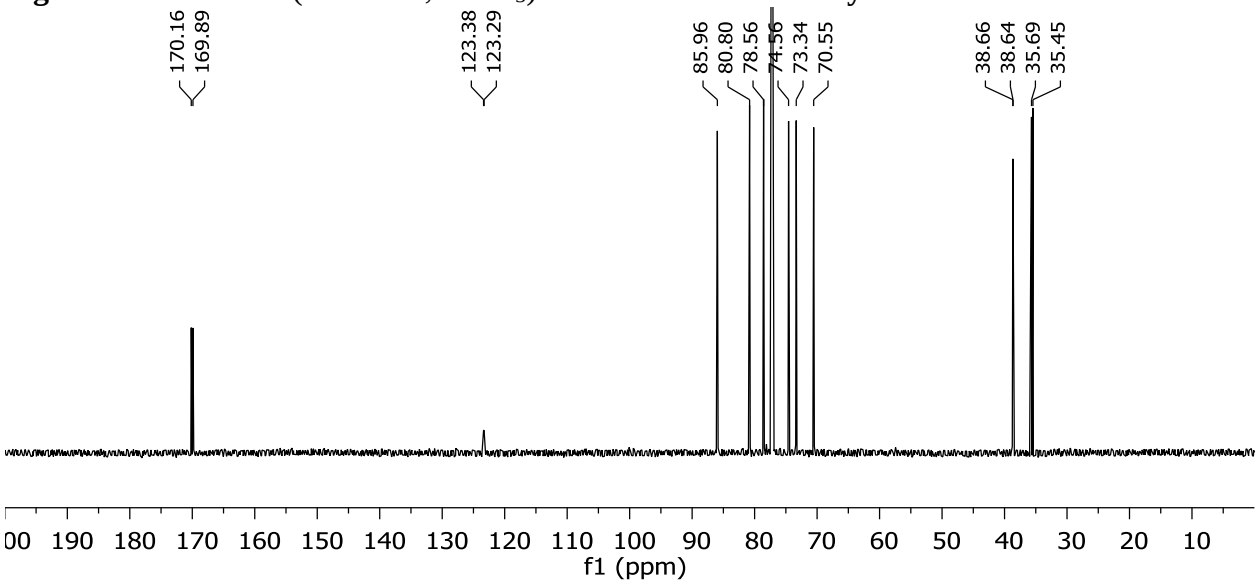

Figure S23. ^{13}C NMR (200 MHz, $CDCl_3$) of **isosorbide monoacrylate**.

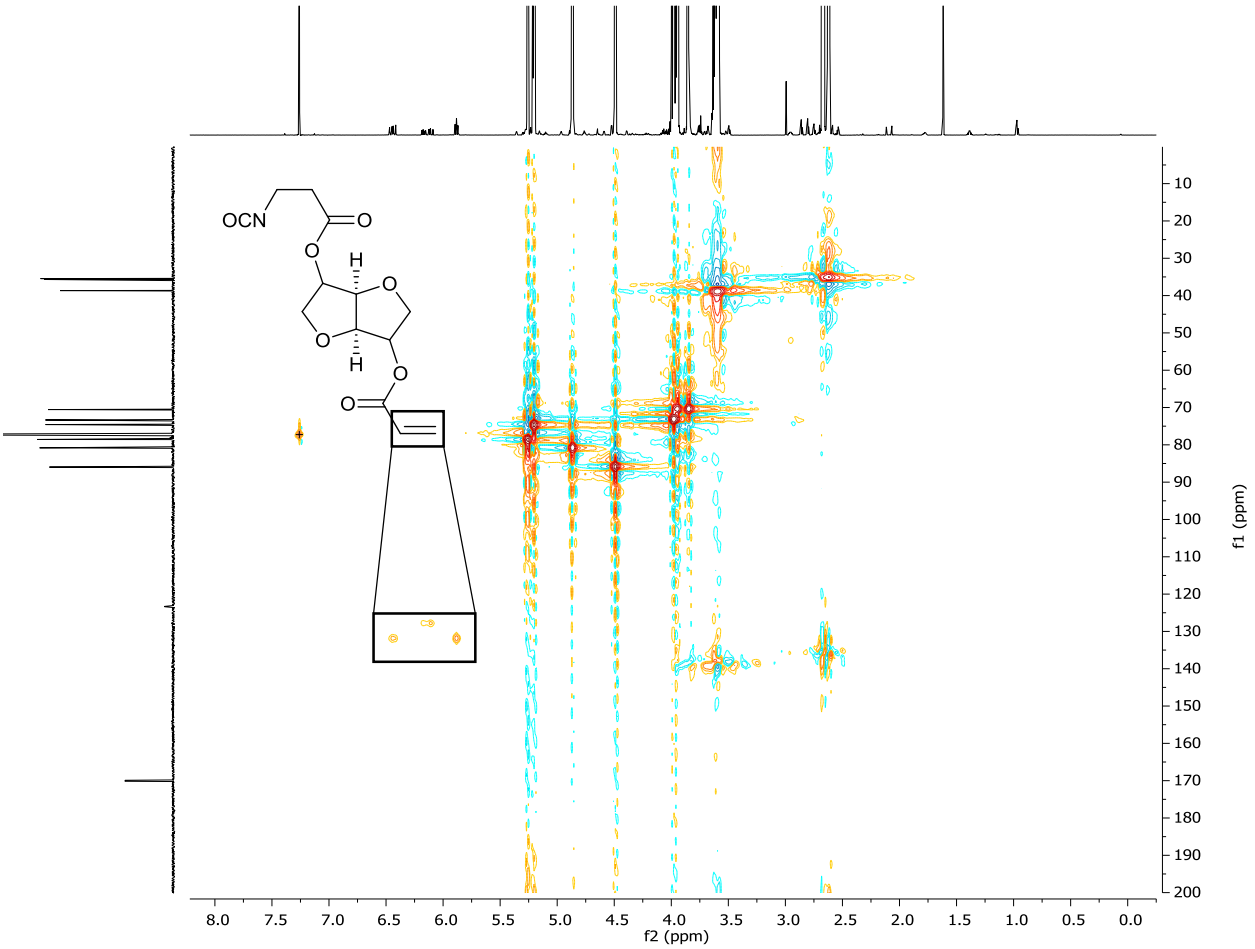

Figure S24. HSQC of **isosorbide monoacrylate**.

References

[1] D. Randall, S. Lee, Eds. *The Polyurethane Book*, Wiley, New York, **2002**, p. 477.

[2] a) D. P. Pfister, Y. Xia, R. C. Larock, *ChemSusChem* **2011**, *4*, 703 – 717; b) M. Desroches, M. Escouvois, R. Auvergne, S. Caillol, B. Boutevin, *Polym. Rev.* **2012,** 52, 38 – 79.

[3] For selected examples of polyurethanes incorporating isosorbide and its isomers as diols, see: a) C. H. Lee, H. Takagi, H. Okamoto, M. Kato, A. Usuki, *J. Polym. Sci. Part A* **2009**, *47*, 6025 – 6031; b) E. C. Varkey, K. Sreekumar, *J. Mater. Sci.* **2010**, *45*, 1912 – 1920; c) M. Beldi, R. Medimagh, S. Chatti, S. Marque, D. Prim, A. Loupy, F. Delolme, *Eur. Polym. J.* **2007**, *43*, 3415 – 3433; d) R. Marin, S. Munoz Guerra, *J. Appl. Polym. Sci.* **2009**, *114*, 3723 – 3736.

[4] For S_N2 approaches to diisocyanate **3** or the corresponding diamine, see: a) J. Thiem, H. Lüders, *Makromol. Chem.* **1986**, *187*, 2775 – 2785; b) F. Bachmann, J. Reimer, M. Ruppenstein, J. Thiem, *Macromol. Chem. Phys.* **2001**, *202*, 3410 – 3419; c) S. Thiyagarajan, L. Gootjes, W. Vogelzang, J. van Haveren, M. Lutz, D. S. van Es, *ChemSusChem* **2011**, 4, 1823 – 1829.

[5] For oxidation–reductive amination approaches to diisocyanate **3** or the corresponding diamine, see: a) G. Limberg, J. Thiem, *Synthesis* **1994**, 3, 317 – 321; b) S. Imm, S. Bahn, M. Zhang, L. Neubert, H. Neumann, F. Klasovsky, J. Pfeffer, T. Haas, M. Beller, *Angew. Chem.* **2011**, 123, 7741 – 7745; *Angew. Chem., Int. Ed.* **2011**, 50, 7599 – 7603; c) U. Dingerdissen, J. Pfeffer, T. Tacke, H. Schmidt, F. Klasovsky, R. Sheldon, M. Volland, M. Rimbach, S. Rinker, **2011**, U.S. patent application US 2011/0251399 A1; d) G. Streukens, C. Lettmann, S. Schneider, **2012**, international patent application WO 2012/010385 A1.

[6] For selected other amines and isocyanates from isosorbide, see: a) F. Bachmann, J. Reimer, M. Ruppenstein, J. Thiem, *Macromol., Rapid Commun.* **1998**, *19*, 21 – 26; b) A. A. Caouthar, A. Loupy, M. Bortolussi, J.-C. Blais, L. Dubreucq, A. Meddour, *J. Polym. Sci. Part A* **2005**, *43*, 6480 – 6491.

[7] For selected other biobased polyisocyanates, see: a) M. R. Kamal, R. C. Kuder, **1972**, U.S. patent 3,691,225; b) J. L. Cawse, J. L. Stanford, R. H. Still, *Makromol. Chem.* **1984**, *185*, 697 – 707; c) P. Bruin, G. J. Venstra, A. J. Nijenhuis, A. J. Pennings, *Makromol. Chem., Rapid Commun*. **1988**, *9*, 589 – 594; d) G. Cayll, S. Kusefoglu, *J. Appl. Polym. Sci.* **2008**, 109, 2948 – 2955; e) L. Hojabri, X. Kong, S. S. Narine, *Biomacromol.* **2009**, 10, 884 – 891; f) L. Hojabri, X. Kong, S. S. Narine, *Biomacromol.* **2010**, 11, 911 – 918; g) D. V. Palaskar, A. Boyer, E. Coloutet, C. Alfos, H. Carmail, *Biomacromol.* **2010**, 11, 1202 – 1211; h) C. N. D. Newmann, W. D. Bulach, M. Rehahn, R. Klein, *Macromol,. Rapid Commun.* **2011**, 32, 1373 – 1378.

[8] M. Patel, M. Crank, V. Domburg, B. Hermann, L. Roes, "Medium and Long-term Opportunities and Risks of the Biotechnological Production of Bulk Chemicals from Renewable Resources," **2006**, http://brew.geo.uu.nl/BREW_Final_Report_September_2006.pdf, pp 75 – 76.

[9] For selected reviews on materials incorporating isosorbide and its isomers, see: a) F. Fenouillot, A. Rousseau, G. Colomines, R. Saint-Loup, J.-P. Pascault, *Prog. Polym. Sci.* **2010**, 35, 578 – 622; b) X. Feng, A. J. East, W. B. Hammond, Y. Zhang, M. Jaffe, *Polym. Adv. Technol.* **2011**, 22, 139 – 150; c) M. Rose, R. Paklovits, *ChemSusChem* **2012**, 5, 167 – 176; d) D. S. van Es, *J. Renew. Mater.* **2013**, *1*, 61 – 72.

[10] For syntheses of isoidide from isosorbide, see: a) L. W. Wright, J. D. Brandner, *J. Org. Chem.* **1964**, 29, 2979 – 2982; b) J. Le Notre, J. van Haveren, D. S. van Es, *ChemSusChem* **2013**, DOI: 10.1002/cssc.201200714; for a synthesis from isomannide, see: c) G. De Coster, K. Vandyck, E. Van der Eycken, J. Van der Eycken, M. Elseviers, H. Röper, *Tetrahedron Asymmetry* **2002**, *13*, 1673 – 1679.

[11] a) J. Thiem, M. Luders, *Starch-Starke* **1984**, *36*, 170 – 176; b) R. Strobeck, M. Rehahn, M. Ballauff, *Makromol. Chem.* **1993**, *194*, 53 – 64; c) R. Gohil, *Polym. Eng. Sci.* **2009**, *49*, 544 – 553; d) R. Quintana, A.M. de Larduya, A. Alla, S. M. Guerra, *High Perform. Polym.* **2012**, *21*, 24 – 30; e) M. Abid, S. Abid, R. El Gharbi, *J. Macromol. Sci. Pure Appl. Chem.* **2012**, 49, 758 – 763.

[12] a) M. Patel, M. Crank, V. Domburg, B. Hermann, L. Roes, "Medium and Long-term Opportunities and Risks of the Biotechnological Production of Bulk Chemicals from Renewable Resources," **2006**, http://brew.geo.uu.nl/BREW_Final_Report_September_2006.pdf, pp 39 – 44; b) K.-K. Cheng, X.-B. Zhao, J. Zeng, J.-A. Zhang, *Biofuels, Bioprod., Bioref.* **2012**, *6*, 302 – 318.

[13] For a discussion on scale-up of Curtius rearrangements, see: D. J. am Ende, K. M. DeVries, P. J. Clifford, S. J. Brenek, *Org. Process Res. Dev.* **1998**, 2, 382 – 392.

[14] The yield of diacid chloride **6a** from pure diacid **5a** was estimated by ^{1}H NMR analysis of the crude mixture with the assumption that the two carboxylic acids behave similarly.

[15] H. H. Bosshard, R. Mory, M. Schmid, H. Zollinger, *Helv. Chim. Acta* **1959**, *42*, 1653 – 1658.

[16] The amount of diacyl azide **7a** was determined in solution by adding ethyl acetate as an internal standard, then diluting a small aliquot with $CDCl_3$ for ^{1}H NMR analysis.

[17] G. R. Palmese, J. J. La Scala, J. M. Sadler, A.-P. T. Lam, **2013**, WO 2013/066461 A2.

[18] For a review of the impact of stereochemistry on polymer properties, see: M. Farina, *Top. Stereochem.* **1987**, *17*, 1 – 111.

CHAPTER 3

UNEXPECTED TACKIFIERS FROM ISOSORBIDE

PUBLISHED: M. D. Zenner, S. A. Madbouly, J. S. Chen, M. R. Kessler, Unexpected Tackifiers from Isosorbide, *ChemSusChem*, **2015**, 8, 448 – 451.

Introduction

Tackifiers, sometimes referred to as rosins or resins, are semisolid or glassy small molecules (monomers or oligomers) that render materials tacky.[1] For example, they can be blended with polymers to create pressure-sensitive adhesives (PSAs)[2] or used as oil additives to modify wetting properties.[3] Major classes of tackifiers include diterpenes (also known as resin acids), terpenes, and petroleum-derived oligomers. Plant-derived tackifiers (diterpenes, terpenes, and their derivatives) are compatible with a broader range of applications. Abietic acid (**1**, Figure 1) is one of the first tackifiers to be discovered. It is no longer in common use, but abietic acid derivatives continue to be important tackifiers.[1b,c]

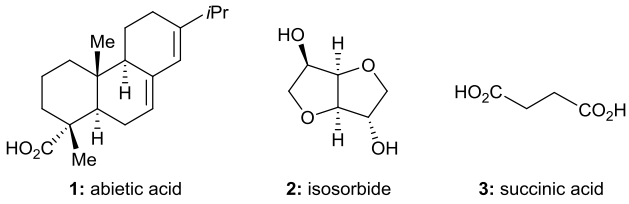

Figure 1. Abietic acid, isosorbide, and succinic acid.

We previously reported[4] the synthesis of a biorenewable diisocyanate (**6**, Scheme 1) from isosorbide (**2**) and succinic anhydride (**4**). Isosorbide[5] is manufactured through a double dehydration of sorbitol. Bio-succinic acid (**3**, Figure 1)[6] is available from fermentation at a price competitive with that of petroleum-derived succinic acid. Both compounds are non-toxic and thermally stable. The first step of our synthesis was a solvent-free esterification of isosorbide (**2**) with succinic anhydride (**4**) to give diacid **5** in quantitative yield. Diacid **5** was so viscous and tacky under ambient conditions that heating to give a free-flowing liquid was necessary for practical transfers of this material. Herein we identify diacid **5** as a promising tackifier and characterize a family of analogues.

Results and Discussion

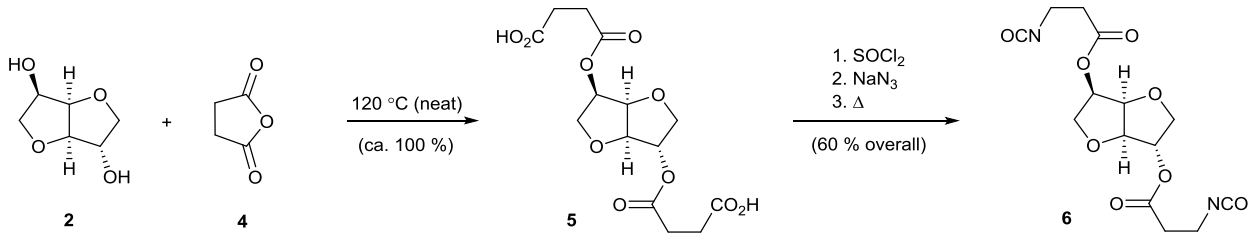

Scheme 1. Synthesis of diisocyanate **6**.

The unusual physical properties of diacid **5** led us to investigate the possibility that it is a tackifier. Consistent with this hypothesis, diacid **5** undergoes a glass transition (T_g = –2 °C as measured by DSC) rather than a melt. Although tackifiers generally are blended with other materials,[1] we chose to further characterize diacid **5** and its analogues in pure form in order to obtain application-independent data.

Although there are many ways to test tack, two protocols in particular stood out as prime candidates. One, a qualitative test, commonly used is the rolling ball tack test, ASTM D3121.[7] For this test, the adhesive is placed at the end of a ramp. The ramp used has a height of 65 mm and an angle of 21° 30′. A steal ball with an 11 mm diameter is rolled down the ramp and across the adhesive being tested. In order to perform the test, the ball is gently pushed down the ramp and travels some distance across the adhesive, and the distance travelled is then measured with a ruler and the values are reported in inch-pounds. While this test is good for quick analysis of an adhesive at room temperature, it lacks the accuracy needed for our

Figure 2. Rolling ball tack test.[2]

[2] Ichemco, Rolling Ball Tack Tester, http://www.ichemco.it/machines/rolling_ball_tack_tester_cheminstruments_tt_100.htm

purposes. For instance, there is very little control over the amount of force used to push the ball from the platform, which can result in a large variation in distance travelled of the ball over the adhesive. There is also a large amount of error in measurement of the distance travelled using a standard ruler.

The second, more commonly used test is the inverted probe tack test, ASTM D2979.[8] For this test, the adhesive is placed, inverted on a surface. A stainless steel probe with a diameter of 5 mm is then raised at a rate of 10 mm·sec^{-1}, and impacts the adhesive with a force of 1 N. The probe is held on the surface at 1N for 1 sec and then lowered at a rate of 10 mm·sec^{-1}. The force required to remove the probe from the adhesive is then recorded as the amount of tack, usually reported in newtons (N). While this method is more accurate and controlled than the rolling ball tack test it still suffers from one major drawback making it unusable for testing of our tackifiers. For the inverted probe tack test, the adhesive is attached to a support, inverted. Applying our tackifiers on this surface would result in the tackifier dripping off the surface, since many of our analogues are free-flowing liquids at room temperature.

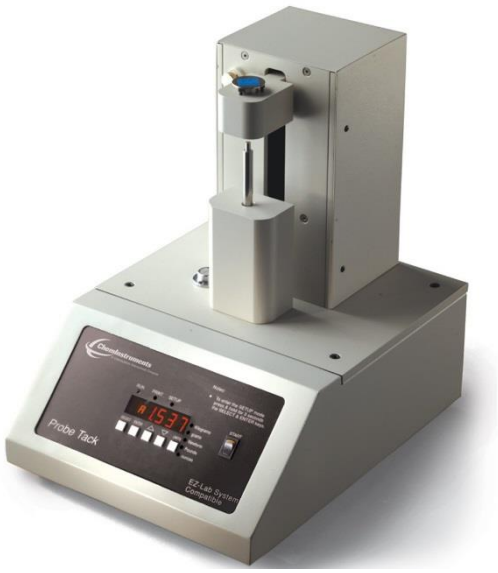

Figure 3. Inverted probe tack test.[3]

Temperature and humidity control was another factor that needed to be addressed for both test protocols. It was possible to control temperature and humidity for the rolling ball tack test with relative ease. All that would be necessary was to construct an environmental chamber, but the inaccuracies associated with the rolling ball tack test made it a nonstarter. While humidity control

[3] ChemInstruments, PT-100 Polyken™ Probe Tack, http://cheminstruments.com/polyken-probe-tack.html/

for the inverted probe tack test was just as solvable as with the rolling ball tack test. Temperature control would prove to be a little more difficult, since heating sample area wasn't possible the entire apparatus would have to be heated to temperatures potentially exceeding 100 °C could melt the plastic and electronics of the machine and cooling to −70 °C could make the plastic brittle and subject to shattering.

We therefore implemented a modified ASTM D2979 protocol[8] to measure tack in a temperature-controlled chamber under a nitrogen atmosphere (to reduce effects of humidity at cryogenic temperatures) using a vertical mechanical load frame (Instron model 5569). A cylindrical stainless steel probe (5 mm diameter) was lowered at 0.5 mm·sec^{-1} until the flat end impacted a 0.1 mm thick layer of diacid **5** (melted onto an aluminium block milled to that depth) with a pressure of 200 kPa. A thermal couple was also taped to the surface of the aluminium block to ensure tack at the stated temperatures were accurate to ±0.2 °C. That pressure was maintained for 1.0 second, and then the probe was raised at 0.5 mm·sec^{-1}. The force (normalized by the cross-sectional area of the probe) required to overcome the adhesive strength of the tackifier and raise the probe off of the surface at different temperatures is shown in Figure 4. No tack was observed below the glass transition temperature. The maximum tack was observed above the glass transition temperature at 15 °C (T_{tack}). As the temperature was further increased, tackiness initially dropped rapidly, but then plateaued over a broad temperature range. At all temperatures, tackifier was found on both the aluminium surface and the stainless steel probe, demonstrating that cohesive failure, not adhesive failure, occurred. Thus, wettability of the tackifier on these surfaces was not a limiting factor for tack. The results are independent of the pressure with which the probe impacts the tackifier and the contact time; we demonstrated at 15 °C that increasing the pressure to 760 kPa, increasing the contact time to 10 sec, or reducing the contact time to the minimum allowed by our

load frame had no effect on the measured tack. The tack properties appear to be indefinitely stable; one sample of diacid **5** has demonstrated unchanged properties over a two year timeframe. We have recently synthesized a 6 mol (2 kg) batch of diacid **5** in a newly constructed, 2 L reactor.

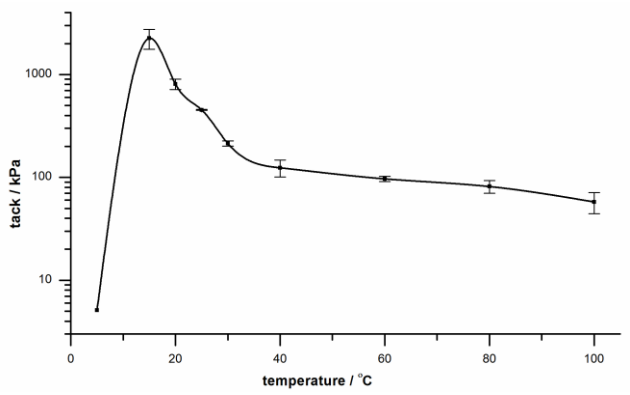

Figure 4. Temperature-dependent tack of diacid **5**. 95 % confidence intervals shown (n = 3). The temperature-response curve was calculated using non-parametric curve fitting.

To evaluate the relevance of the measured tack, we compared diacid **5** with abietic acid (**1**), isosorbide (**2**), and succinic acid (**3**) (see Table 1). Tack is an emergent property of diacid **5**; neither isosorbide (**2**) nor succinic acid (**3**) is tacky. This property is particularly surprising since short oligomers of isosorbide and succinic acid have been used to raise the glass transition temperature and reduce the tackiness of polyesters.[9] Diacid **5** is more tacky than abietic acid (**1**) under our testing conditions. To visualize the level of tack, a thin layer of diacid **5** was melted onto the end of a steel cylindrical rod (1.3 cm^2 cross-section) and cooled to 15 °C (T_{tack}). When the rod was pressed by hand against a 7.2 kg steel cylindrical block (block at ambient temperature) and then pulled upward, the layer of diacid **5** transmitted enough force to lift the block before cohesive failure occurred (see Figure 5). This process could be repeated without reapplying diacid **5**.

We then investigated the effect of structural changes on tack properties. Changing the stereochemistry of the bicyclic core (diacid **7**, see Table 1 and Figures 6 and 7) has no significant effect on materials properties. Altering the length of the alkyl chain (diacid **8**) or introducing unsaturation (diacid **9**) changes both the glass transition temperature and the temperature at which maximum tack is observed, but does not significantly alter the maximum tack level. [10]

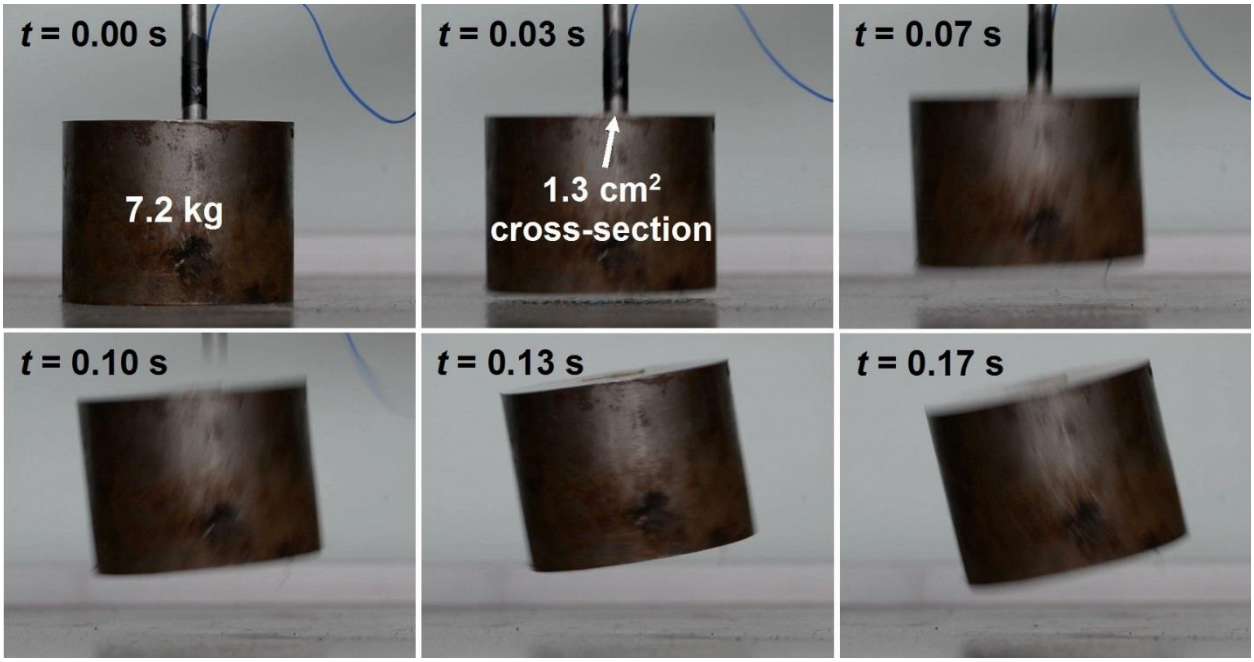

Figure 5. Time-lapse photography of a 7.2 kg steel block (at ambient temperature) being lifted by a layer of diacid **5** at the end of a steel cylindrical rod (1.3 cm^2 cross-section) at 15 °C (T_{tack}).

We speculated that hydrogen bonding may be important for the function of our tackifiers. To test this hypothesis, we prepared methyl ester analogues **10** – **12**.[11] In all cases the maximum tack level of the methyl ester was comparable to that of the corresponding diacid, proving that hydrogen bonding was not necessary for tack. The more notable property change upon conversion to a methyl ester is lowering of the glass transition temperature and the temperature at which maximum tack is observed by approximately 30 °C. Thus, modification of the carboxylic acid groups offers a means to adjust the useful temperature range of these materials.

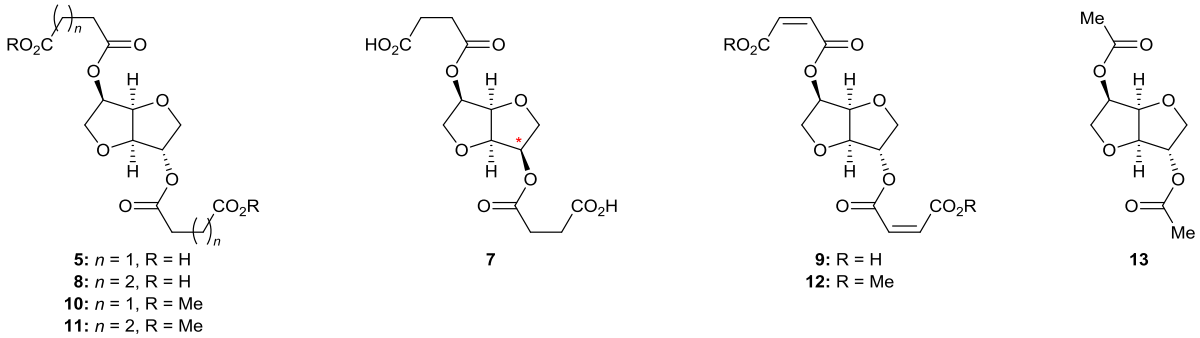

Figure 6. Structures of test substances **5**, **7** – **13**.

Table 1. Selected materials properties for new compounds and controls.

Compound	T_g / °C[a]	T_{tack} / °C[b]	Tack / kPa[c]	η_0 / Pa·s[d]
diacid **5**	–2	15	2300 ± 500	1.5×10^5
diacid **7**	0	15	2300 ± 300	1.4×10^5
diacid **8**	–25	–15	2400 ± 500	5.2×10^6
diacid **9**	10	35	2000 ± 300	9.1×10^3
methyl ester **10**	–35	–15	1500 ± 400	2.7×10^4
methyl ester **11**	–50	–40	1200 ± 500	4.4×10^4
methyl ester **12**	–14	0	1700 ± 400	7.9×10^4
diacetate **13**	melt	NA	< 5[e]	ND
isosorbide (**2**)	melt	NA	< 5[e]	ND
succinic acid (**3**)	melt	NA	< 5[e]	ND
abietic acid (**1**)	71	90	480[f]	ND

[a] Determined by DSC. Samples were heated at 10 °C·min^{-1}. [b] Temperature at which maximum tack was observed. Determined to the nearest 5 °C by modified ASTM D2979 protocol. [c] Determined at T_{tack}. 95 % confidence intervals reported (n = 3). Cohesive failure occurred at all temperatures for compounds **5**, **7** – **12**. [d] Determined at T_{tack}. [e] Measured both above and below the compound's melting point. [f] Compound was transiently tacky, but only one measurement could be obtained before it became non-tacky. NA = not applicable. ND = not determined.

The peripheral carboxyl groups also are important for stabilizing the tacky properties of this class of compounds; truncating the linear segment can destabilize the glassy phase in which tack is observed. For example, the diacetate derivative of isosorbide (**13**) undergoes a glass transition when impure and is tacky in its glassy phase. However, purified diacetate **13** melts rather than undergoing a glass transition, and lacks tack both above and below its melting point.

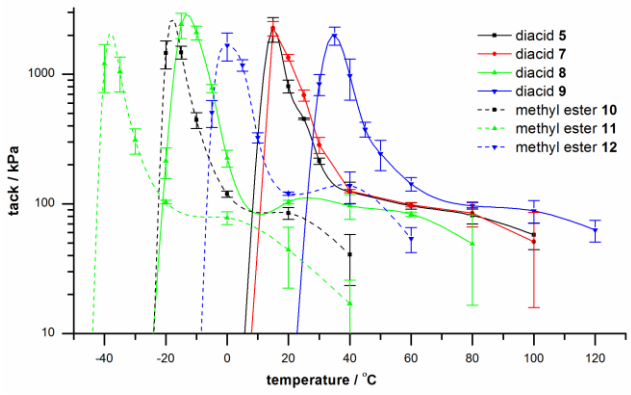

Figure 7. Temperature-dependent tack of compounds **5**, **7** – **12**. Temperature-response curves were calculated using non-parametric curve fitting.

Viscoelastic properties of our tackifiers were investigated by dynamic rheology. No single temperature was appropriate for comparative viscosity measurements of all of our tackifiers since they

become tacky over a broad range of temperatures; therefore, we compared them at different temperatures, selecting for each tackifier the temperature at which it is most tacky (T_{tack}, see Table 1). As shown in Figure 8, small-amplitude oscillatory shear flow experiments revealed complex viscosities that are strongly dependent on tackifier structure. The zero-shear viscosity (η_0, see Table **1**) was determined using the Carreau–Yasuda model[12]

$$|\eta^*| = \eta_0 [1 + (\tau_\eta \omega)^a]^{(n-1)/a}$$

where η^* is the measured viscosity, τ_η is the characteristic viscous relaxation time (a constant), ω is the angular frequency, and n and a are variables determined by nonlinear regression analysis. Surprisingly, whereas all the methyl ester tackifiers (**10** – **12**) have similar zero-shear viscosities when compared in this manner, the zero-shear viscosity for the carboxylic acid tackifiers (**5**, **7** – **9**) is strongly dependent on compound structure. For example, the zero-shear viscosity for diacid **8** (5.2×10^6 Pa·s) is over 500 times higher than that for diacid **9** (9.1×10^3 Pa·s). We speculate that this unexpected variation in viscosity is due to differences in hydrogen bonding;[10] more analogues are being prepared in order to test and clarify this explanation.

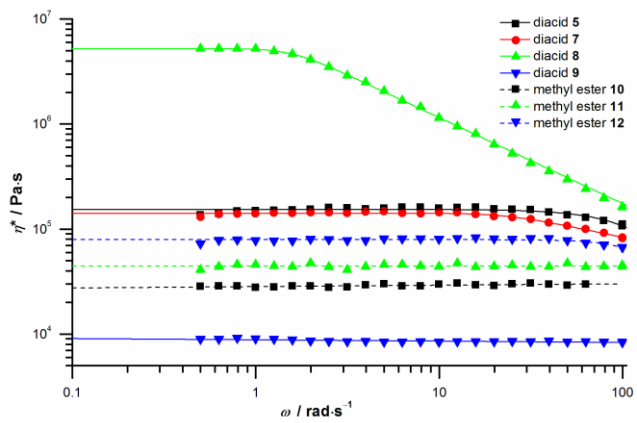

Figure 8. Angular frequency-dependent complex viscosity of compounds **5**, **7** – **12**. All measurements were performed at T_{tack} (see Table 1). Frequency–response curves were calculated by fitting the data to the Carreau–Yasuda model.

Our lead tackifier, diacid **5**, was also subjected to small-amplitude oscillatory shear flow experiments. The sol–gel transition (T_{gel}), defined as the temperature at which the storage (G') and loss (G'') moduli are equal, was determined as a function of angular frequency. The sol–gel transition marks a phase transition between a solid-like state (at lower temperature) and a liquid-

like state (at higher temperature). Figure 9 shows the temperature-dependent dynamic shear moduli (G' and G'') at different angular frequencies. The sol–gel transition temperature rises with increasing angular frequency (see Figure 9f). Interestingly, the transition temperature is similar to the temperature at which maximum tack was observed in direct tack measurements (T_{tack} = 15 °C).

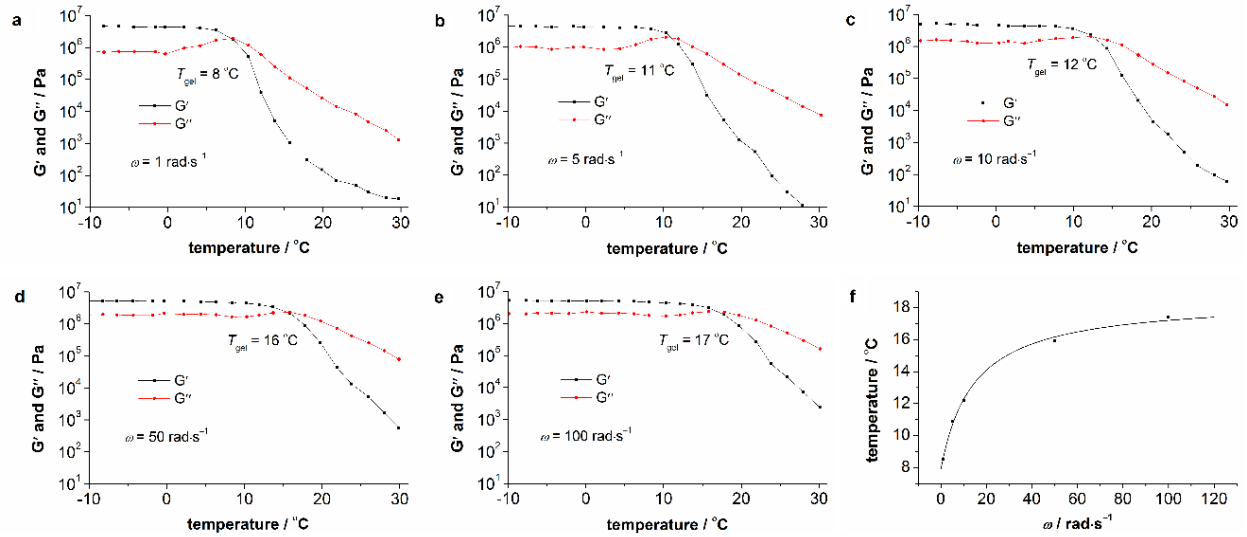

Figure 9. Determination of angular frequency-dependent T_{gel} for diacid **5**. Samples were cooled at 2 °C·min^{-1}. a: 1 rad·s^{-1}. b: 5 rad·s^{-1}. c: 10 rad·s^{-1}. d: 50 rad·s^{-1}. e: 100 rad·s^{-1}. f: Angular frequency-dependent T_{gel} as estimated by non-parametric curve fitting.

Conclusion

In summary, we identified a new family of low-cost tackifiers that are prepared in one or two steps from isosorbide and have up to 100 % bio-content. The useful temperature of these tackifiers can be adjusted over a broad range. Synthesis and characterization of additional members of this family and evaluation of these tackifiers as components of pressure-sensitive adhesives are underway.

I would like to thank Samy Madbouly for his help with and contribution of rheological experiments and analysis. I would also like to thank Dr. Mahendra Thunga for help training me on the Instron Load Frame and Dr. Danny Vennerberg for his insights into testing the tackifiers.

Experimental Section

General procedures. Unless otherwise noted, all reactions were performed with stirring under an argon atmosphere under anhydrous conditions. Isosorbide was purchased from Acros Organics. Isomannide was purchased from Sigma-Aldrich. Other reagents were purchased at the most economical grade. All chemicals were used as received, without purification. Dry *N*,*N*-dimethylformamide (DMF) was obtained by passing ACS grade DMF through a Glass Contour solvent purification system. Yields of materials refer to spectroscopically (^{1}H NMR) homogeneous samples. Flash column chromatography was performed using Grace Davison Davisil silica gel (60 Å, 35 – 70 μm). Thin-layer chromatography (TLC) was performed on Grace Davison Davisil silica TLC plates using UV light and common stains for visualization. The pressures for vacuum distillations were measured during the collection of the distillate. NMR spectra were calibrated using residual undeuterated solvent as an internal reference. Apparent couplings were determined for multiplets that could be deconvoluted visually.

Differential scanning calorimetry (DSC) was performed on ca. 5 mg samples under a helium atmosphere at a heat rate of 10 °C·min^{-1}; samples were then cooled back down at a rate of 10 °C·min^{-1} for a second heat.

Tack testing was performed via a modified ASTM D2979 standard. The tests were performed on a load frame (Instron model 5569) fitted with a temperature control box. A continuous nitrogen gas purge was used to maintain ≤ 30 % relative humidity. An aluminum plate was milled to a depth of 0.1 mm and the test substance was melted onto the plate. Tack was measured in triplicates making sure no one physical point was tested more than once. Temperature of the sample was

monitored via a Control Company model 4015 traceable thermocouple, attached to the aluminum plate. The probe was lowered at a rate of 0.5 mm·sec^{-1}, until it was in contact with the sample at an average force of 200 kPa. The probe was held at this pressure for one second, then raised at a rate of 0.5 mm·sec^{-1}.

The viscoelastic behavior of different types of tackifiers was investigated using an AR2000ex rheometer (TA Instruments) with 25 mm diameter parallel plates. The following rheological experiments were performed:

1. Strain sweep at constant angular frequency and temperature to determine the linear viscoelastic regime of the tackifiers.
2. Angular frequency sweep at $T_{\text{max tack}}$ for different tackifiers. The zero-shear viscosities (η_o) were also calculated by fitting the complex viscosity η^* vs. ω data to the Carreau-Yasuda model.
3. A temperature sweep at different constant angular shear frequencies ($\omega = 0.5 - 100$ rad·s^{-1}) to evaluate the T_{gel} for different tackifiers.

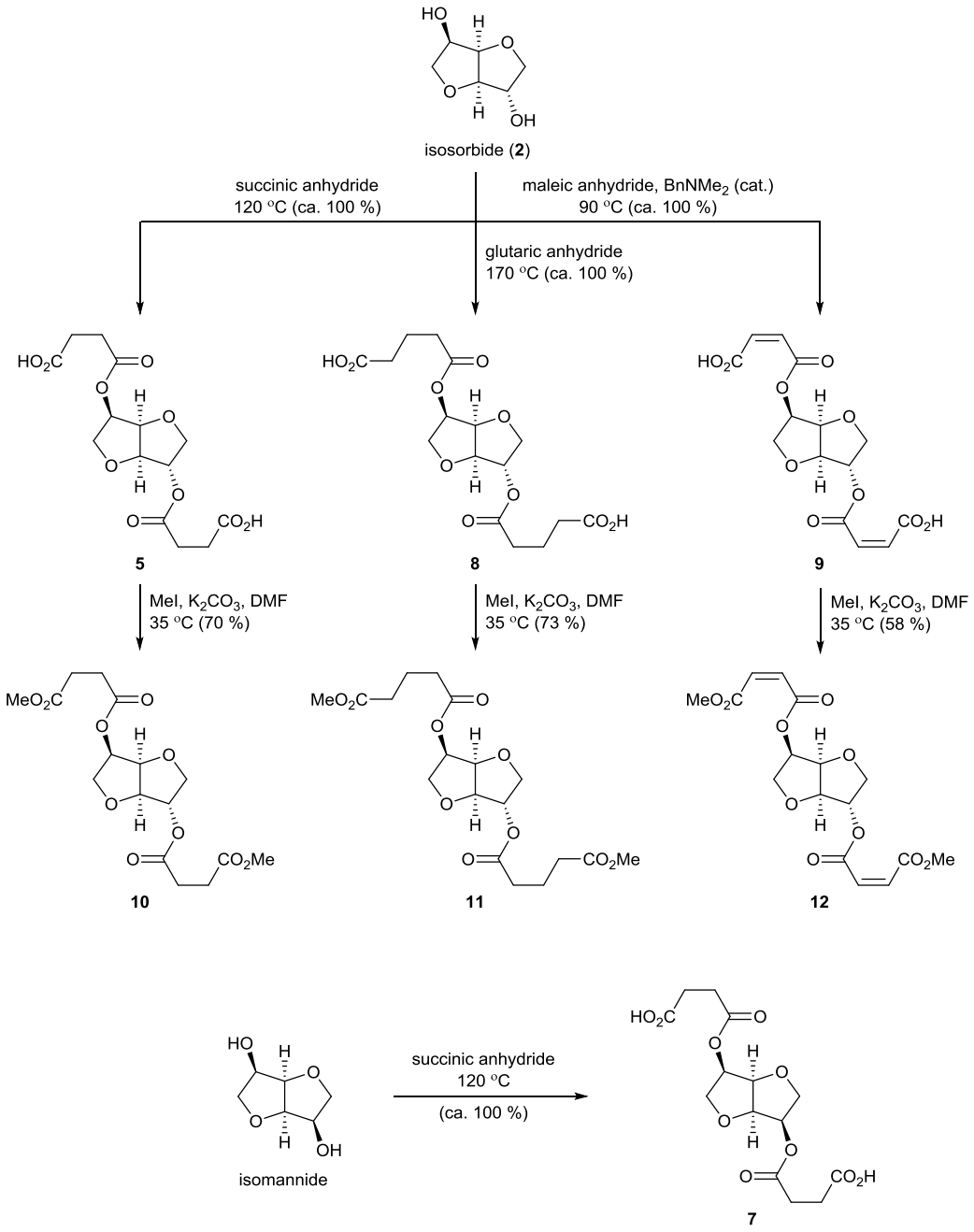

Scheme 1. Synthesis of tackifiers.

The synthesis of diacids **5** and **7**[4] and **9**[5] have been previously reported.

[4] M. D. Zenner, Y. Xia, J. S. Chen, M. R. Kessler, *ChemSusChem*, **2013**, 6, 1182 – 1185.
[5] G. R. Palmese, J. J. La Scala, J. M. Sadler, A.-P. T. Lam, **2013**, WO 2013/066461 A2.

Diacid 8. A mixture of isosorbide (14.6 g, 100 mmol) and glutaric anhydride (26.2 g, 230 mmol, 2.3 equiv.) were added to a pressure flask and heated. Note: the flask must be fully immersed into the oil bath to minimize evaporation of glutaric anhydride. The mixture was heated to 170 °C for 72 h producing a dark amber, viscous oil. Vacuum sublimation of glutaric anhydride from crude material gave diacid **8** for analysis. **8**: R_f = 0.35 (99.5 % EtOAc / Hexanes); $[\alpha]_D^{23}$ = +112.7 $cm^3 \cdot g^{-1} \cdot dm^{-1}$ (c = 1.00 $g \cdot cm^{-3}$, $CHCl_3$); IR (thin film): ν_{max} = 3183, 1736 cm^{-1}; ^1H NMR (600 MHz, $CDCl_3$): δ = 5.20 (br, 1H), 5.17 (q, J = 5.5 Hz, 1H), 4.84 (t, J = 5.0, 1H), 4.48 (d, J = 4.7, 1H), 3.99 – 3.95 (m, 2H), 3.94 (dd, J = 10.1, 6.4 Hz, 1H), 3.81 (dd, J = 10.0, 5.4 Hz, 1H), 2.54 – 2.37 (m, 8H), 2.05 – 1.91 (m, 4H) ppm; ^{13}C NMR (150 MHz, $CDCl_3$): δ = 178.65, 178.50, 172.40, 172.07, 85.99, 80.79, 78.19, 74.14, 73.42, 70.55, 33.21, 32.99, 32.94, 32.85, 19.92, 19.81 ppm; HRMS (ESI-QTOF) calcd for $C_{16}H_{22}O_{10}Na^+$ [M + Na^+]: 397.1105, found: 397.1109.

Methyl ester 10. To a crude mixture of diacid **5** (34.6 g, 100 mmol) and potassium carbonate (55.2 g, 400 mmol, 4 equiv.) in DMF (200 mL) at 35 °C was added methyl iodide (25 mL, 400 mmol, 4 equiv.) dropwise. After 24 h at 35 °C, the reaction mixture was dilute with 200 mL water. The reaction mixture was extracted with 4 × 100 mL ethyl acetate. The resultant organic phase was then washed with 1 × 400 mL water and 1 × 400 mL brine, then dried over $MgSO_4$. The reaction mixture was concentrated under reduced pressure to give crude dimethyl ester as a transparent yellow oil. Crude methyl ester **10** was distilled (247 – 248 °C, 800 mTorr) to give a light yellow oil (26.3 g, 70 % yield). **10**: R_f = 0.36 (60 % EtOAc / Hexanes); $[\alpha]_D^{23}$ = +28.7 $cm^3 \cdot g^{-1} \cdot dm^{-1}$ (c = 1.00 $g \cdot cm^{-3}$, $CHCl_3$); IR (thin film): ν_{max} = 1739 cm^{-1}; ^1H NMR (600 MHz, $CDCl_3$): δ = 5.20 (br, 1H), 5.16 (q, J = 5.5 Hz, 1H), 4.81 (t, J = 5 Hz, 1H), 4.47 (d, J = 4.6 Hz, 1H), 3.96, (d, J = 2.2 Hz, 2H), 3.92 (dd, J = 10.0, 6.0 Hz, 1H), 3.80 (dd, J = 10.0, 5.3 Hz, 1H), 3.69 (s, 3H), 3.68 (s, 3H),

2.71 – 2.59 (m, 8H) ppm; ^{13}C NMR (150 MHz, $CDCl_3$): δ = 172.66, 172.63, 171.79, 171.49, 85.97, 80.85, 78.37, 74.32, 73.40, 70.50, 52.04, 52.02, 29.18, 28.95, 28.93, 28.88 ppm; HRMS (ESI-QTOF) calcd for $C_{16}H_{23}O_{10}^+$ [M + H$^+$]: 375.1286, found: 375.1292.

Methyl ester 11. Methyl ester **11** was synthesized from diacid **8** following the above procedure. Vacuum distillation (214 – 216 °C, 320 mTorr) gave methyl ester **11** (73 % yield) as a colorless oil. **11**: R_f = 0.3 (40 % EtOAc / Hexanes); $[\alpha]_D^{23}$ = +80.9 $cm^3 \cdot g^{-1} \cdot dm^{-1}$ (c = 1.00 $g \cdot cm^{-3}$, $CHCl_3$); IR (thin film): ν_{max} = 1736 cm^{-1}; ^{1}H NMR (600 MHz, $CDCl_3$): δ = 5.19 (br, 1H), 5.15 (q, J = 5.6 Hz, 1H), 4.82 (t, J = 5.1 Hz, 1H), 4.46 (d, J = 4.7 Hz, 1H), 3.97 – 3.94 (m, 2H), 3.93 (dd, J = 10.0, 6.0 Hz, 1H), 3.80 (dd, J = 9.9, 5.1 Hz, 1H), 3.67 (s, 6H), 2.44 (dt, J = 7.3, 1.0 Hz, 2H), 2.42 – 2.35 (m, 6H), 2.00 – 1.91 (m, 4H) ppm; ^{13}C NMR (150 MHz, $CDCl_3$): δ = 173.44, 173.33, 172.40, 172.09, 86.08, 80.84, 78.16, 74.07, 73.50, 70.56, 51.79, 51.75, 33.25, 33.06, 33.05, 33.02, 20.19, 20.09 ppm; HRMS (ESI-QTOF) calcd for $C_{18}H_{26}O_{10}Na^+$ [M + Na$^+$]: 425.1418, found: 425.1425.

Methyl ester 12. Methyl ester **12** was synthesized from diacid **9** following the above procedure. Flash column chromatography (50% EtOAc / hexanes) gave methyl eser **12** (58 % yield) as a light yellow oil. **12**: R_f = 0.34 (50 % EtOAc / Hexanes); $[\alpha]_D^{23}$ = +66.7 $cm^3 \cdot g^{-1} \cdot dm^{-1}$ (c = 1.00 $g \cdot cm^{-3}$, $CHCl_3$); IR (thin film): ν_{max} = 1731 cm^{-1}; ^{1}H NMR (600 MHz, $CDCl_3$): δ = 6.35 – 6.26 (m, 4H), 5.35 (d, J = 3.3 Hz, 1H), 5.30 (q, J = 5.6 Hz, 1H), 4.88 (t, J = 5.0 Hz, 1H), 4.63 (d, J = 4.6 Hz, 1H), 4.11 – 4.00 (m, 3H), 3.87 (dd, J = 10.0, 5.3 Hz, 1H), 3.82 (s, 3H), 3.81 (s, 3H) ppm; ^{13}C NMR (150 MHz, $CDCl_3$): δ = 165.55, 165.34, 164.32, 130.78, 129.92, 129.68, 128.73, 85.57, 80.80, 78.65, 74.64, 72.97, 70.17, 52.28, 52.26 ppm; HRMS (ESI-QTOF) calcd for $C_{16}H_{19}O_{10}^+$ [M + H$^+$]: 371.0973, found: 371.0979.

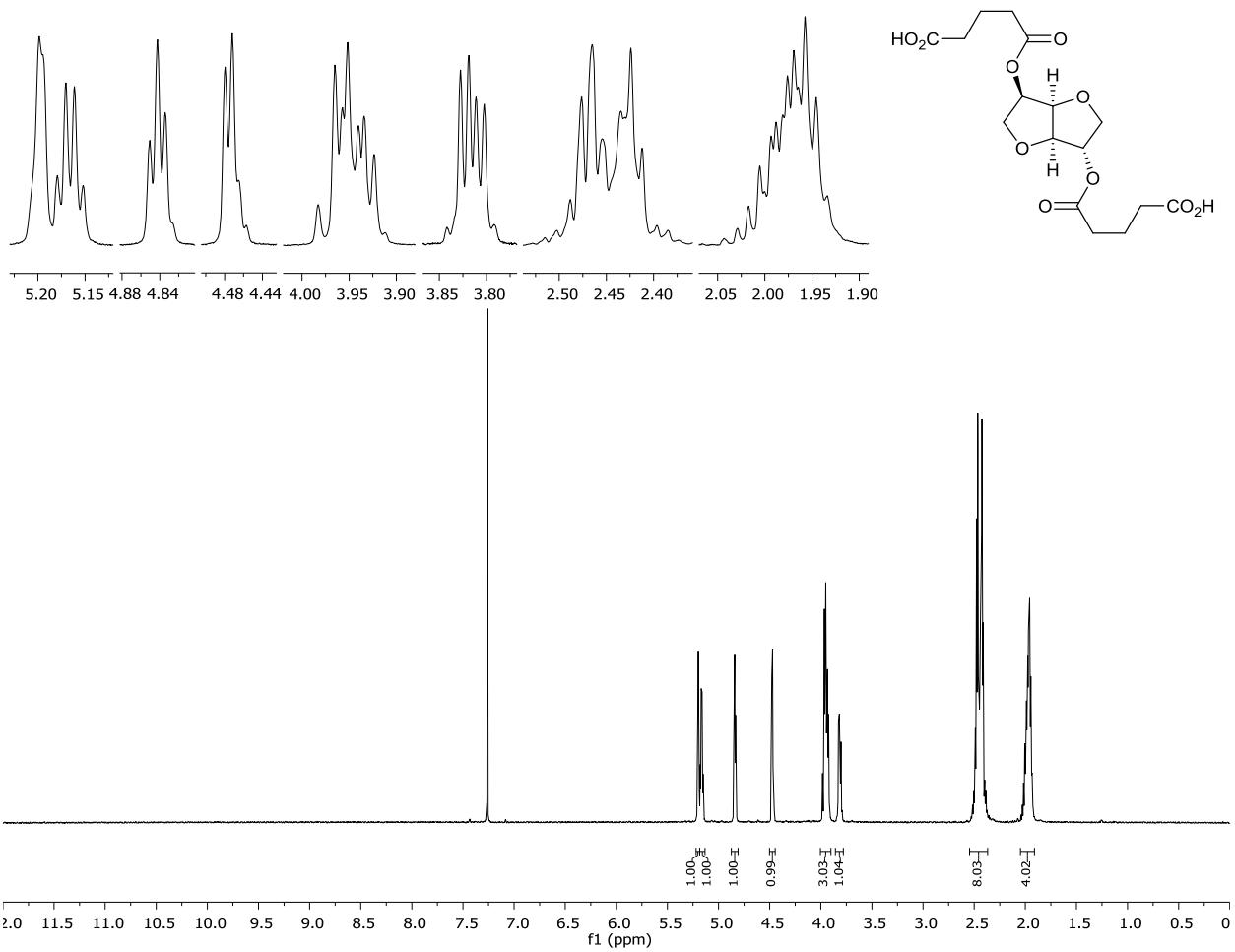

Figure S1. ^{1}H NMR (600 MHz, $CDCl_3$) of diacid **8**

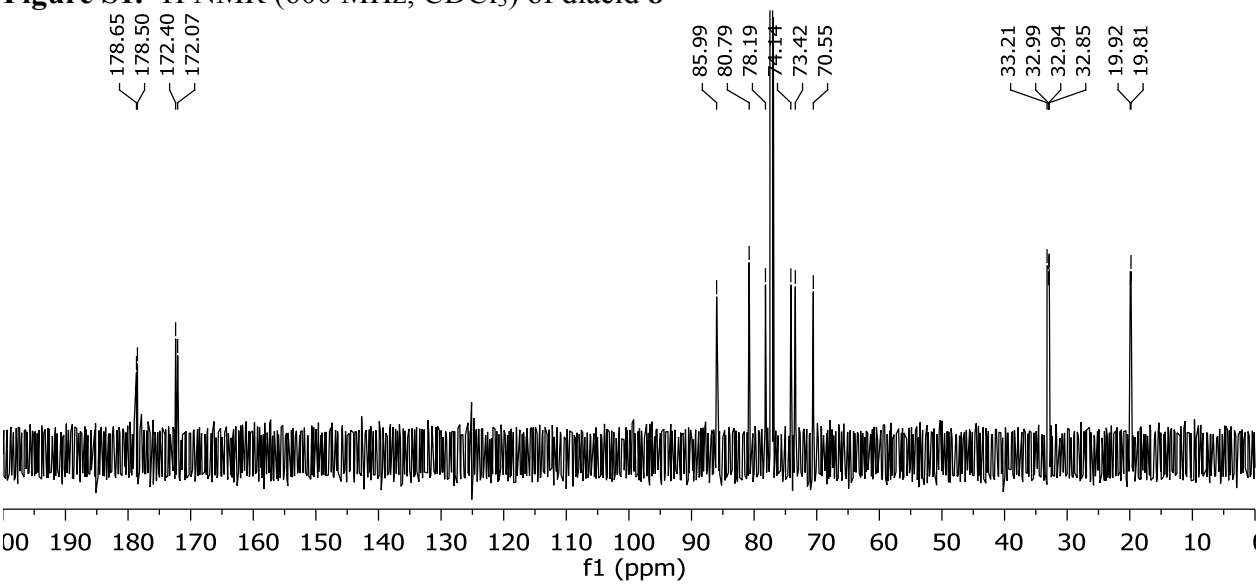

Figure S2. ^{13}C NMR (150 MHz, $CDCl_3$) of diacid **8**

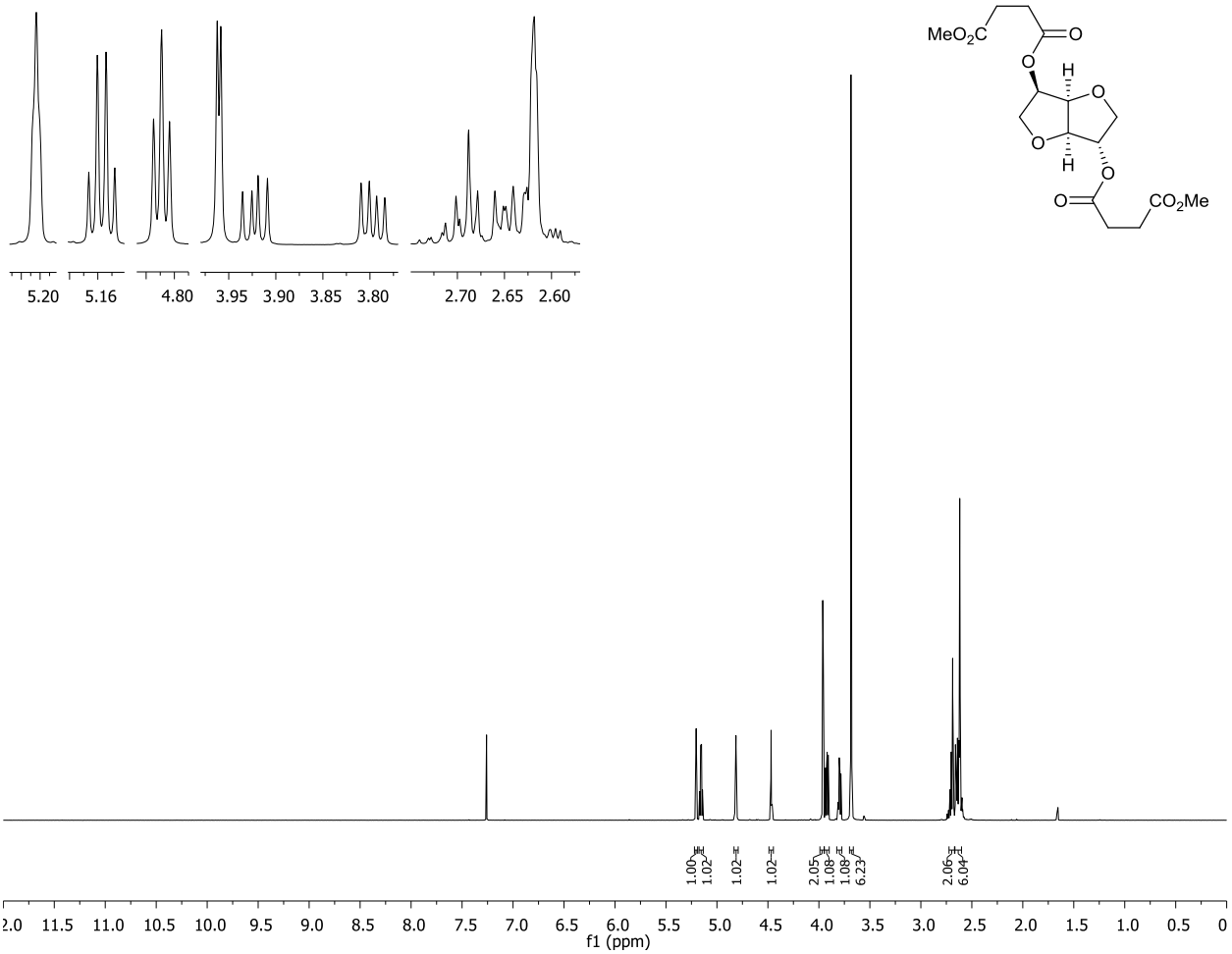

Figure S3. ^{1}H NMR (600 MHz, $CDCl_3$) of methyl ester **10**

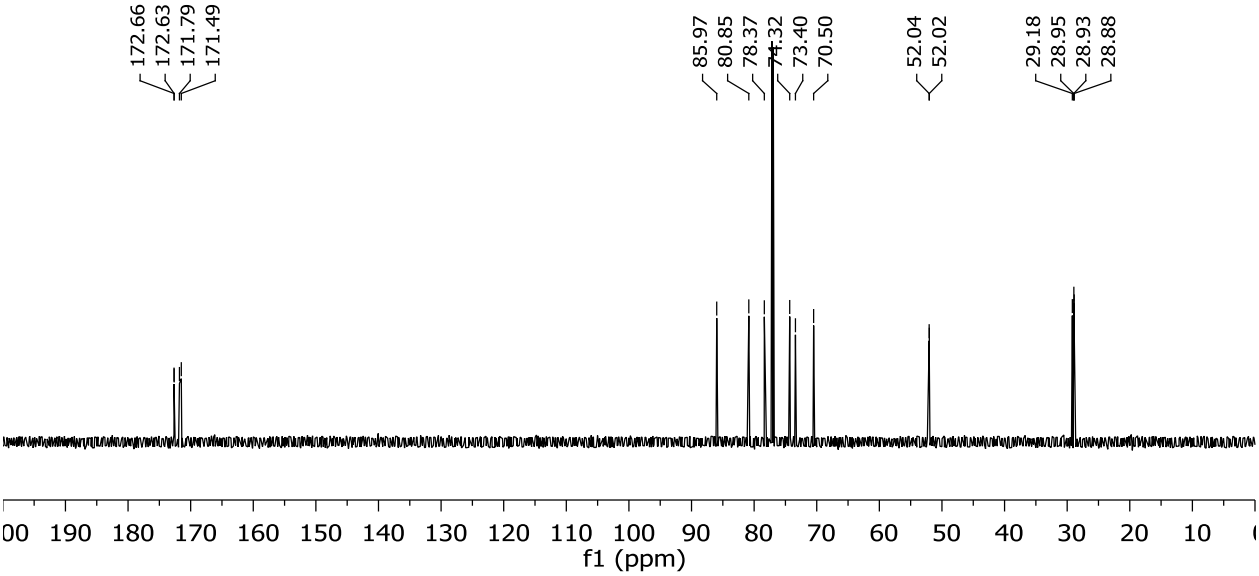

Figure S4. ^{13}C NMR (150 MHz, $CDCl_3$) of methyl ester **10**

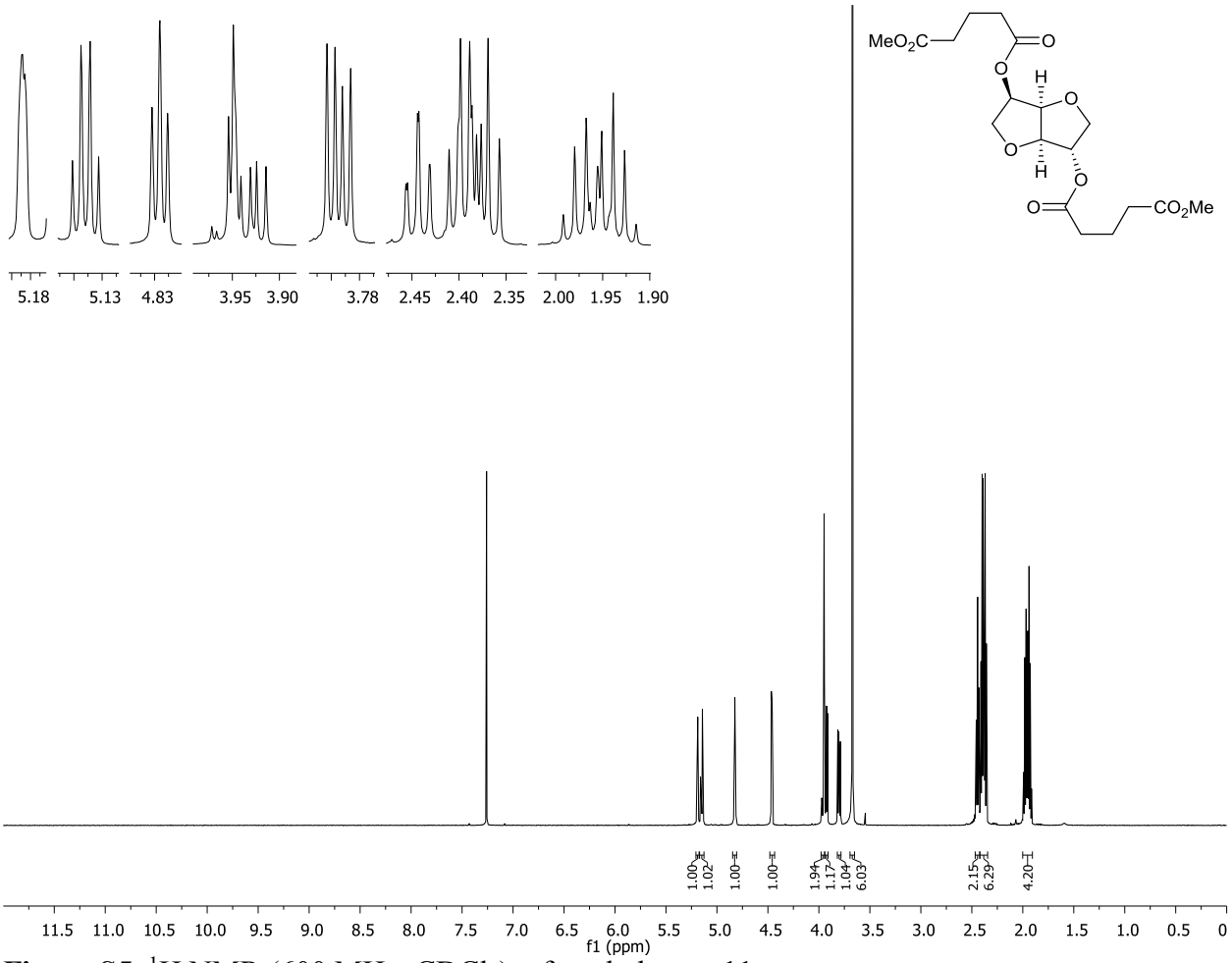

Figure S5. ^{1}H NMR (600 MHz, $CDCl_3$), of methyl ester **11**

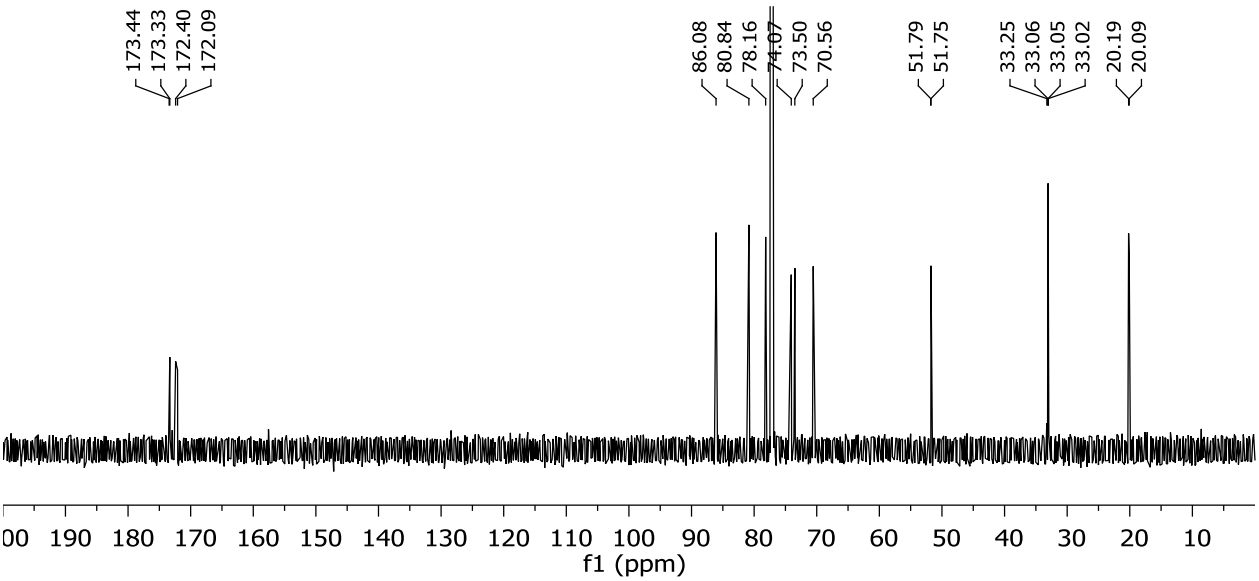

Figure S6. ^{13}C NMR (150 MHz, $CDCl_3$) of methyl ester **11**

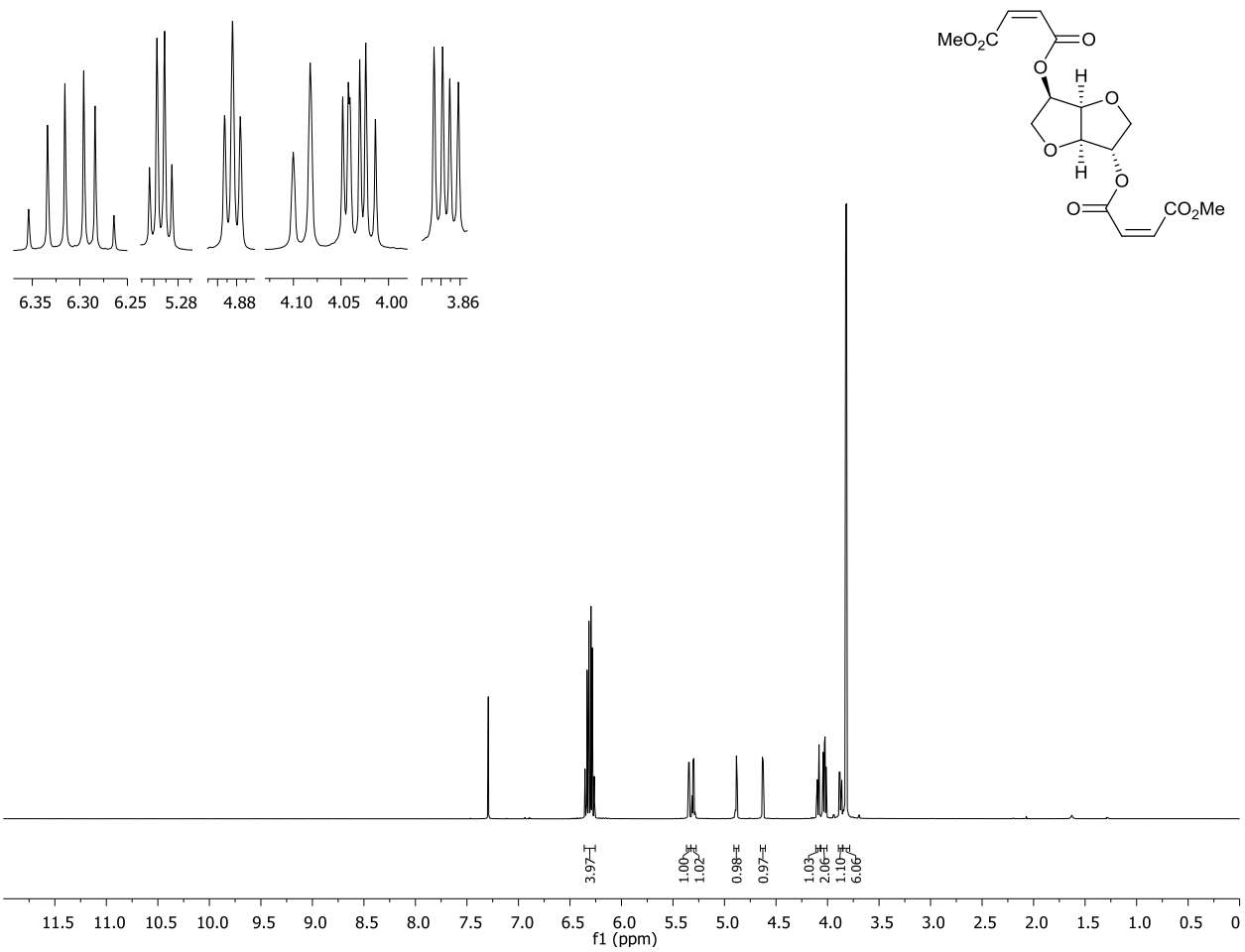

Figure S7. ^{1}H NMR (600 MHz, $CDCl_3$) of methyl ester **12**

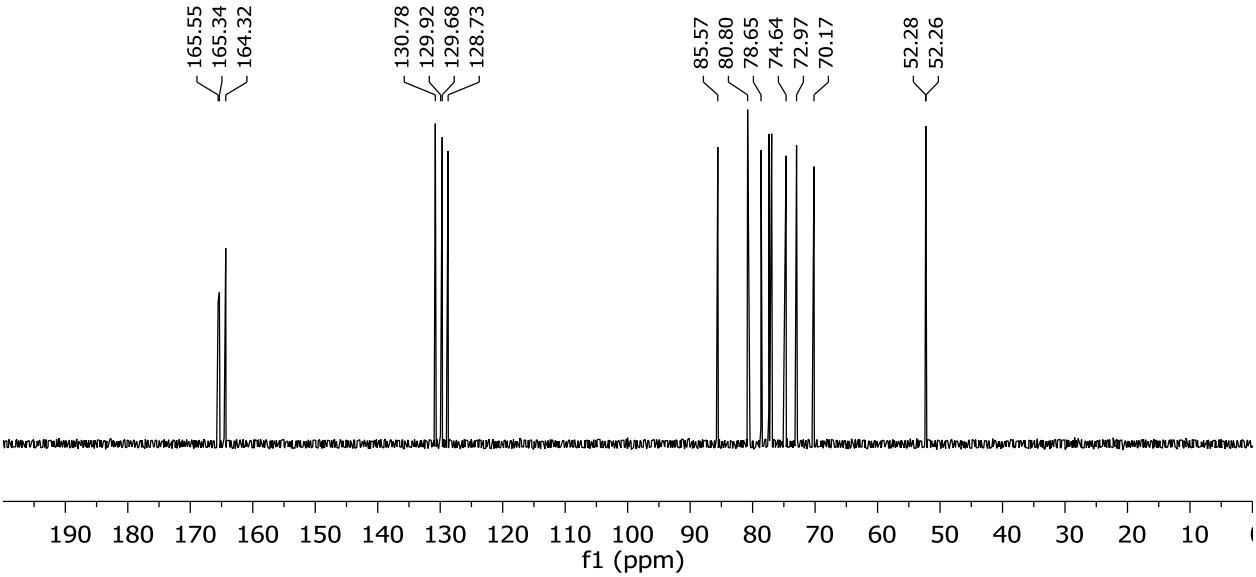

Figure S8. ^{13}C NMR (150 MHz, $CDCl_3$) of methyl ester **12**

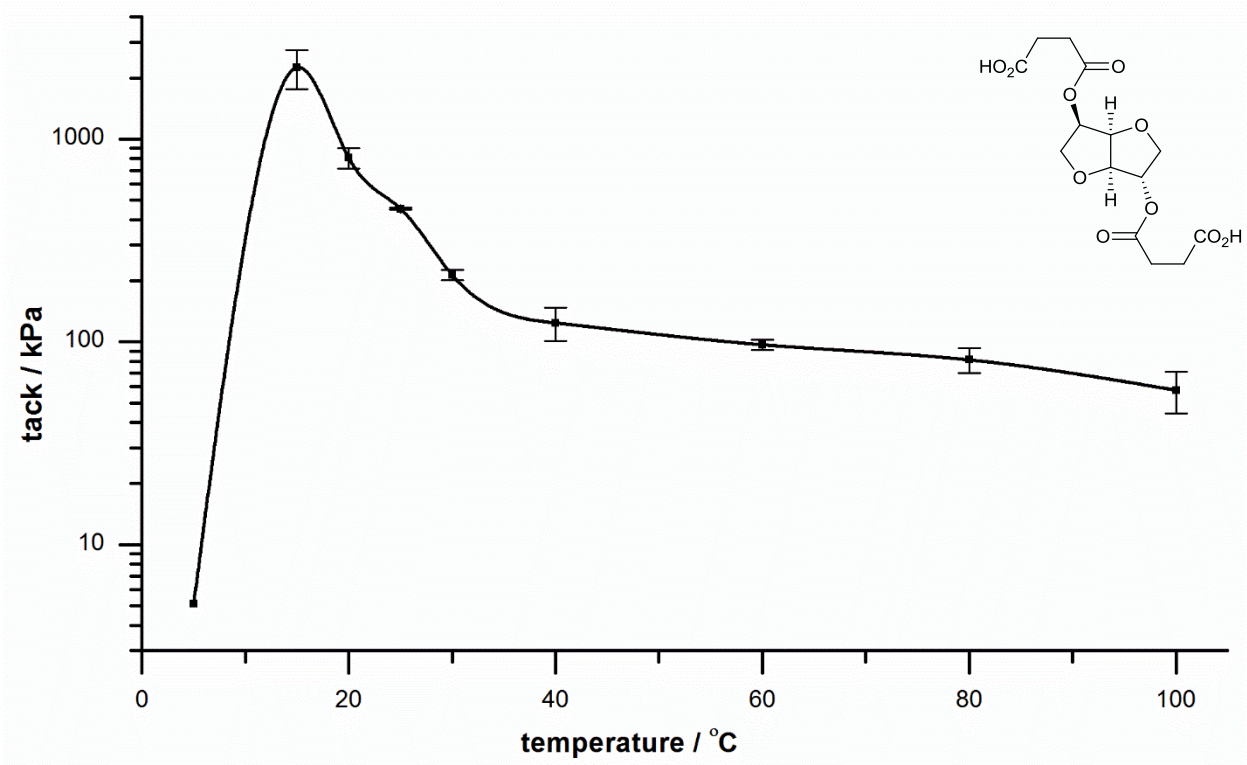

Figure S9. Tack vs. temperature curve (modified ASTM D2979 standard) for diacid **5**

Note: Tack at 10 °C is not reported because at that temperature, the sample sometimes showed no tack and sometimes showed near-maximum tack.

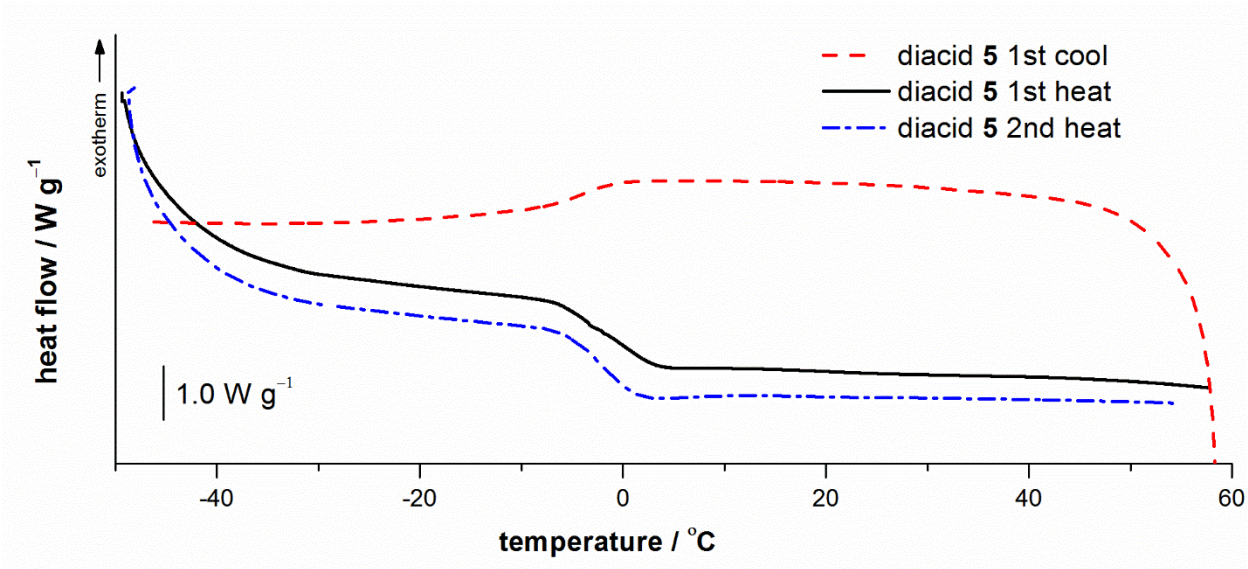

Figure S10. DSC curves (He, 10 °C min^{-1}) for diacid **5**

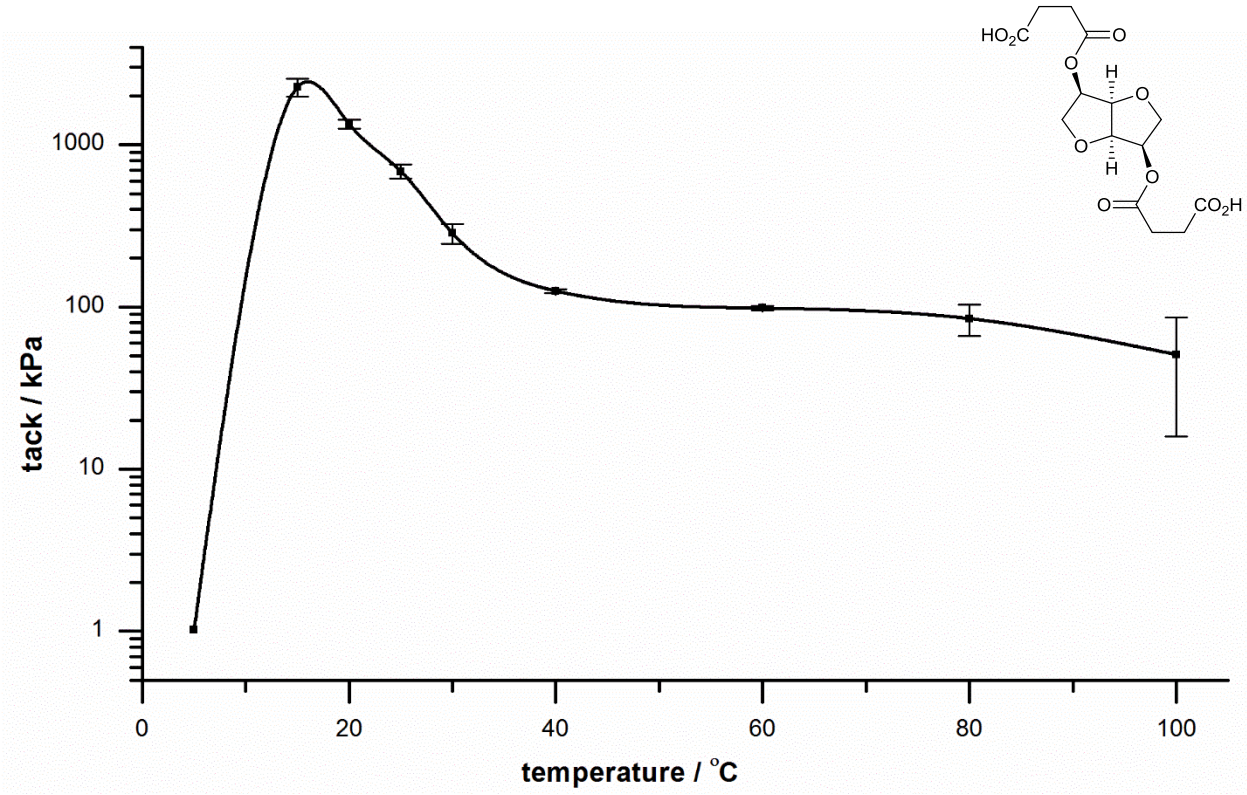

Figure S11. Tack vs. temperature curve (modified ASTM D2979 standard) for diacid **7**

Note: Tack at 10 °C is not reported because at that temperature, the sample sometimes showed no tack and sometimes showed near-maximum tack.

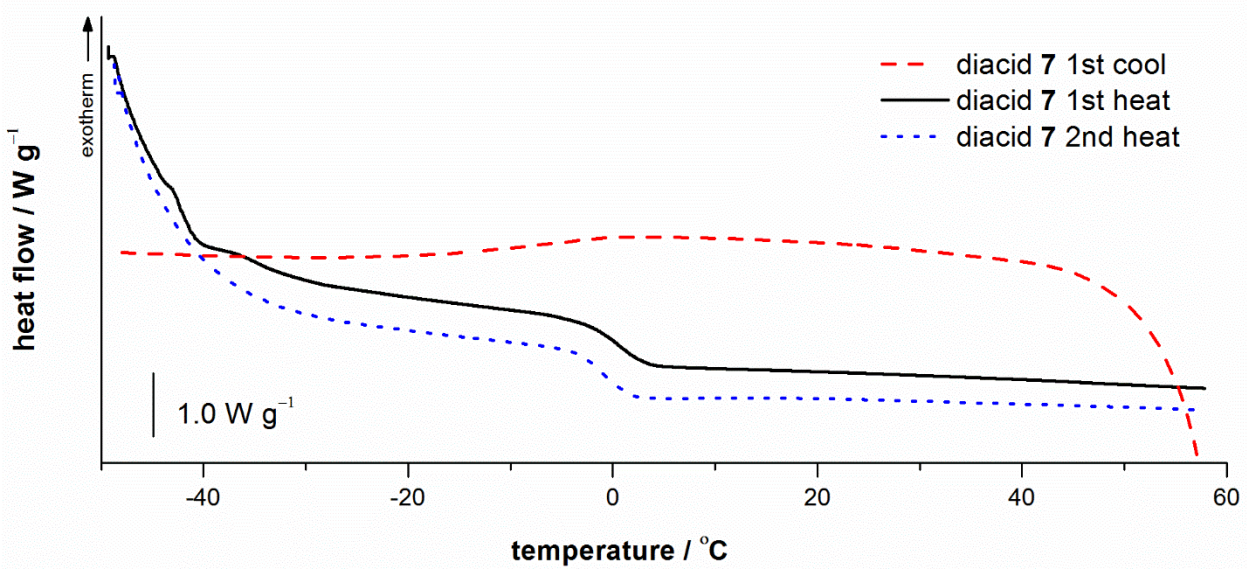

Figure S12. DSC curves (He, 10 °C min^{-1}) for diacid **7**

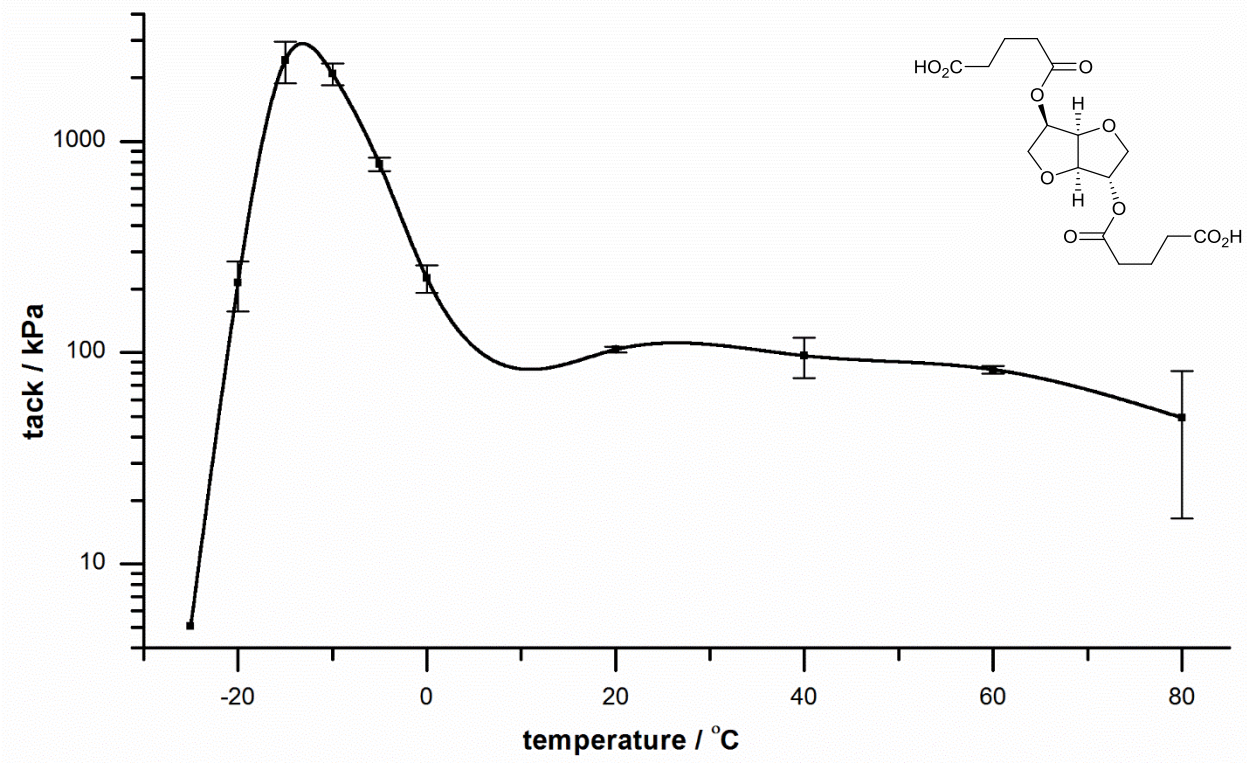

Figure S13. Tack vs. temperature curve (modified ASTM D2979 standard) for diacid **8**

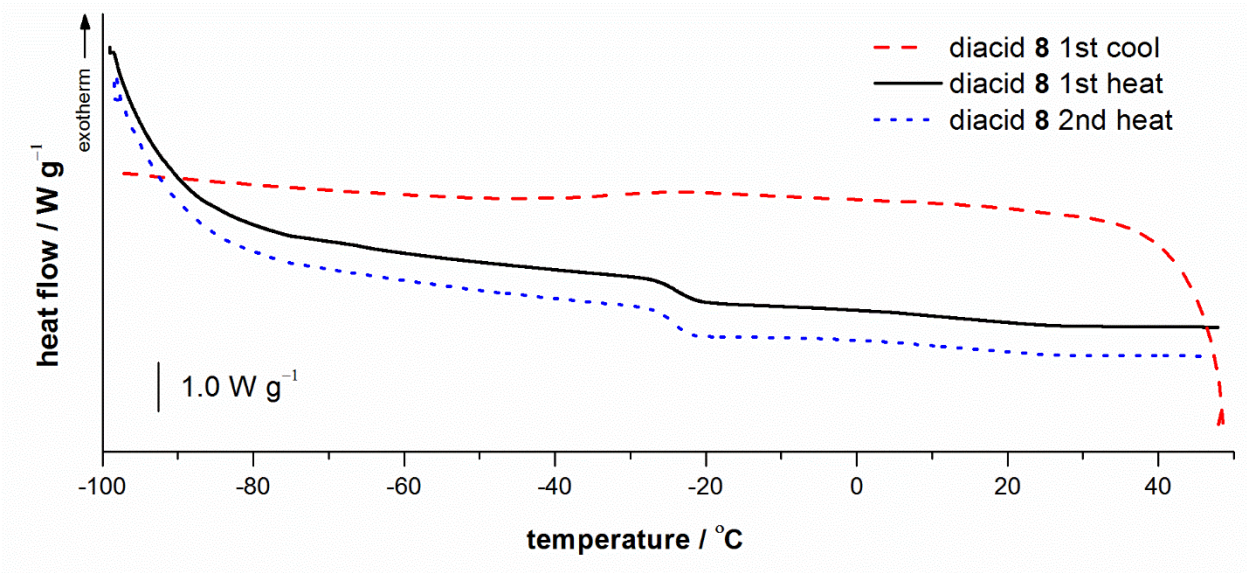

Figure S14. DSC curves (He, 10 °C min^{-1}) for diacid **8**

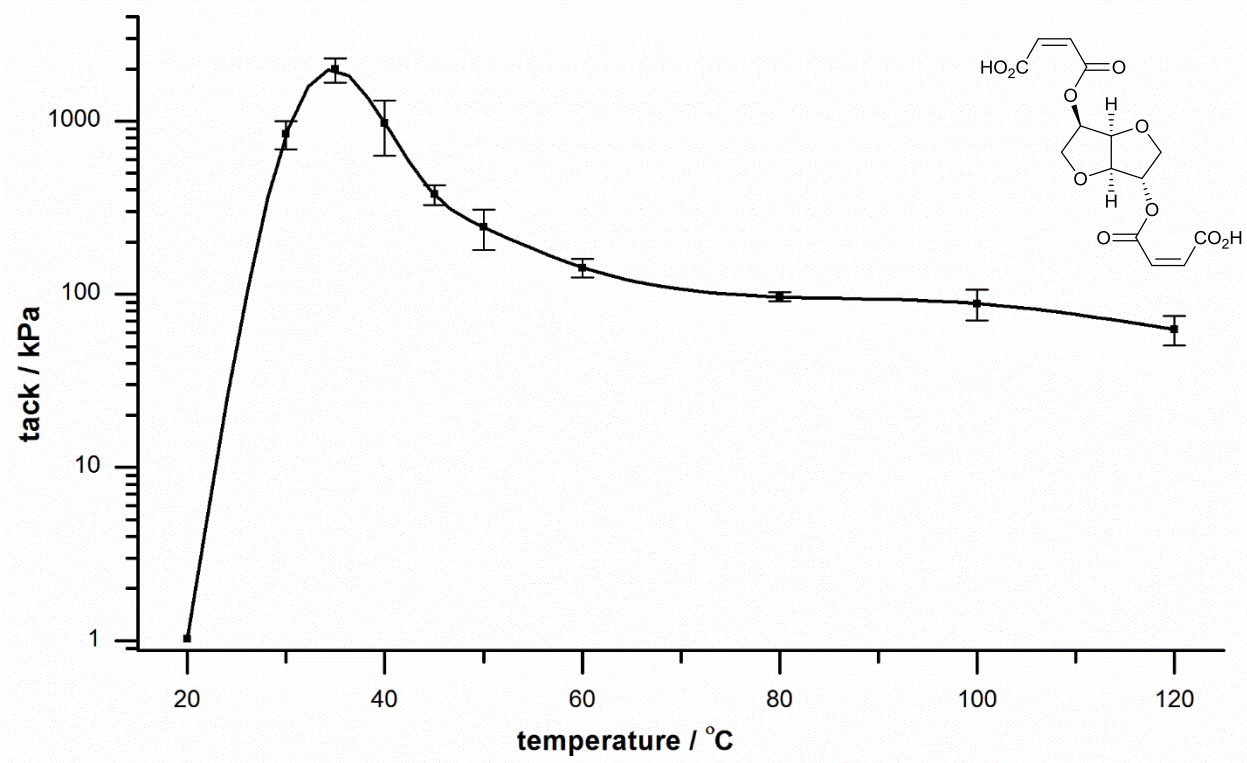

Figure S15. Tack vs. temperature curve (modified ASTM D2979 standard) for diacid **9**

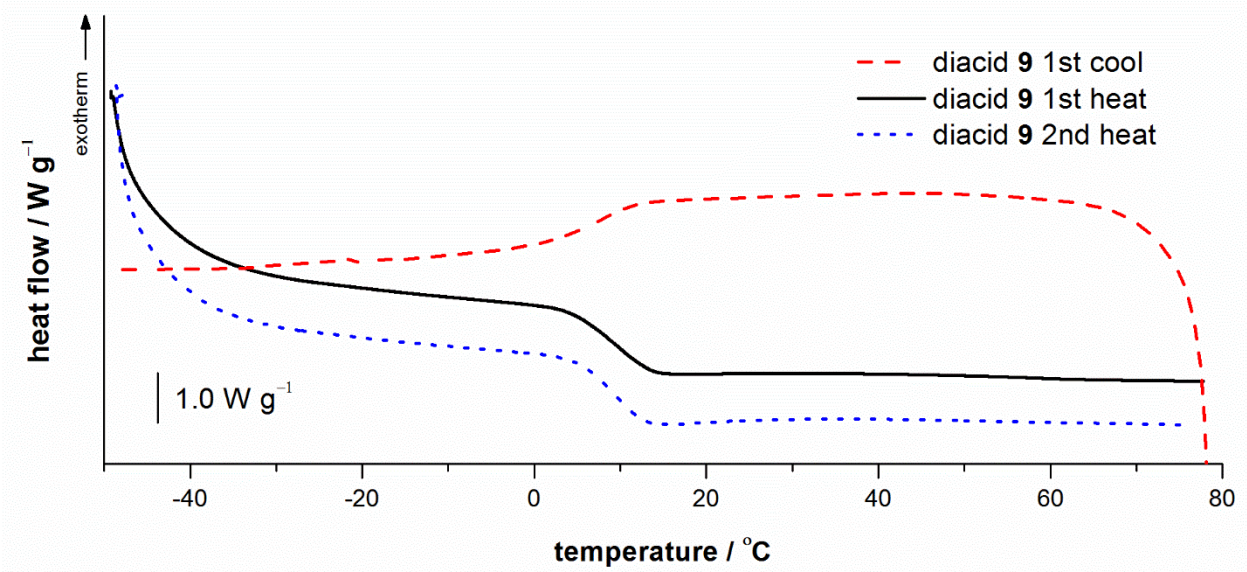

Figure S16. DSC curves (He, 10 °C min^{-1}) for diacid **9**

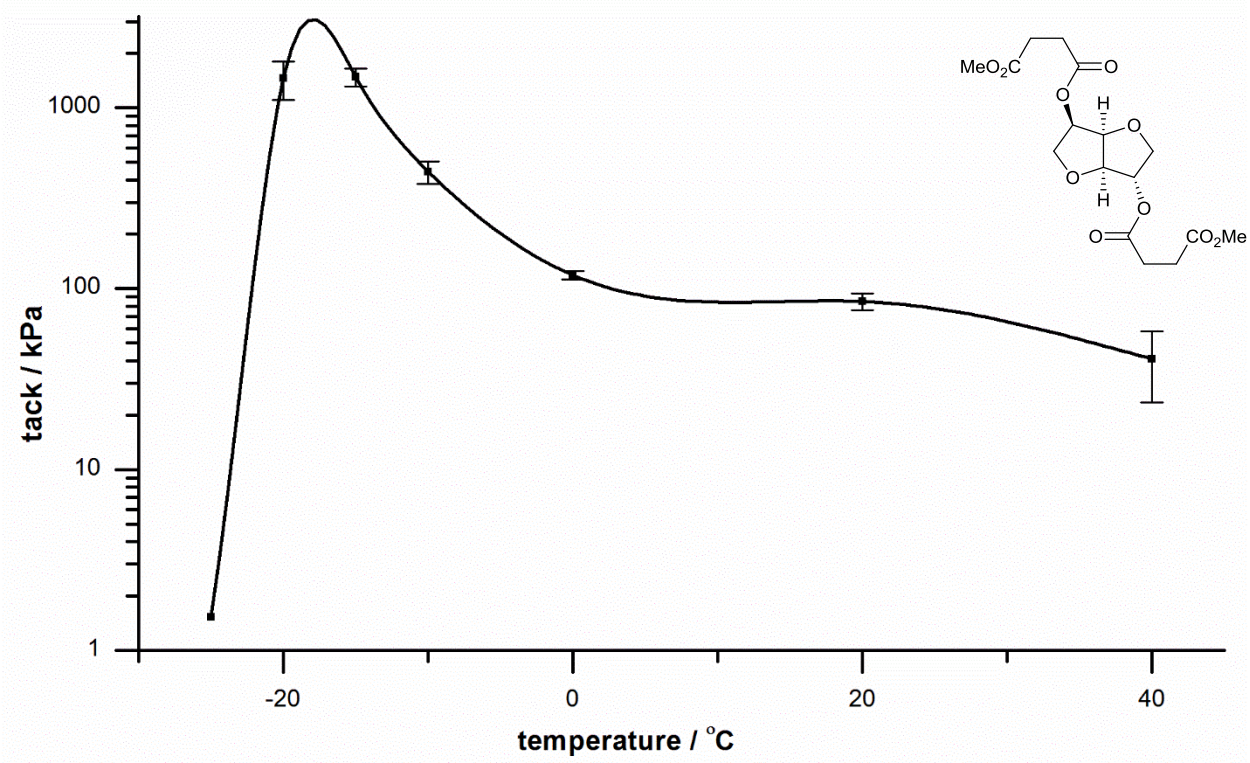

Figure S17. Tack vs. temperature curve (modified ASTM D2979 standard) for methyl ester **10**

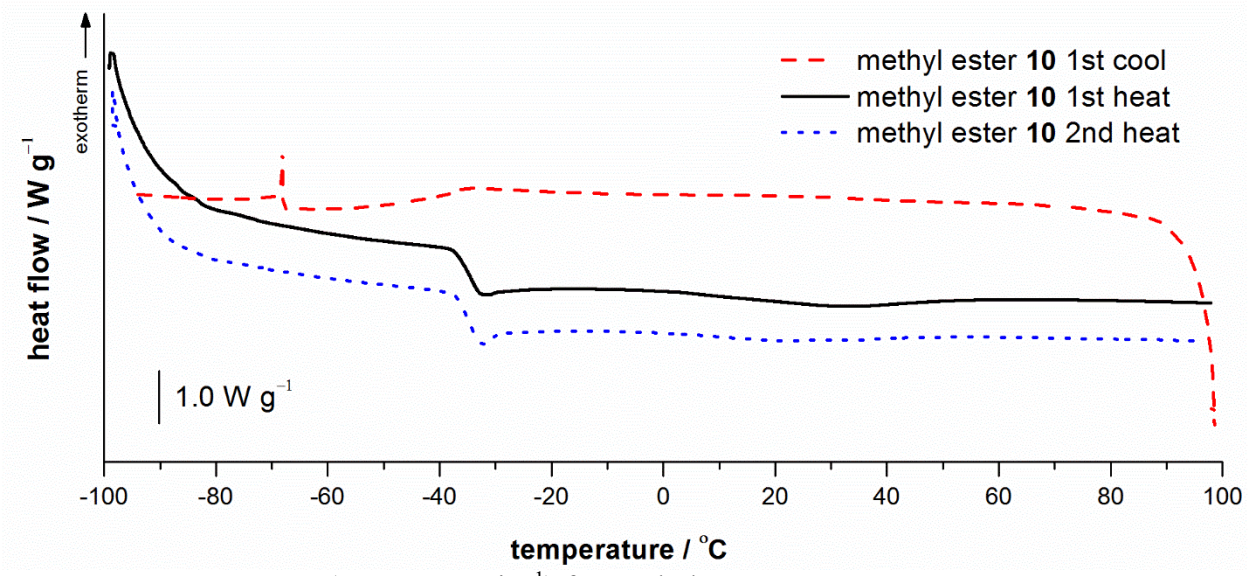

Figure S18. DSC curves (He, 10 °C min^{-1}) for methyl ester **10**

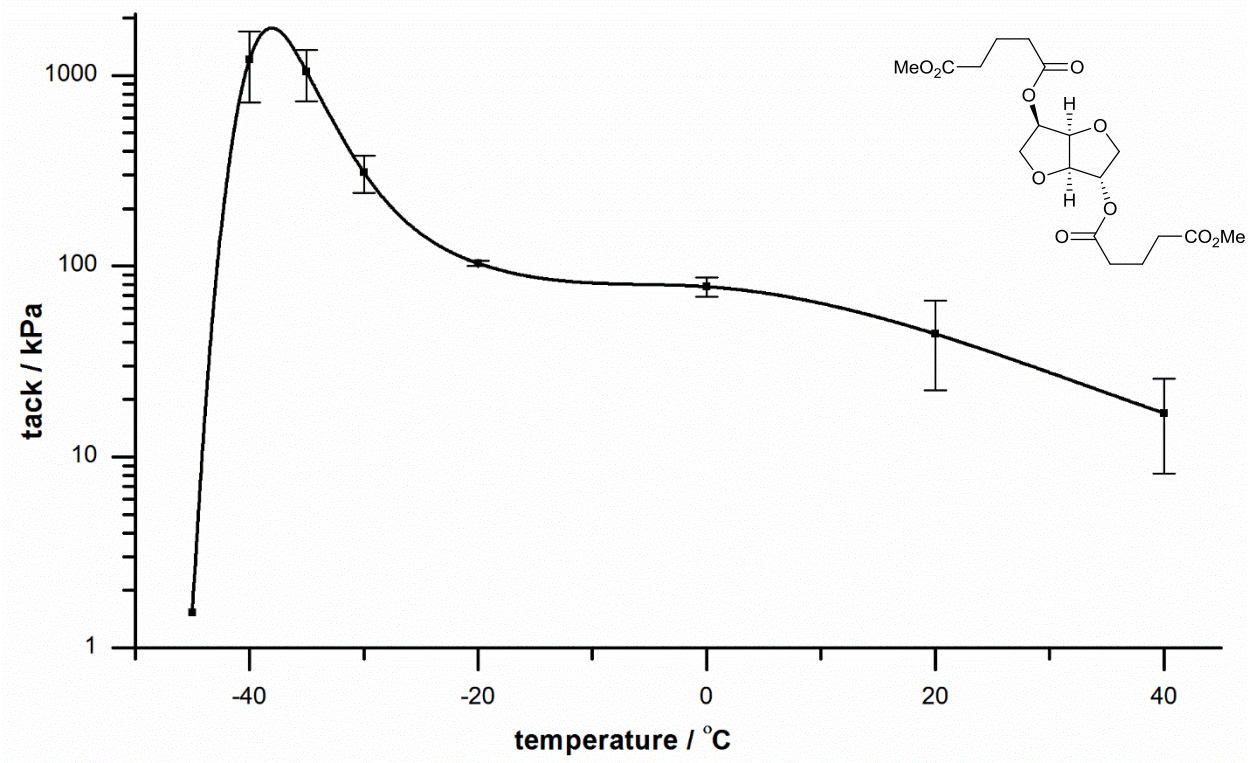

Figure S19. Tack vs. temperature curve (modified ASTM D2979 standard) for methyl ester **11**

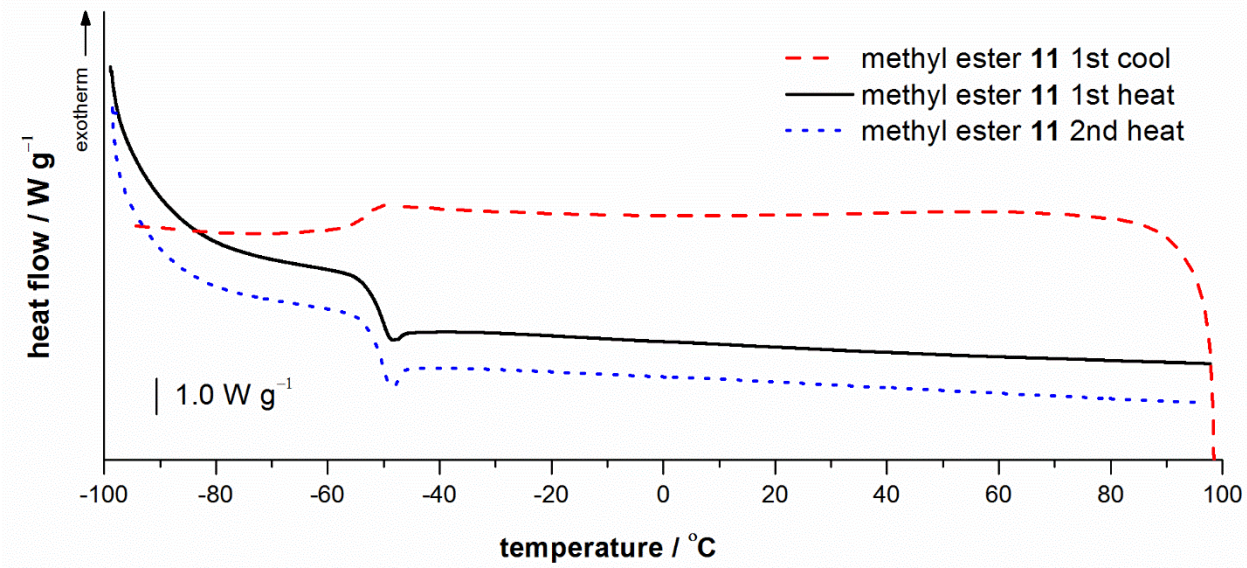

Figure S20. DSC curves (He, 10 °C min^{-1}) for methyl ester **11**

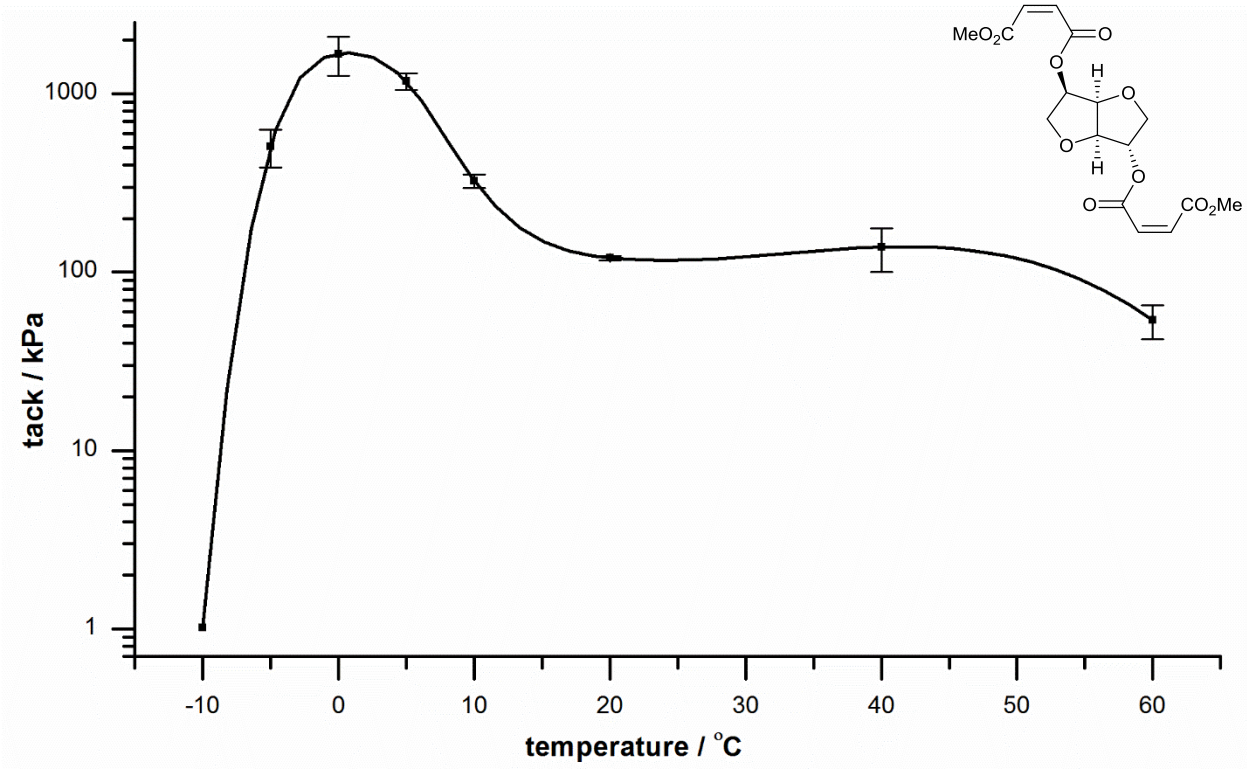

Figure S21. Tack vs. temperature curve (modified ASTM D2979 standard) for methyl ester **12**

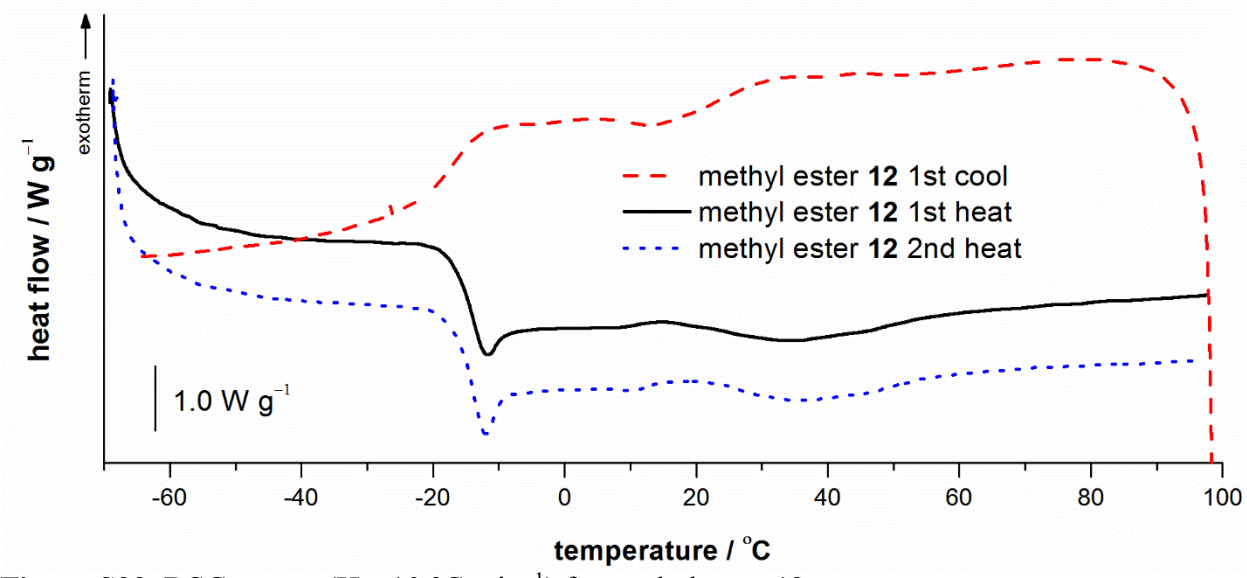

Figure S22. DSC curves (He, 10 °C min^{-1}) for methyl ester **12**

References

[1] For the definition of tack and tackifiers, see: a) Standard Terminology of Adhesives D907-11a, *American Society for Testing and Materials*, Philadelphia, PA, Vol. 15.06, **2012**, 33 – 44; for some reviews on tackifiers, see: b) I. Benedek, M. M. Feldstein (eds.), *Technology of Pressure-Sensitive Adhesives and Products*, CRC Press, Boca Raton, **2009**, p. 576; c) A. V. Pocius, *Adhesion and Adhesives Technology*, 2nd ed., Hanser, Cincinnati, **2002**, pp. 242 – 259.

[2] Y. Hu, C. W. Paul, "Block Copolymer-Based Hot-Melt Pressure-Sensitive Adhesives" in *Technology of Pressure-Sensitive Adhesives and Products* (I. Benedek, M. M. Feldstein, eds.), CRC Press, Boca Raton, **2009**, pp. 3-1 – 3-45.

[3] a) V. J. Levin, R. J. Stephan, A. I. Leonov, "Tackiiers and Antimisting Additives" in *Lubricant Additives: Chemistry and Applications*, 2nd ed., CRC Press, Boca Raton, **2009**, pp. 357 – 375.

[4] M. D. Zenner, Y. Xia, J. S. Chen, M. R. Kessler, *ChemSusChem*, **2013**, 6, 1182 – 1185.

[5] a) D. S. van Es, *J. Renew. Mater.* **2013**, 1, 61 – 72; b) M. Rose, R. Paklovits, *ChemSusChem.* **2012**, 5, 167 – 176; c) F. Fenouillot, A. Rousseau, G. Colomines, R. Saint-Loup, J.-P. Pascault, *Prog. Polym. Sci.* **2010**, 35, 578 – 622.

[6] a) J. B. McKinlay, C. Vieille, J. G. Zeikus, *Appl. Microbiol. Biotechnol.* **2007**, *76*, 727 – 740; b) C. S. K. Lin, R. Luque, J. H. Clark, C. Webb, C. Du, *Biofuels, Bioproducts and Biorefining* **2011**, *6*, 88 – 104; c) K.-K. Cheng, X.-B. Zhao, J. Zeng, J.-A. Zhang, *Biofuels, Bioproducts and Biorefining* **2012**, *6*, 302 – 318.

[7] Standard Test Method for Tack of Pressure-Sensitive Adhesives by Rolling Ball D3121-06, *American Society for Testing Materials*, Philidelphia, PA, **2006**

[8] Standard Test Method for Pressure-Sensitive Tack of Adhesives Using an Inverted Probe Machine D2979 – 01, *American Society for Testing Materials*, Philidelphia, PA, Vol. 15.06, **2012**, 212 – 214.

[9] J. V. Kurian, Y. Liang, United States Patent US6,737,481, **2004**.

[10] Hydrogen-bonded carboxylic acid FTIR stretches: 3527 (diacid **5**), 3620 (**7**), 3422 (**8**), and 3527 (**9**) cm^{-1}.

[11] The methyl esters were scrupulously purified by vacuum distillation (**10** and **11**) or column chromatography (**12**).

[12] a) P. J, Carreau, D. C. R. De Kee, R. P. Chabra, *Rheology of Polymeric System: Principles and Applications*, Hanser/Gradner Publications, Cincinnati OH, **1997**, p. 520; b) P. J. Carreau, D. De Kee, *The Canadian Journal of Chemical Engineering*, **1979**, 57, 3 – 15.

CHAPTER 4

DIVERGENT THERMAL POLYMERIZATION PATHWAYS OF TWO ISOSORBIDE-MALEIC ACID DERIVATIVES

M. D. Zenner, J. S. Chen, S. A. Madbouly, **manuscript in progress**

Introduction

Isosorbide (**1**, Figure 1) is a sorbitol-derived diol used in the production of a vasodilator and the manufacture of a specialty solvent for cosmetics.[1–4] Due to its rigidity, thermal stability, and lack of toxicity, isosorbide is also widely viewed as a promising biorenewable filler,[5,6] monomer,[7–11] or monomer precursor.[12–17] We recently designed an isosorbide- and succinic acid-based diisocyanate in which 100% of the carbon content can be derived from biorenewable resources.[18] As an unexpected offshoot of this work, we identified a series of promising tackifiers, including diacids **2** and **3**.[19] Used extensively in pressure-sensitive adhesives, tackifiers are glassy small molecules (monomers or oligomers) that instantaneously form a non-covalent bond to a surface (i.e., are tacky).[20–23]

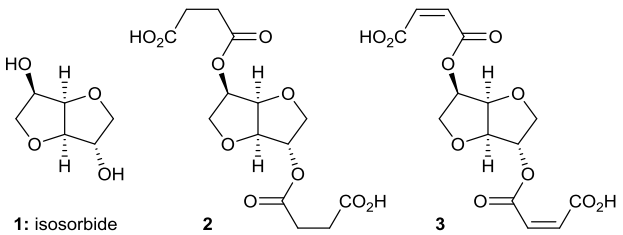

Figure 1. Isosorbide (**1**) and two isosorbide-based tackifiers (**2** and **3**).

We reasoned that the ability to introduce additional chemical functionality such as the alkenes in maleic acid-derived tackifier **3** should allow us to design "smart" tackifiers that would change properties, either reversibly or permanently, in response to pre-defined external stimuli. As a test case, we hypothesized that thermally-induced radical polymerization of diacid **3** should yield a heavily-crosslinked thermoset. Herein we show that the related dimethyl ester (**5**, Scheme 1) undergoes the expected radical polymerization, but diacid **3** forms a polyester thermoplastic.

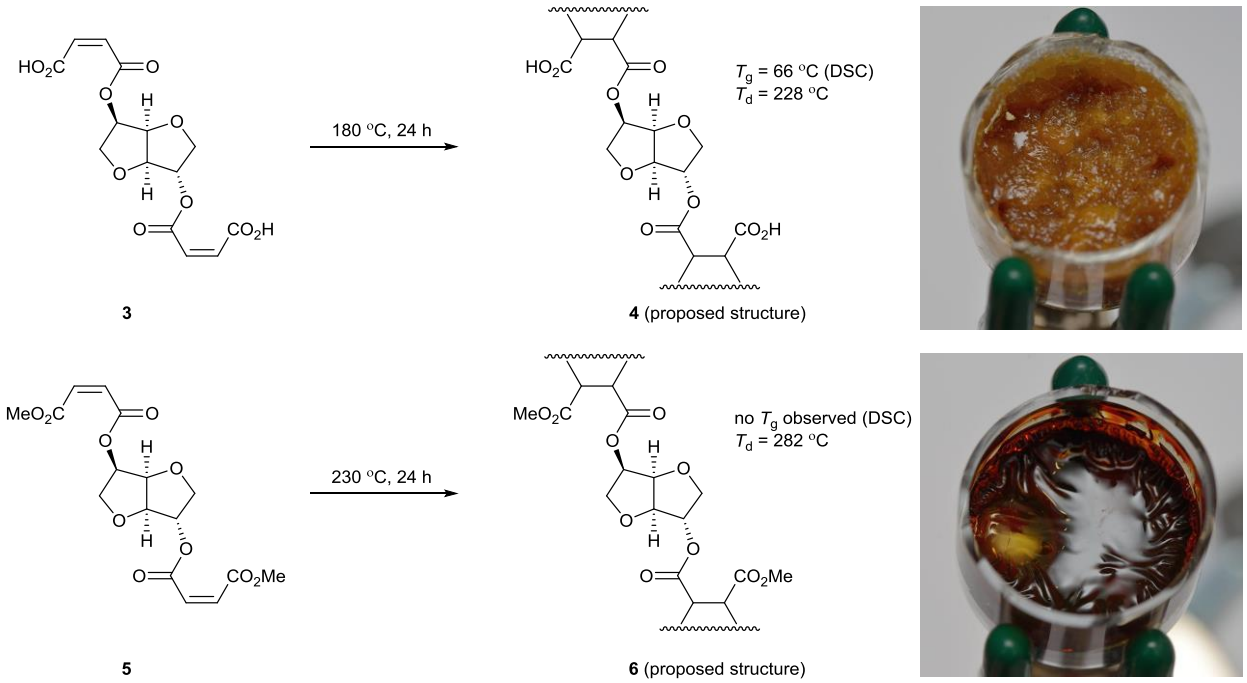

Scheme 1. Thermal polymerization of monomers **3** and **5**.

Results and Discussion

Diacid **3** and the corresponding dimethyl ester (**5**, Scheme 1) were heated to polymerization. Interestingly, methyl ester **5** was much less prone to polymerization than diacid **3**; diacid **3** polymerized at 180 °C, but methyl ester **5** did not react until 230 °C. Furthermore, the physical appearances of the resultant polymers also differed significantly. Whereas diacid **3** polymerized into a light-colored solid with an uneven surface (**4**, initially-proposed structure), methyl ester **5** turned into a dark-colored solid with a smooth surface (**6**). The high polymerization temperatures were not surprising since maleates are known to resist radical homopolymerization (but can co-polymerize with other alkenes such as styrene).[25] Maleate homopolymerizations often proceed through an initial alkene isomerization to the more-readily polymerized fumarate isomer.[26–29] However, the large difference in the required temperature for polymerization of diacid **3** and methyl ester **5** and in the morphology of the resultant polymers (**4** and **6**) alerted us to the

possibility of different polymerization mechanisms. Therefore, we decided to further characterize the two polymerizations.

We then turned to ^{1}H NMR spectroscopy to characterize the polymerization pathways. Aliquots of a polymerization of diacid **3** were obtained at time points from 0 minutes to 120 minutes (see Figure 2). The end point of 120 minutes was chosen because aliquots obtained at later time points did not fully dissolve.

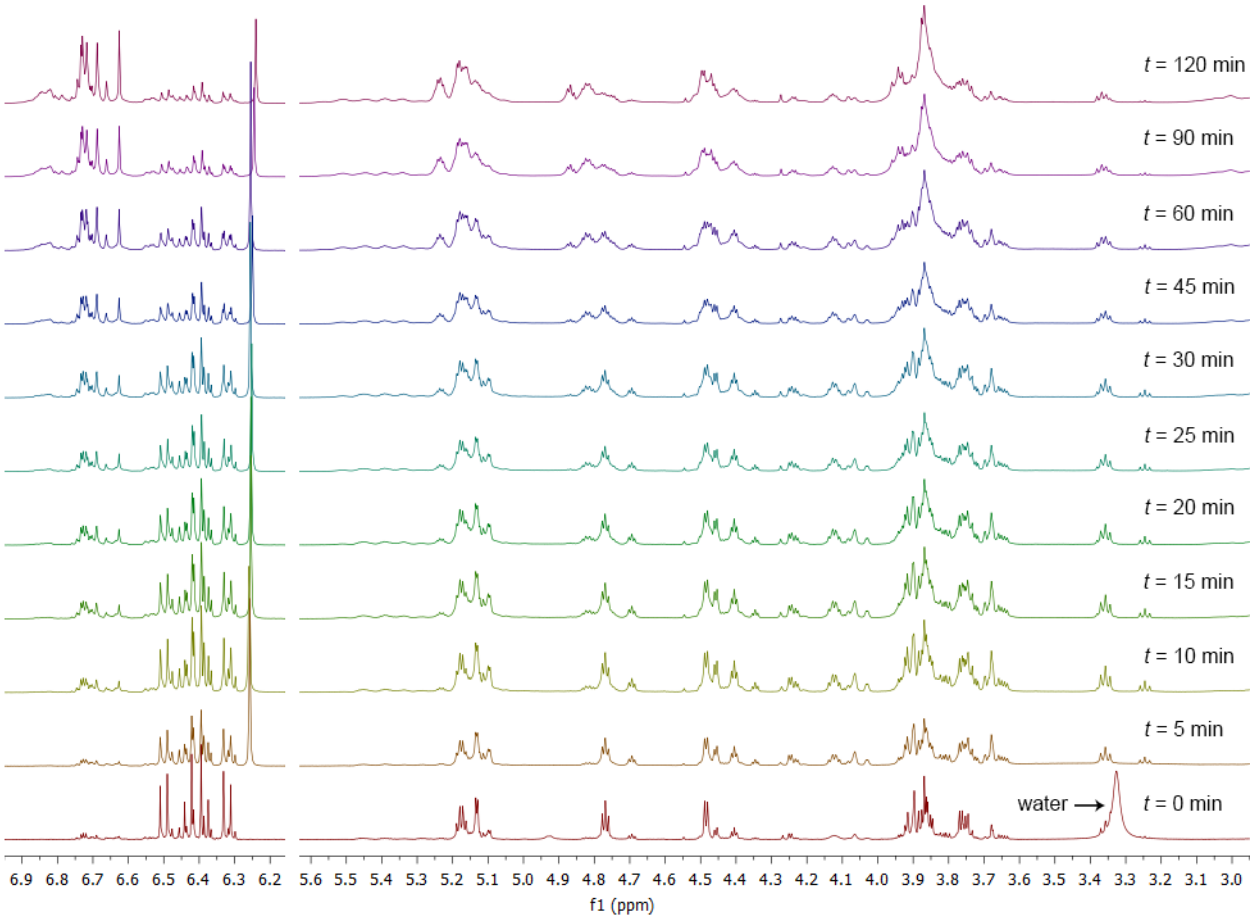

Figure 2. Time-dependent ^{1}H NMR spectra of the polymerization of diacid **3.**

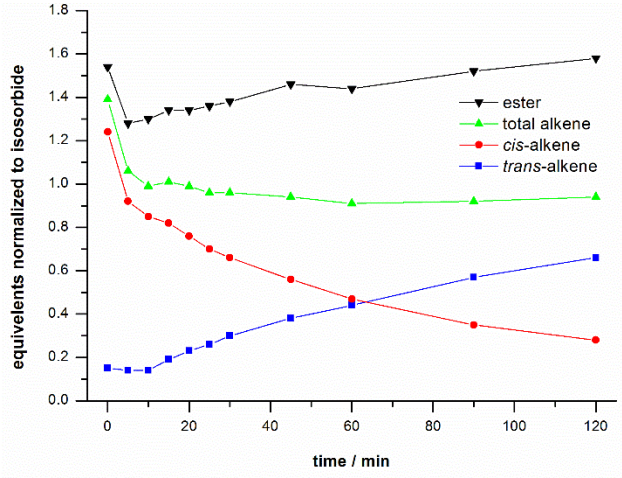

Figure 3. Time-dependent number of equivalents (normalized to isosorbide content) of ester and alkene during the polymerization of diacid **3**.

We determined by a phase-edited HSQC spectrum (see Supporting Information) that although multiple isosorbide-containing species were present, one of the hydrogens present at the isosorbide ring fusion was always found in a narrow chemical shift range (4.56 to 4.30 ppm). No other hydrogens were observed in this region of the spectrum, and therefore the integration of this region corresponded to the isosorbide content of the sample. By analyzing unreacted diacid **3** and a sample of diacid **3** that had been heated for 120 minutes by ^{1}H NMR spectroscopy in the presence of an internal standard (*N*,*N*-dimethylformamide), we further determined that no isosorbide was lost or decomposed under these reaction conditions. Therefore, absolute quantities of various chemical fragments in the aliquots could be determined from the ^{1}H NMR spectra by setting the integration of the chemical shift range from 4.56 to 4.32 ppm to one proton. The amounts of ester (5.28 to 5.04 ppm), *cis*-alkene (6.58 to 6.28 ppm; integrated range does not overlap maleic anhydride or maleic acid), and *trans*-alkene (6.93 to 6.65 ppm; integrated range does not overlap fumaric acid) as a function of time are plotted in Figure 3.

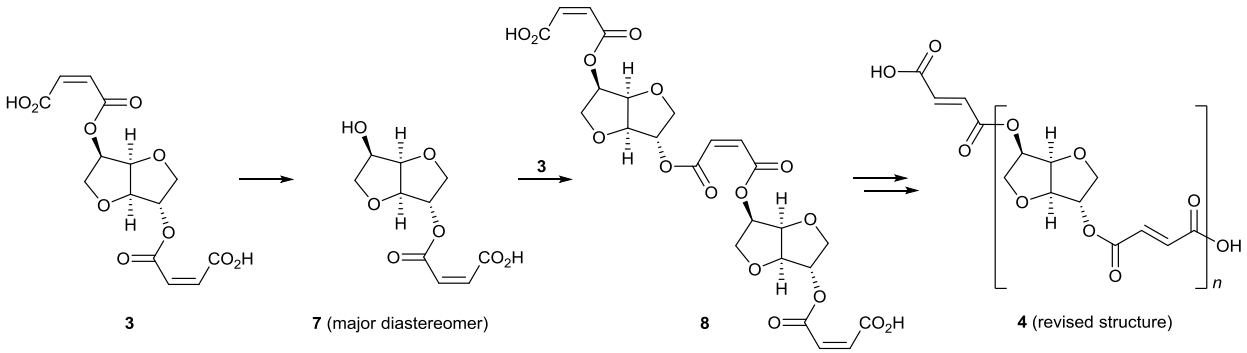

Scheme 2. Proposed polymerization Mechanism for diacid **3**

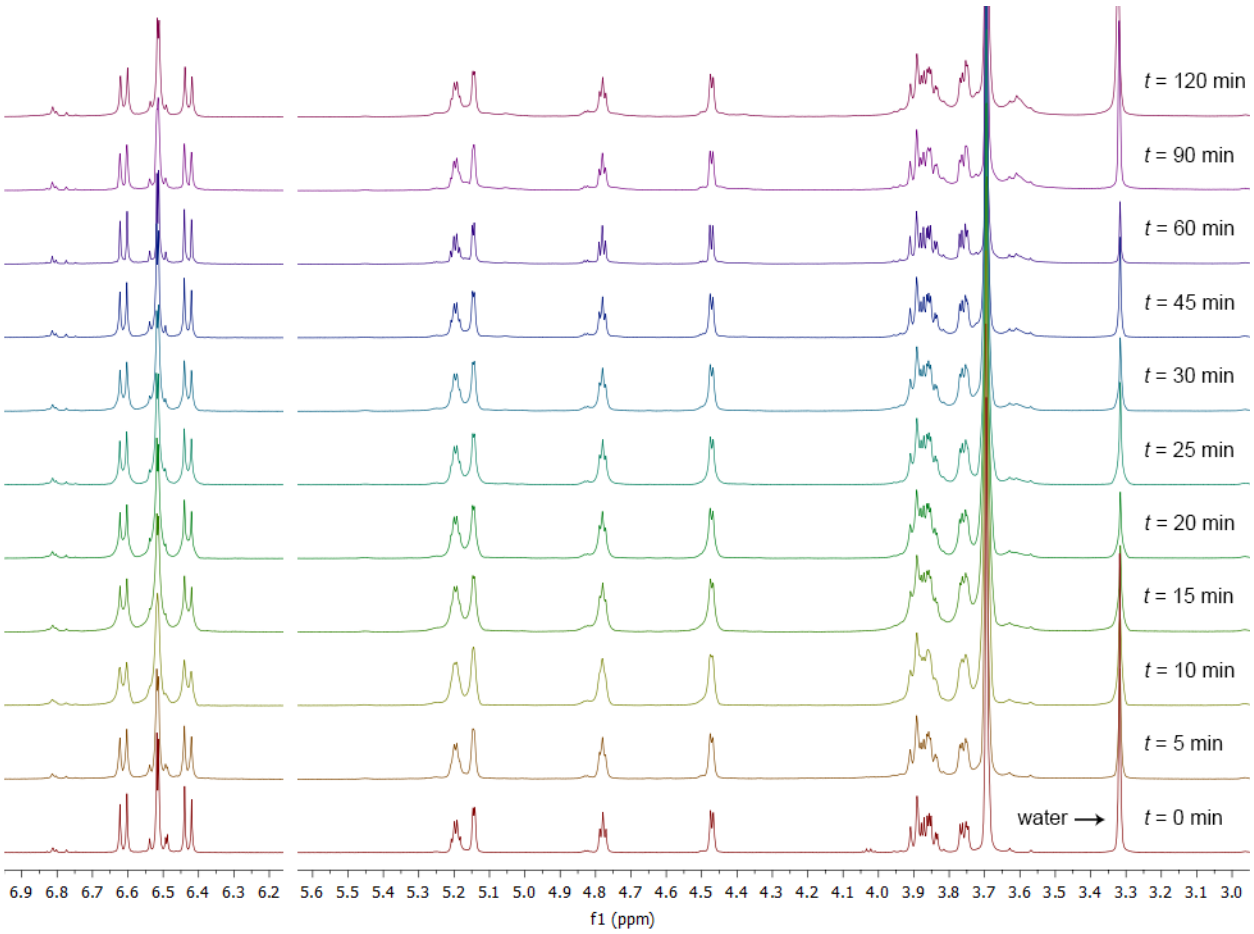

Figure 4. Time-dependent ^{1}H NMR spectra of the polymerization of dimethyl ester **5**.

Analysis of the data from the polymerization of diacid **3** revealed a loss of ester linkages and *cis* alkenes during the early stages of the reaction (t = 0 – 5 min) consistent with rapid expulsion of maleic anhydride (see **7**, Scheme 2). Afterwards, the number of ester linkages per isosorbide unit climbed back up while the number of alkenes per isosorbide unit stabilized near 1.0. This is consistent with a condensation reaction to form an ester linkage between the free hydroxyl group of

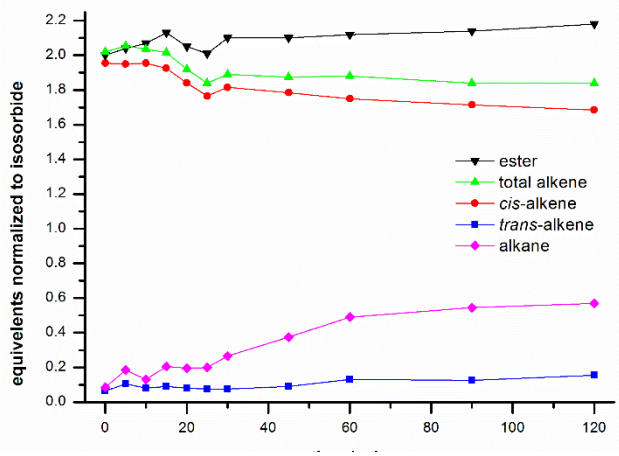

Figure 5. Time-dependent number of equivalents (normalized to isosorbide content) of ester, alkene, and alkane during the polymerization of dimethyl ester **5**.

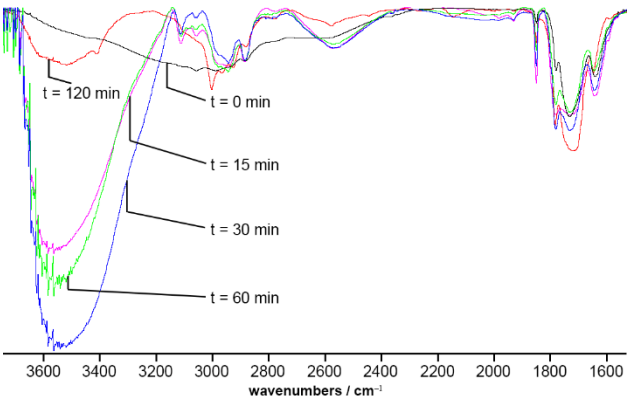

Figure 6. Time-dependent IR spectra during the polymerization of diacid **3.**

compounds such as **7** and a maleate carboxylic acid to form oligomeric species such as **8**. Furthermore, the alkenes undergo a thermodynamically-favorable isomerization under the reaction conditions, slowly converting maleates into fumarates. The combination of further polymerization and alkene isomerization yields polyester **4** (revised structure). The NMR spectra of the aliquots do not show evidence of radical polymerization under these reaction conditions.

The polymerization of dimethyl ester **5** was analyzed by ^{1}H NMR spectroscopy in the same manner (see Figures 4 and 5). In sharp contrast with the polymerization of diacid **3**, the polymerization of dimethyl ester **5** did not involve ester bond cleavage or subsequent condensation polymerization. Furthermore, a new NMR signal appeared between 3.65 and 3.54 ppm, providing direct experimental evidence for the radical polymerization pathway depicted in Scheme 1. The concentration of *trans*-alkene stayed low even though maleates generally isomerize to fumarates before undergoing radical polymerization.[25–29] This result is consistent with a slow alkene isomerization step and a fast polymerization of the *trans* alkene.

Since ^{1}H NMR spectroscopy suggested an unexpected polymerization pathway for diacid **3**, we turned to IR spectroscopy and rheology for further verification of this result. IR spectra of selected aliquots (Figure 6) provided additional evidence for the polymerization pathway outlined in Scheme 2. Initially the IR spectrum showed predominantly intramolecular hydrogen bonding consistent with maleate mono-acids. A strong hydroxyl stretch consistent with free alcohols quickly appeared. This new stretch reduced in intensity after 30 minutes, but did not completely

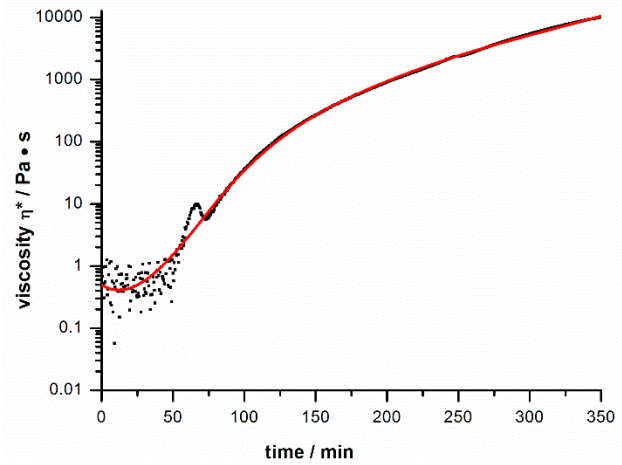

Figure 7. Time-dependent complex viscosity (η*) at 180 °C and 10 rad s^{-1} during the polymerization of diacid **3**.

disappear because the oligomeric material present after 120 minutes of heating contained some fumarate mono-acids.

The polymerization of diacid **3** was also followed by dynamic rheology (see Figure 7). No change in complex viscosity (η*) was observed in the first 50 minutes. Afterwards, viscosity increased, with viscosity reaching 11,200 Pa s (at 180 °C) after 350 minutes at 180 °C. The smooth increase in viscosity suggested that the polymerization pathway characterized in the first 120 minutes is the same one operative at later time points.

A 120 minute aliquot from the polymerization of diacid **3** was reacted with methyl iodide in the presence of potassium carbonate to convert the carboxylic acids into methyl esters for analysis by gel permeation chromatography (GPC).[30] At this early stage of polymerization, the weight-averaged molecular weight (M_w) was 1451 and the number-averaged molecular weight (M_n) was 710.

We wondered whether the oligomeric material formed by heat-treating diacid **3** for 120 minutes (hereafter referred to as **4′**) might be a higher-temperature tackifier. The glass transition temperature (T_g) for oligomer **4′** was determined by DSC to be 49 °C (compare with 10 °C for diacid **3**).[19] Temperature-dependent tack was determined using our previously-

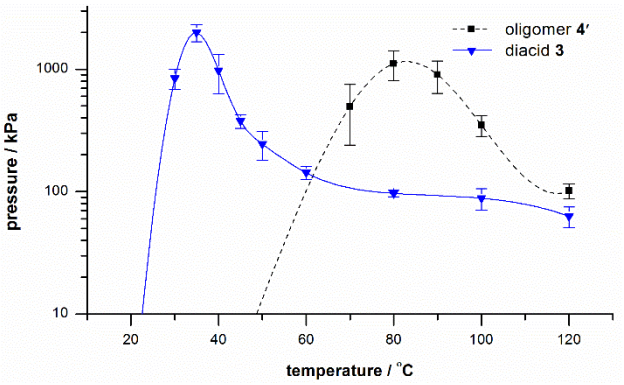

Figure 8. Temperature-dependent tack of diacid **3** [19] and oligomer **4′** (prepared by heating diacid **3** at 180 °C for 120 minutes).

described modified ASTM D2979 protocol.[19] As shown in Figure 8, oligomerization resulted in tack at a higher temperature range, with oligomer **4′** most tacky at 80 °C (compare with 35 °C for diacid **3**). The oligomeric material was a little less tacky (1100±300 kPa for oligomer **4′**, compare with 2000±300 kPa for diacid **3**), but high tack was available over a broader temperature range. Thus, oligomerization of isosorbide-based tackifiers such as diacid **3** offers a potential means to access derivatives that perform at a higher temperature range.

Conclusion

In conclusion, ^{1}H NMR spectroscopy revealed divergent thermal polymerization pathways for an isosorbide- and maleic acid-based diacid (**3**) and a closely related dimethyl ester (**5**). Whereas dimethyl ester **5** underwent the expected radical polymerization, diacid **3** polymerized through expulsion of maleic anhydride followed by subsequent condensation reactions. Characterization of the tack properties of an oligomer generated by partial polymerization of diacid **3** (i.e., **4′**) demonstrated that oligomers of isosorbide and simple diacids may be useful as higher-temperature tackifiers.

I would like to thank Samy Madbouly for his help with and contribution of rheological experiments and analysis.

Experimental Section

General Procedures. Unless otherwise noted, all reactions were performed with stirring under an argon atmosphere under anhydrous conditions. Isosorbide was purchased from Acros Organics. Isomannide was purchased from Sigma-Aldrich. Other reagents were purchased at the most economical grade. All chemicals were used as received, without purification. Dry *N*,*N*-dimethylformamide (DMF) was obtained by passing ACS grade DMF through a Glass Contour solvent purification system. The pressures for vacuum distillations were measured during the

collection of the distillate. Yields of materials refer to distilled and spectroscopically (^{1}H NMR) homogeneous samples. NMR spectra were calibrated using residual undeuterated solvent as an internal reference. Apparent couplings were determined for multiplets that could be deconvoluted visually. Gel permeation chromatography (GPC) measurements performed using two 10μm AM-gel columns connected in series (guard, HMW, and LMW) with a UV-Vis and RI detector. Analyses were performed using $CHCl_3$ at 40 °C as the solvent with a flow rate of 1.0 mL·min^{-1}. Calibration was based on polystyrene standards as well as synthesized monomer and dimer of our compounds.

Differential scanning calorimetry (DSC) was performed on ca. 5 mg samples under a helium atmosphere, outfitted with a quench cooler, at a heat rate of 10 °C·min^{-1}; samples were then cooled back down at a rate of 20 °C·min^{-1} for a second heat. Tack testing was performed via a modified ASTM D2979 standard. Following modifications are as follows: The tests were performed on an Instron Load Frame fitted with a temperature control box. A continuous nitrogen purge was used and internal humidity was monitored using a Control Company, model 4185 traceable hygrometer, and was maintained at or below 30 % relative humidity. An aluminum plate was milled to a depth of 0.1 mm. Tack was measured in triplicates making sure no one point was measured more than once. Temperature of the sample was monitored via a Control Company, model 4015 traceable thermocouple, attached to the aluminum plate. The probe was lowered at a rate of 0.5 mm·sec^{-1}, until it was in contact with the sample at an average force of 200 kPa. The probe was held at this pressure then raised at a rate of 0.5 mm·sec^{-1}. The viscoelastic behavior of the tackifier was investigated using ARES strain-controlled rheometer (Rheometrics Scientific) with 25 mm diameter parallel plates.

Oligomerization procedure of diacid 3. Diacid **3** (5.0 g, 14.6 mmol) was added to a 20 ml vial with a small stir bar. The vial (exposed to air) was then immersed into an oil bath preheated to 180°C. Time started when the stir bar was freely rotating at approximately 650 rpm as indicated by the dial. Small aliquots were taken and stored for NMR, FTIR and GPC at selected time points.

Conversion to methyl ester. At time points 15, 30, 60, and 120 min, small aliquots were taken at converted to methyl esters for GPC analysis. An example procedure is shown for t = 120 min. To a crude solution of oligomer **4′** (356.6 mg, .96 mmol) in DMF (5 mL) at 23 °C, potassium carbonate (700 mg, 2 mmol, 2.5 equiv.) was added. The reaction was heated to 35 °C and methyl iodide (0.31 mL, 5 mmol, 2.5 equiv.) was added dropwise. After 24 h at 35 °C, the reaction mixture was dilute with 5 mL water. The reaction mixture was extracted with 3 × 5 mL ethyl acetate. The resultant organic phase was then washed with 2 × 10 mL water and 1 × 10 mL brine, then dried over $MgSO_4$. The reaction mixture was concentrated under reduced pressure to give crude dimethyl ester as a transparent yellow oil.

Internal standard check of isosorbide. Before polymerization: In a vial, diacid **3** (4.990 g, 14.6 mmol) was dissolved in 5 mL of DMSO. DMF (0.56 mL, 7.3 mmol) was then added. ^{1}H NMR was then taken to determine the amount of isosorbide present compared to a known amount DMF. After Polymerization: A separate sample of diacid **3** (5.016 g, 14.6 mmol) was placed in a preheated oil bath at 180 °C for 120 min. The product was then dissolved in 6 mL of DMSO and DMF (0.56 mL, 7.3 mmol) was added. ^{1}H NMR was taken and the amount of isosorbide present after heating was determined.

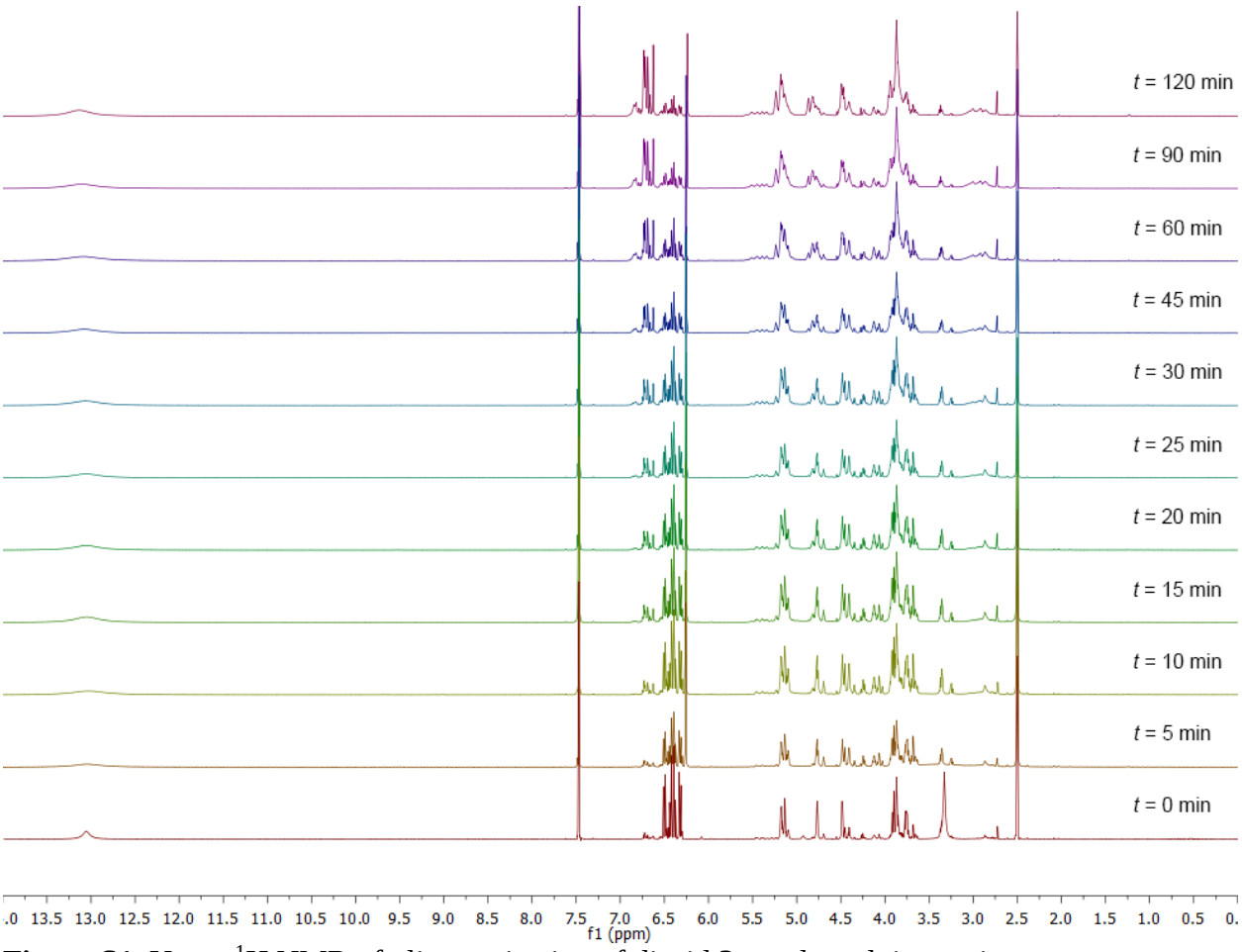

Figure S1. Uncut ^{1}H NMR of oligomerization of diacid **3** at selected time points.

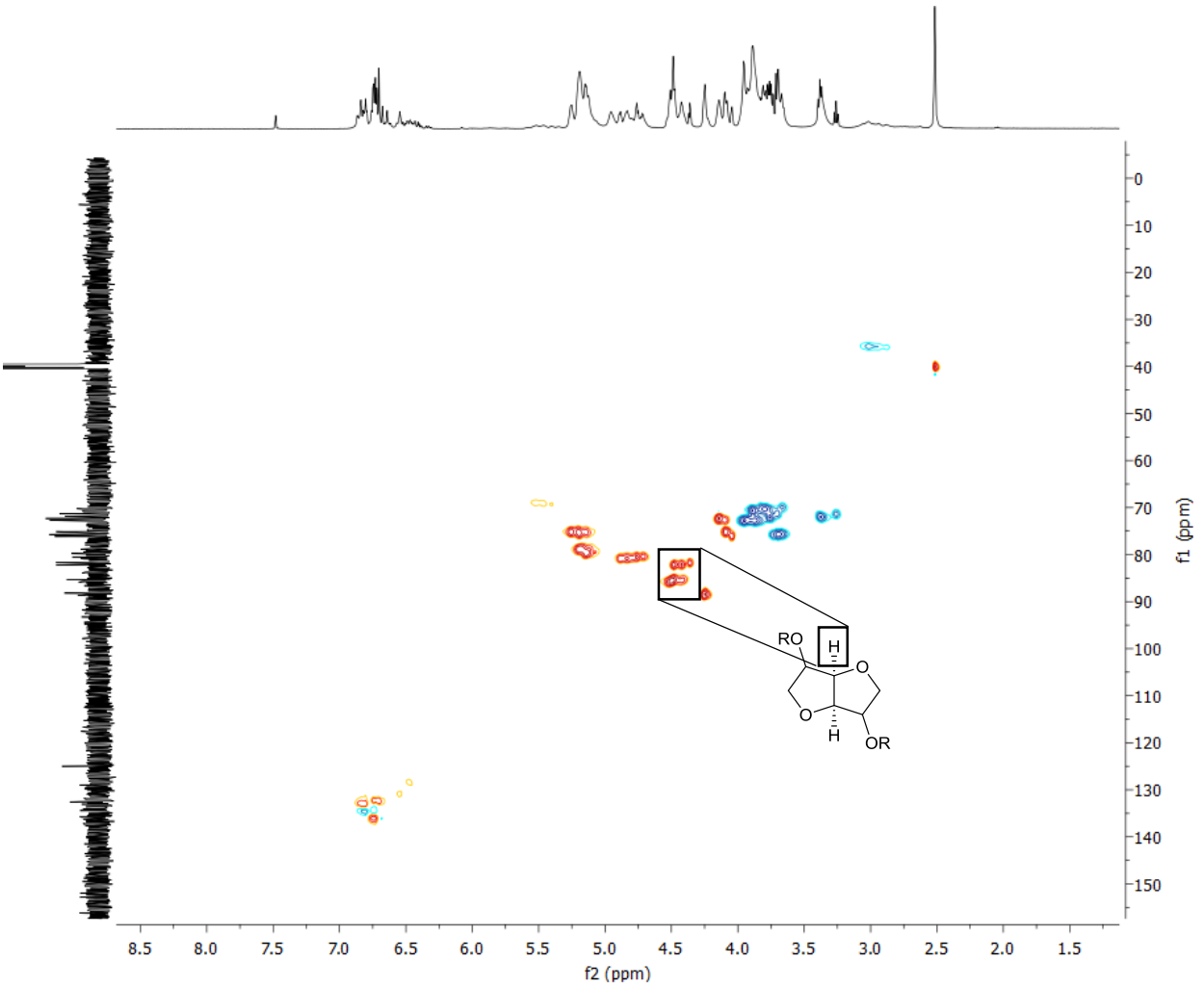

Figure S2. HSQC NMR of oligomer 4′. Proton reference on isosorbide was determined by HSQC NMR (single bond proton-carbon correlation).

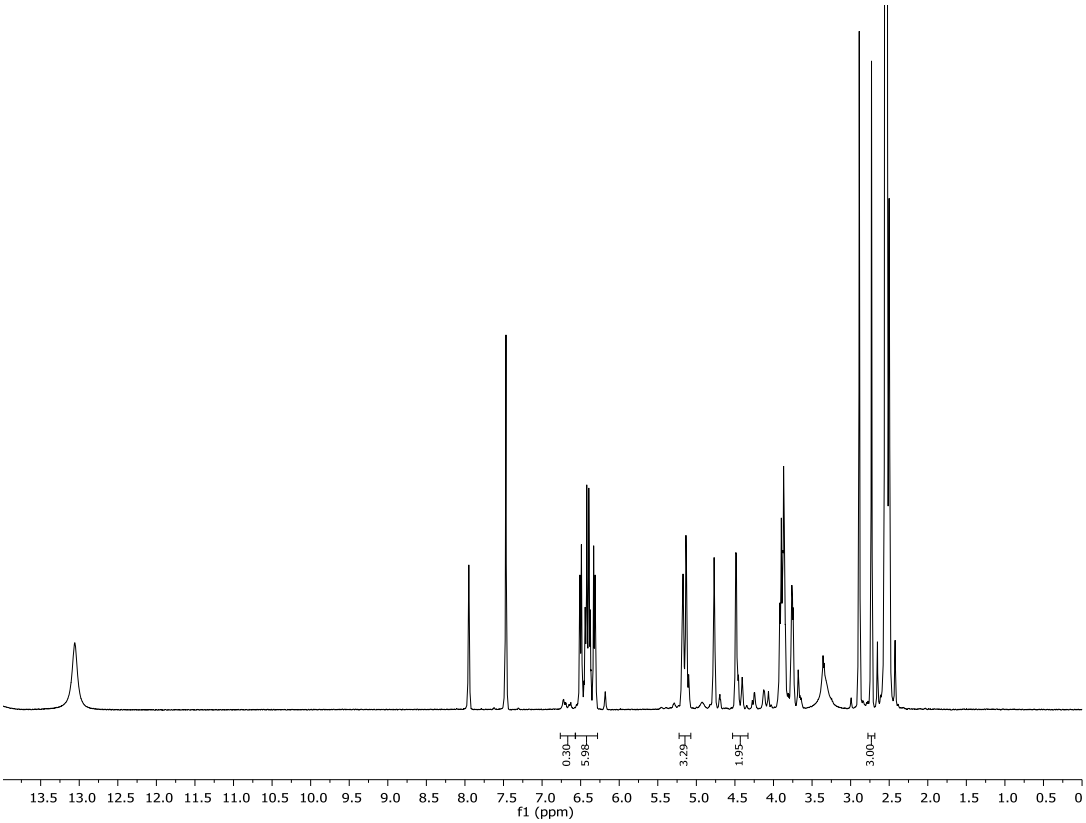

Figure S3. ^{1}H NMR of diacid **3** in DMSO-d_6 with DMF as internal standard.

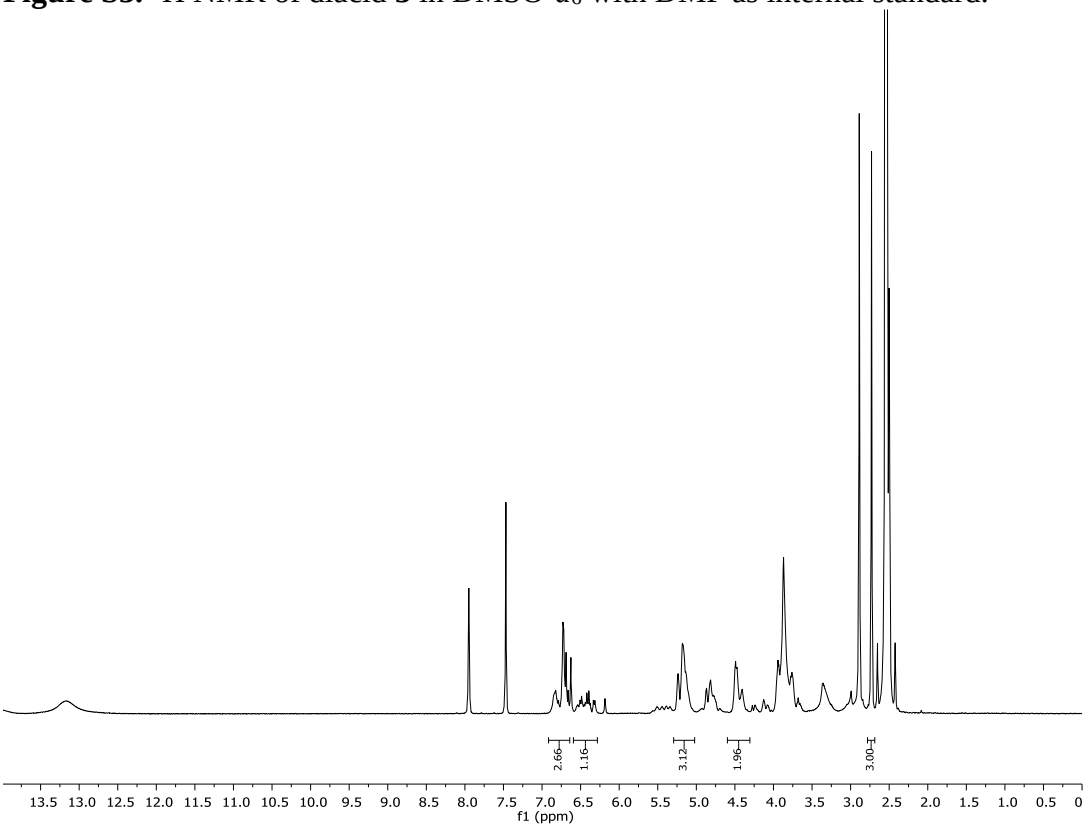

Figure S4. ^{1}H NMR of oligomer **4′** in DMSO-d_6 with DMF as internal standard.

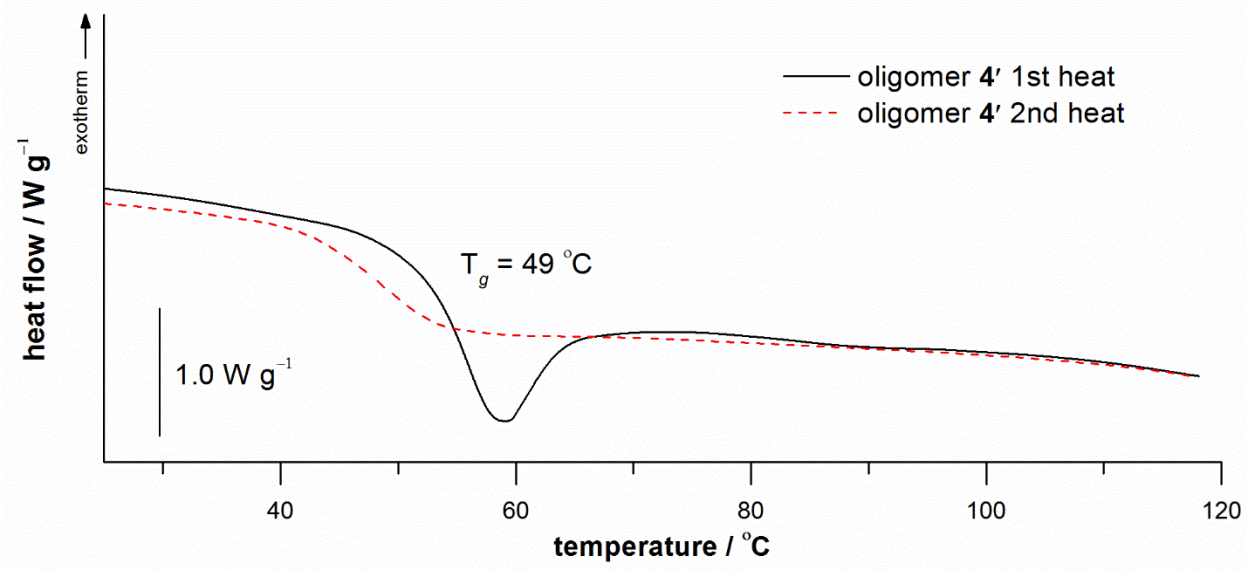

Figure S5. DSC curves (He, 10 °C min^{-1}) for oligomer **4′.**

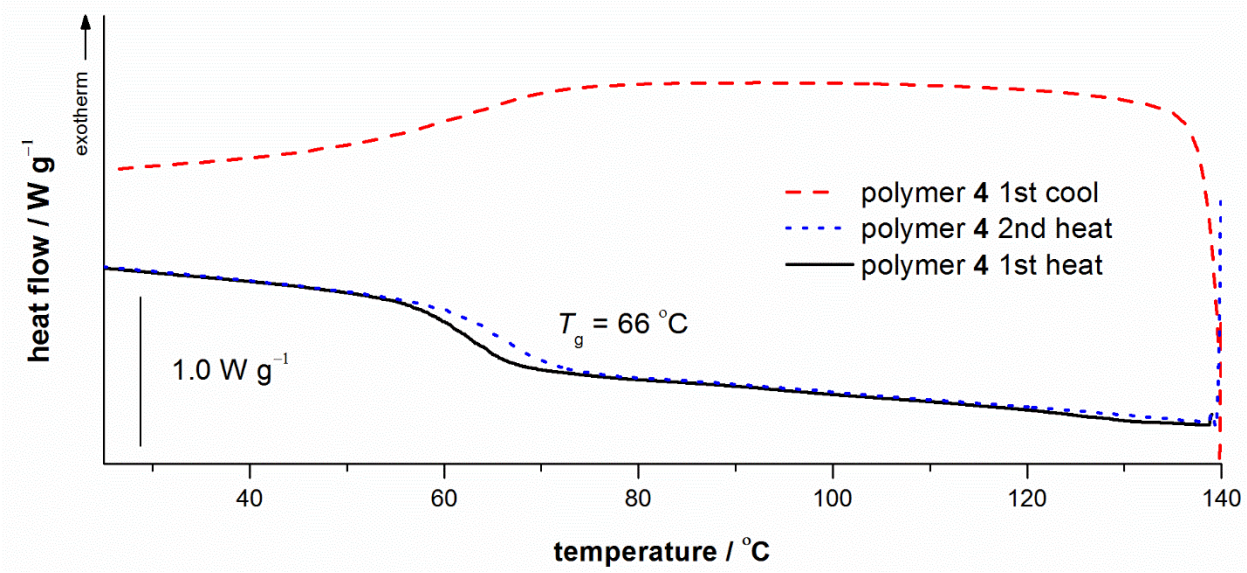

Figure S6. DSC curves (He, 10 °C min^{-1}) for polymer **4.**

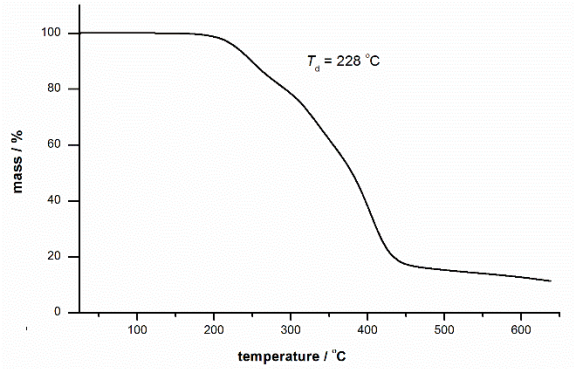

Figure S7. TGA curve (air, 20 °C min^{-1}) for polymer **4**

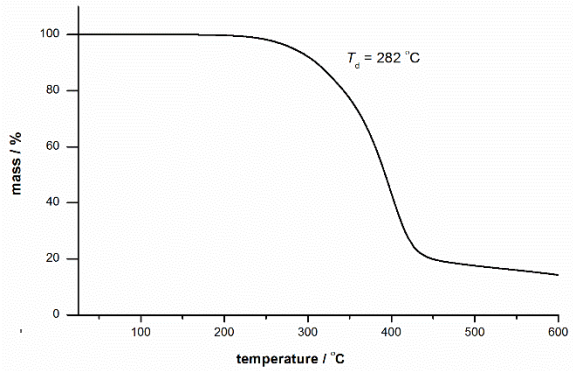

Figure S8. TGA curve (air, 20 °C min^{-1}) for polymer **6**

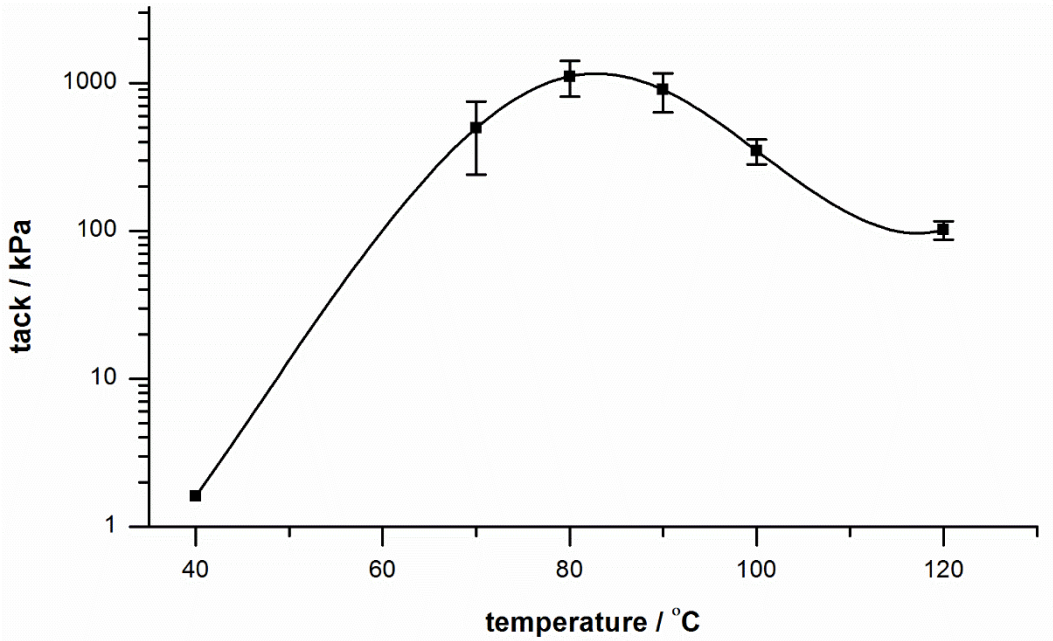

Figure S9. Tack vs. temperature curve (modified ASTM D2979 standard) for oligomer **4′**

Note: Tack at 60 °C is not reported because at that temperature, the sample sometimes showed no tack and sometimes showed near-maximum tack.

References

[1] M. Patel, M. Crank, V. Domburg, B. Hermann, L. Roes, *Medium and Long-term Opportunities and Risks for the Biotechnological Production of Bulk Chemicals from Renewable Resources*, **2006**. http://www.bio-economy.net/applications/files/Brew_pro-ject_report.pdf

[2] F. Fenouillot, A. Rousseau, G. Colomines, R. Saint-Loup, J.-P. Pascault, *Prog. Polym. Sci.* **2010**, 35, 578.

[3] X. Feng, A. J. East, W. B. Hammond, Y. Zhang, M. Jaffe, *Polym. Adv. Technol*. **2011**, 22, 139.

[4] D. S. van Es, *J. Renew. Mater.* **2013**, 1, 61.

[5] B. Delfort, S. Joly, T. Lacome, P. Gateau, F. Paille, *European Patent*, **2001**, EP 1 106 616 A2.

[6] P. W. Shepperd, M. Pankonmen, J. T. Gross, *International Patent*, **2012**, WO 2012/128858 A1.

[7] M. Okada, Y. Okada, K. Aoi, J. Polym. Sci.: Part A: Polym. Chem. **1995**, 33, 2813.

[8] M. Okada, Y. Okada, A. Tao, K. Aoi, *J. Appl. Polym. Sci.* **1996**, 62, 2257.

[9] C.-H. Lee, H. Takagi, H. Okamoto, M. Kato, A. Usuki, *J. Appl. Polym. Sci.: Part A: Polym. Chem.* **2009**, 47, 6025.

[10] M. Garaleh, T. Yashiro, H. R. Kricheldorf, P. Simon, S. Chatti, Macromol. Chem. Phys. **2010**, 211, 1206.

[11] R. Marin, A. Alla, A. Martinez de Ilarduya, S. Munoz-Guerra, *J. Appl. Polym. Sci.* **2012**, 123, 986.

[12] F. Bachmann, J. Reimer, M. Ruppenstein, J. Thiem, *Macromol. Rapid Commun.* **1998**, 19, 21.

[13] F. Bachmann, J. Reimer, M. Ruppenstein, J. Thiem, *Macromol. Chem. Phys.* **2001**, 202, 3410.

[14] X. Feng, A. J. East, W. B. Hammond, Y. Zhang, M. Jaffe, *Polym. Adv. Technol.* **2011**, 22, 139.

[15] J. Wu, P. Eduards, S. Thiyagarajan, J. van Haveren, D. S. van Es, C. E. Koning, M. Lutz, C. F. Guerra, *ChemSusChem*, **2011**, 4, 599.

[16] M. Rose, R. Paklovits, *ChemSusChem.* **2012**, 5, 167.

[17] J. Wu, P. Eduard, S. Thiyagarajan, L. Jasinska-Walc, A. Rozanski, C. F. Guerra, B. A. J. Noordover, J. van Haveren, D. S. van Es, C. E. Koning, *Macromolecules*, **2012**, 5069.

[18] M. D. Zenner, Y. Xia, J. S. Chen, M. R. Kessler, *ChemSusChem*, **2013**, 6, 1182.

[19] M. D. Zenner, S. A. Madbouly, J. S. Chen. M. R. Kessler, *ChemsSusChem*, **2015**, 8, 448 – 451.

[20] A. V. Pocius, *Adhesion and Adhesives Technology* (Ed. 2), Hanser, Cincinnati, **2002**, pp. 242 – 259.

[21] I. Benedek, M. M. Feldstein (eds.) *Technology of Pressure-Sensitive Adhesives and Products*, CRC Press, Boca Raton, **2009**, p. 576.

[22] J. Miguel, M.-Martínez, "Rubber-Based Pressure-Sensitive Adhesives" in *Technology of Pressure-Sensitive Adhesives and Products*, (I. Benedek, M. M. Feldstein, eds.), CRC Press, Boca Raton, **2009**, pp. 2-12 – 2-13.

[23] Standard Terminology of Adhesives D907 – 11a, *American Society for Testing and Materials*, Philadelphia, PA, Vol. 15.06, **2012**, 33.

[24] G. R. Palmese, J. J. La Scala, J. M. Sadler, A.-P. T. Lam, *International Patent*, **2013**, WO 2013/066461 A2.

[25] Y. Zhu, B. Geng, A. Xu, L. Zhang, S. Zhang, *Des. Monomers Polym.* **2013**, 16, 286.

[26] J. R. Damewood Jr., *Macromol.* **1985**, 18, 1795.

[27] M. Yoshioka, A. Matsumoto, T. Otsu, *Polym. J.* **1991**, 23, 1249.

[28] T. Otsu, K. Shiraishi, A. Matsuoto, *J. Polym. Sci.: Part A: Polym. Chem.* **1993**, 31, 885.

[29] A. Matsumoto, T. Otsu, *Macromol. Symp.* **1995**, 98, 139

[30] Methyl esters were formed in order to protect the GPC and to improve solubility in chloroform.

CHAPTER 5

CONCLUSION AND FUTURE DIRECTIONS

As oil supplies continue to dwindle, it is becoming increasingly important to find suitable replacements for current, petroleum based, materials. Isosorbide has been the focus of much research in recent years as a replacement for hard segments of polymers as well as for use in other materials. In this manuscript we reported the synthesis and characterization of bio-based materials from isosorbide.

Our first project was the synthesis and characterization of a 100 % biobased diisocyanate and representative polyurethanes from isosorbide. In order to access stereochemically pure diisocyanates, a tethered approach using various anhydrides, were used. A two-step Curtius Rearrangement was selected rather than a one-step approach such as the Schmitt Rearrangement for its increased safety. We have successfully synthesized an isosorbide-based diisocyanate from the starting materials isosorbide and succinic anhydride in four steps with a 60 % overall yield from isosorbide. One problem encountered during the synthesis an isosorbide based diisocyanate from a succinate tether was the potential of an E1cB elimination during distillation. This problem can be solved by using a gluterate tether in place of a succinate linker. We have also reduced waste and increased safety of our synthesis through further optimization of our synthetic route. With the diacid, acid chloride and first step of the Curtius Rearrangement optimized, we are now turning our attention to the optimization of the second step of the Curtius Rearrangement using various transition metal catalysts. Once fully optimized, a representative 1 mole (340 g) batch of crude diisocyanate will be synthesized.

It was during the synthesis of our isosorbide-based diisocyanate that an unanticipated discovery of an isosorbide-based tackifier was discovered. Isosorbide-based diacid tackifiers and

derivatives from various anhydrides synthesized and characterized. It was our belief the hydrogen bonding of our diacid based tackifiers were leading to this emergent property of tack. To test this, methyl esters were synthesized and subsequently tested for tack. It was found that these materials remain tacky, with max tack comparable to that of the diacids, but with max tack approximately 30 °C cooler. Further derivatives are being synthesized to investigate the molecular aspect of these isosorbide-based tackifiers to hopefully gain insight into the molecular aspects of tack. A collaboration with a computational group has also been formed to further analyze the molecular aspects of tack, to hopefully gain some insight into these unique molecules.

The extra functionality of our maleate-based tackifier led us to investigate further ways to modify our tackifiers into other materials, such as higher temperature tackifiers or curable adhesives. The presence of internal alkenes led us to investigate radical polymerization, which would result in a highly crosslinked thermoset. We noticed that, depending on the structure of the monomer, the polymerizations went at different temperatures and resulted in differing morphology. With this in mind, we set out to determine the structure of the polymerized product. We discovered the polymerization process was not radical, but a condensation polymerization for our diacid-based tackifier. With this in mind, we are now pursuing higher temperature tackifiers through oligomerization of our tackifiers through a more efficient and cost effective means.